Thesis for the Degree of Doctor of Philosophy

Controlled Fabrication of Thermoresponsive Elastin-like Polypeptide Microparticles

온도 민감성 엘라스틴 유래 폴리펩타이드 마이크로입자의 구조제어

February 2014

By

Cheng, Jie

Department of Biosystems & Biomaterials

Science and Engineering

SEOUL NATIONAL UNIVERSITY

Thesis for the Degree of Doctor of Philosophy

Controlled Fabrication of Thermoresponsive Elastin-like Polypeptide Microparticles

February 2014

By

Cheng, Jie

Department of Biosystems & Biomaterials

Science and Engineering

SEOUL NATIONAL UNIVERSITY

Thesis for the Degree of Doctor of Philosophy

Controlled Fabrication of Thermoresponsive Elastin-like Polypeptide Microparticles

A Thesis Submitted to the Faculty of Seoul National University

in Partial Fulfillment of the Requirements for

the Degree of Doctor of Philosophy

By

Cheng, Jie

Advisor : Professor Jinho Hyun, Ph.D.

February 2014

Department of Biosystems & Biomaterials

Science and Engineering

SEOUL NATIONAL UNIVERSITY

Department of Biosystems & Biomaterials

Science and Engineering

SEOUL NATIONAL UNIVERSITY

Supervisory Committee Approval

of Thesis submitted by

Cheng, Jie

This thesis has been read by each member of the following supervisory committee and has been found to be satisfactory.

Chairman of Committee :

_____

Lee, Kihoon

Vice Chairman of Committee :

_____

Hyun, Jinho

Member of Committee :

_____

Park, Younghwan

Member of Committee :

_____

Park, Jongshin

Member of Committee :

_____

Lim, Dongwoo

Controlled Fabrication of Thermoresponsive Elastin-like Polypeptide Microparticles

온도 민감성 엘라스틴 유래 폴리펩타이드 마이크로입자의 구조제어

지도교수 현 진 호

이 논문을 박사 학위논문으로 제출함

2013년 12월

서울대학교 대학원
바이오시스템·소재학부
바이오소재전공
정 걸

정걸의 박사 학위논문을 인준함

2014년 2월

위 원 장 이 기 훈 (인)

부위원장 현 진 호 (인)

위 원 박 영 환 (인)

위 원 박 종 신 (인)

위 원 임 동 우 (인)

Abstract

Elastin-like polypeptide (ELP, MW: 85kDa) containing lysine-residues was genetically synthesized and a series of thermoresponsive ELP microstructures were fabricated by using emulsion and non-emulsion methods. The transition temperature (T_t) of ELP was ~37 ^oC at a concentration of 200μM. Temperature-triggered folding of ELP molecules involved changes in secondary and tertiary structures. Firstly, a series of polypeptide microcapsules (MCs) with positively thermoresponsive pores were fabricated using two-step cross-linking w/o emulsion method. The shell thickness of MCs could be easily adjusted by changing the glutaraldehyde crosslinking time. The MCs prepared in this method had positively thermoresponsive pores. The increase of temperature above T_t opened the pore windows both at the surface and inside the shell. The pore morphology of ELP MCs could be adjusted by the addition of BSA. Secondly, both the ELP-based microbeads and microcapsules could be obtained by controlling the phase separation in the water-in-oil emulsion and subsequently by crosslinking with glutaraldehyde. The responsiveness and morphology of ELP microstructures could be controlled through the temperature used during the crosslinking process in a water-in-oil emulsion. The ELPs' behavior inside the emulsion could be controlled by the experimental temperature. ELP microbeads prepared below T_t had positively thermoresponsive pores. ELP microcapsules prepared above T_t had negatively thermoresponsive pores. ELP MCs were also prepared at the temperature of their transition state. Interestingly, these ELP MCs demonstrated bidirectional thermoresponsiveness, closing their

pores at both higher and lower temperatures. Thirdly, ELP microbeads were prepared by temperature triggered phase separation of ELP molecules in water solution at a temperature higher than T_t. The microbead prepared in this method had negatively thermoresponsive pores. Above T_t, ELP chains folded and were compressed so tightly that no pores could be observed. On the contrary, the compressed ELP chains extended and gave rise to pores formation below T_t.

Keywords: Elastin-like polypeptide, Microparticles, Negative and positive thermoresponsiveness, Microcapsules, Microbeads.

Student number: 2009-31280

CONTENTS

List of Tables

List of Figures

I. Introduction

The exploitation of protein/peptide based materials is an increasing concern due to their broad applications in biotechnology, nanotechnology, bioelectronics and biomedicine. Advances in gene cloning technology and materials science are enabling the development of new protein/peptide materials for novel applications. Among protein-based polymers, Elastin-like polypeptides (ELPs) are biopolymers of the pentapeptide repeat Val-Pro-Gly-Xaa-Gly derived from human tropoelastin, where the "guest residue" Xaa can be any of the natural amino acids except Pro. Besides biocompatibility, biodegradability, and non-immunogenicity, stimuli-responsive characteristics, in particular their thermoresponsive characteristic, make ELPs a very promising candidate for drug delivery and other biomedical applications.[1, 2] ELPs are soluble in aqueous solution below the inverse transition temperature (T_t), and once the temperature is increased above T_t, ELPs will undergo a sharp phase transition leading to self-assembly and aggregation of the polypeptides. This unique property also makes purification simple and cost-effective compared to other protein purification methods.

Microparticles (microbeads and microcapsules) have been widely used as delivery platform for drugs, medical imaging agents and cells. Recently, much attention has been focused on developing stimuli responsive microparticles to meet the need for better control of drug administration and active agent delivery. Possible stimuli being applied for microparticles include pH [3], temperature [4-6], light [7-9], magnetic fields [10-13], ultrasound[14, 15] and

electrical fields [16, 17]. However, from a biomedical point of view, temperature change is a considerably valuable stimulus to trigger drug release due to its simple, effective, and safe natures. Sometimes, such as inflammation and cancer which are always accompanied by an increase in body temperature, a positive thermoresponsive drug release system, meaning that rapid drug release occurs above a certain temperature and stops below this temperature, is urgently needed. On the other hand, sometimes, a negative thermoresponsive drug release system in which rapid drug release occurs below a certain temperature and sustained release above this temperature is also needed.

Due to the remarkable superiority in biocompatibility and biodegradability, protein-based microcapsules for controlled and sustained release have attracted a lot of attentions for drug delivery and other extensive applications. However, there are some challenges remained for preparing protein-based microcapsules. Until now, the fabrications of protein-based microcapsules are mainly focused on two approaches, one is dependent on the self-assembly of small amphiphilic polypeptide [18, 19], the other one is dependent on layer by layer electrostatically adsorb a protein molecule onto a charged emulsion droplet or solid template [20, 21]. The former always are confined to small protein not exceeding a molecular weight of 10kDa, whereas, despite the later method is able to fabricate larger-protein-based microcapsules, an obvious defect, which is dependent on the protein charge, is negligent. As we know, protein charge is very sensitive to pH changes in the surrounding environment,

making this method very sensitive to pH. Therefore it is imperative to search a simple and more stable large-protein-based microcapsules fabrication method.

Thermoresponsive microcapsules (MCs) are promising carriers for achieving on-demand release of drugs. So far, most of these thermo-responsive MCs are made with poly(N-isopropylacrylamide)(poly-NIPAAM) and its derivatives [22]. However, these MCs made with poly-NIPAAM have a number of shortcomings, such as non-biodegradability, cytotoxicity and slow thermo-responsive rate, which will restrict their use in pharmaceutical applications [23, 24]. According to the literatures, poly (N-isopropylacrylamide)(pNIPAAm) has been widely used to prepare negative thermo-responsive drug release hydrogel system due to its lower critical solution temperature (T_t) of ~32 ℃. At high temperature (above T_t), pNIPAAm hydrogel MC shrinks and forms a dense skin layer at the gel surface. The skin layer prevents drug diffusion, leading to the creation of an on-off pulsatile drug release in response to temperature. Positive thermoresponse is also realizable for pNIPAAm polymer, but needs some additional processes such as coating pNIPAAm hydrogel with release-holes-containing membrane, grafting pNIPAAm hydrogel main chains with hydrophilic polymer(HEMA)[25], copolymerizing pNIPAAm hydrogel with other polymer[26], or putting pNIPAAm hydrogel into the holes of an inert membrane [27].

In this thesis, the lysine-residues containing ELPs were genetically synthesized and a series of ELP microstructures with negatively and

positively thermoresponsive properties have been fabricated by using emulsion and non-emulsion method.

1. Microcapsule prepared by two-step method at low temperature inside water in oil (W/O) emulsion

Elastin-like polypeptide (ELP)/bovine serum albumin (BSA) protein microgel capsules (MCs) with thermoresponsive pore windows were successfully prepared using a template-free water in oil emulsion method. The pores at the surface and in the interior shell could be changed between a closed state and an opened state under thermal stimuli. Above the transition temperature (T_t) of ELP, both small and big molecules including rhodamine B, FITC and BSA were loaded into the hollow cores of the MCs. The selective release of entrapped molecules could be achieved by controlling the environmental temperature.

2. Microstructures prepared by one-step method at high temperature inside water in oil (W/O) emulsion

The responsiveness and morphology of ELP microstructures could be controlled through the temperature used during the crosslinking process in a water-in-oil emulsion. The ELPs' behavior inside the emulsion could be controlled by adjusting the experimental temperature. The ELP molecules are hydrophilic at low temperatures, allowing them to fully extend due to the level of hydration; these conditions generate ELP microbeads with positively thermoresponsive pores. At higher temperatures, the ELP molecules are

hydrophobic, leaving them completely folded and compressed inside water droplets; these conditions generate ELP microcapsules with negatively thermoresponsive pores. ELP microcapsules were also prepared at the temperature of their transition state. Interestingly, these ELP microcapsules demonstrated bidirectional thermoresponsiveness, closing their pores at both higher and lower temperatures. The dominance of inter- or intramolecular crosslinkings depended on the diblock nature and local concentration of the ELPs; this parameter determined the surface morphology of the ELP microstructures.

3. ELP microbead prepared at high temperature inside water solution.

A negative thermoresponsive ELP microberad system prepared by temperature induced phase separation in aqueous solution. The microparticles were prepared by increasing the temperature above T_t of ELP, and then ELPs phase separated from the aqueous solution and coacervated to form micro-scale particles. Because of the primary amines in the ELP chain, these microparticles were simply crosslinked with glutardaldehyde. The inherent thermo-responsive nature of ELPs imbues these microparticles with thermo-responsive characteristic.

II. Literature Survey

2.1. Elastin-like polypeptide

2.1.1. Synthesis and purification of elastin-like polypeptides

Elastin-like polypeptides (ELPs) are biodegradable polypeptide of the pentapeptide repeat Val-Pro-Gly-Xaa-Gly, in which the “guest residue” Xaa can be any of the natural amino acids except for proline [28]. ELPs have elastic property due to a particular repeating elastomeric peptide sequence. Additionally, ELP shows inverse phase transition, which is the characteristic chemophysical properties responding to the external stimuli such as temperature, pressure, ion concentration, and pH.

Both the chemically and genetically based synthesis can be used to synthesize ELPs. The chemical method is based on solid phase synthesis, which have a lot of obvious limitations such as peptide length, scale and high cost. Since a genetically encoded synthesis method was firstly developed by Urry et al [29], a series of genetic synthesis method were reported [30-32]. The sequence and length of ELPs can be precisely controlled with the genetic method. And the high yield is another merit for the genetic method [33].

Although a number of strategies to rapidly assemble repetitive polypeptide genes have been developed, including PCR cloning [34, 35], concatemerization [36], and seamless cloning [37, 38]. The recursive directional ligation (RDL) method could be the most suitable one for ELP synthesis due to its merit of simplicity [30](Figure 1). RDL is a controlled

stepwise oligomerization process, which requires two restriction enzyme recognition sites to ligate genes for direction of a head-to-tail. After ligation, recognition site of the ligated site disappears and original restriction enzyme recognition sites of only two-ends remain. Finally, DNA fragment grows in sequential steps. RDL provides the ability to control specific sequences, molecular weight, and architecture. In addition, RDL is also a useful method for the synthesis of genes that encode block polymers (e.g., ELP complex block copolymer, ELP fusion protein), and therefore recently various functional ELPs have been produced [39, 40].

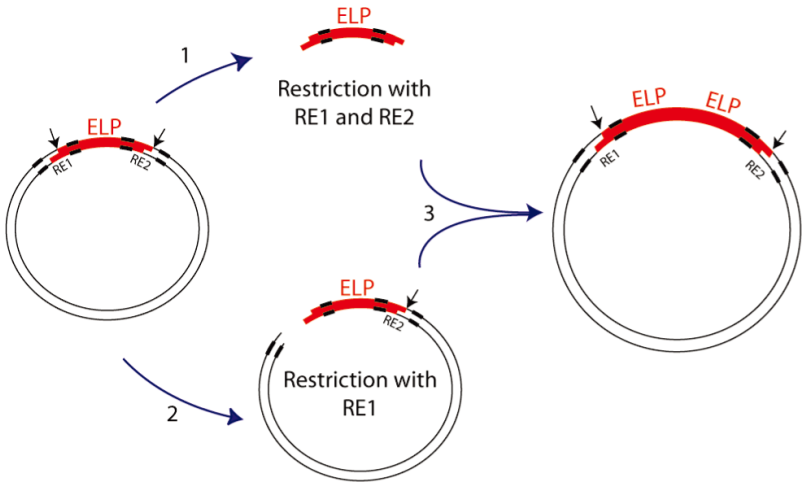

Figure 1. **Recursive directional ligation [41].**

2.1.2. Thermal behavior and the corresponding structural change of elastin-like polypeptides

ELP is typical thermoresponsive material, which exhibits a phase transition temperature (T_t) or lower critical solution temperature (LCST). Being a genetically engineered negative thermoresponsive biopolymer, below the lower critical solution temperature (T_t), the uncrosslinked ELP chains are hydrophobic hydrated and soluble in water with a random coil structure. However above T_t the ELP chains will liberate the bound water molecules and fold taking a beta-turn structure, followed by phase separation and self-assembly to form a state that is 63% water/37% ELP polypeptide by weight [42, 43].

Two of the most widely studied systems which display lower critical solution temperature behavior are ELPs and pNIPAAm. However, there is a critical difference between ELP and PNIPAM phase transition system. The key difference between this pNIPAAm and ELP is that the amide moiety of pNIPAAm is pendent rather than part of the backbone [44]. Like ELPs, pNIPAAm will also separate out of solutions above their T_t value [45-48]. However, pNIPAAm undergoes hydrophobic collapse/aggregation without the formation of specific secondary or tertiary structures. On the other hand, above T_t ELPs fold and aggregate to form significant Beta-turn/Beta-spiral secondary/tertiary structure formation [49-53].

At low temperature (below T_t), all ELP chains existed in a disordered way (random coil), once the temperature increased above T_t, ELP chains started to

fold and took an ordered structure (β-turn/β-spiral). This changing from free chains to a micro-scale particle involved a secondary structure transition which was determined by CD spectra. Two main CD peaks (a band at ～198 nm and a band at ～212 nm) have been clearly observed. The band at ~198 nm assigns to random coil structure and the band at ~212 nm should arise from type Ⅱ β–turn/β-spiral structure.[54-57] Fourier- transform infrared (FT-IR) spectroscopic measurement also can be used to determine the secondary structure change. Amide I band ATR/FTIR studies are suitable to investigate structural differences in ELPs of increasing hydrophobicity in the collapsed state. Unlike CD, FTIR is more suitable for probing the secondary structure of the collapsed ELPs since light scattering is not nearly as problematic at IR wavelengths [58]. Amide I peaks have been extensively used to probe secondary structures of ELPs [59-63]. According to literatures, the peaks near 1619 and 1663 cm^{-1} most likely arise from Beta-turn and Beta-aggregate structure. However, the resonance near 1644 cm^{-1} can be assigned to random coil and perhaps some distorted Beta-sheet structure. The change in secondary structure below and above T_t can be probed by fitting amide I peak to Gaussion components [61]. The components show that there is a significant increase at 1624 cm^{-1} indicative of an increase Beta-sheet structure as the temperature is raised. This aspect of the structural change in ELP is well represented by the traditional band fitting to components (Figure 2).

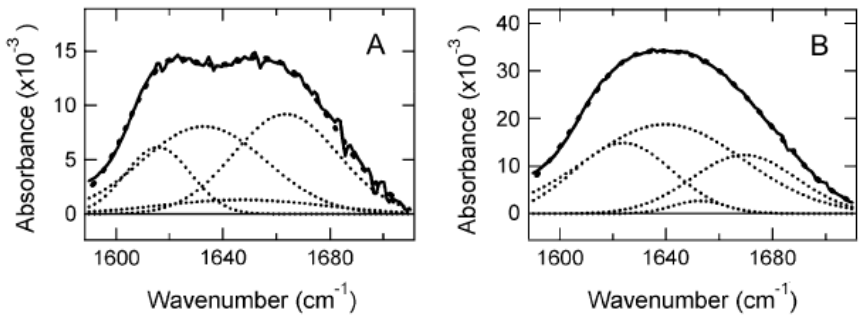

Figure 2. Fits to amide I band of the 61-kDa ELP (lighter solid lines) at (A) below and (B) above T_t [61].

2.1.3. Applications based on elastin-like polypeptide

Elastin-like polypeptide (ELP), an artificial smart polypeptide, has successfully prepared by a number of different strategies. ELPs are biopolymers of the pentapeptide repeat Val-Pro-Gly-Xaa-Gly derived from human tropoelastin, where the “guest residue” Xaa can be any of the natural amino acids except for Pro. Besides biocompatibility, biodegradability, and non-immunogenicity, stimuli-responsive characteristics, in particular their thermo-responsive characteristic, make ELPs a very promising candidate for widespread applications including tissue engineering, drug delivery, nanostructure design, protein purification, and so on.

2.1.3.1. Purification of ELP-fused recombinant protein

Unlike other proteins, which always requires complex and costly process such as chromatographic separation to be purified, ELP is temperature responsive and can be purified easily with inverse transition cycling (ITC) method. As demand of the recombinant protein in therapeutic drug is increased, economical and large-scale protein purification method is desirable. With the help of ELP tag, the target protein incorporated with ELP can be purified with ease by ITC method [30, 33, 64]. Thanks to the advance in DNA recombinant technology, various protein genes can be joined with ELP gene and be co-expressed. After co-expressed, target-ELP fusion protein could be purified by ITC method. And to separate the target peptide from ELP tag, a cleavable peptide gene is always inserted between target peptide and ELP

gene. Therefore, upon treating fusion protein with protease or dithiothreitol, the target peptide will be cut off and separate from ELP tag. And another circulation of ITC will precipitate ELPs leading to only target peptides remain in supernatant [65]. ELP based purification method is a very powerful strategy to purify protein and always with a purity over 95%. And this method has a dramatic potential to replace the existing protein purification method.

2.1.3.2. Micropatterning

A stimuli-responsive-based micropatterning technique has been wildly used for the spatial control of DNAs, proteins and cells. Derivatives of poly(N-isopropylacrylamide) (pNIPAAM), a most well-known thermo-responsive polymer with a low critical solution temperature of 32 ^{o}C, are reported to be effective for the control of cell attachment through their reversible hydration/dehydration transition induced by temperature change [66-69].

As a thermoresponsive biopolymer, ELPs can been micropatterned on the biochip surface, which have been used as biochip sensors to detect the ELP-tagged biomolecules in the bulk solution through hydrophobic interactions between ELPs grafted on the surface and ELP tag [70-72]. ELP-tagged biomolecules can be selectively immobilized on the biochip surface through hydrophobic interaction at a temperature higher than T_t of ELP, where ELPs on the surface of biochip provided a strong driving force to bind ELP-tagged biomolecules because both ELPs on the surface and ELP-tag were in their conformationally collapsed and dehydrated state. A drop in temperature is

sufficient to release the immobilized ELP-tagged biomolecules, due to ELP will take a secondary structural change to embed its hydrophobic side groups and interact with water molecules.

ELP grafted surface also can be used to micropattern cells. Hydrophobic and hydrophilic surfaces have been widely studied and modified with a series of methods to promote cell adhesion [73-75]. Surface modification based on ELP-micropatterning is a wonderful method to modify the surface of biomedical devices. Temperature can induce ELP phase transition between hydrophobic and hydrophilic state, as a result, the cell affinity to surface will also be changed. A hydrophobic surface is more beneficial to cell adhesion, while a hydrophilic surface is unfavorable. Cell adhesion can be easily controlled by adjusting environmental temperature on the ELP patterned surface. In addition, cells are commonly harvested by treating with EDTA-trypsin, which is a harmful process to cell health. This unfavorable process can be avoided by using ELP patterned surface and cells can be harvested by easily changing environmental temperature.

2.1.3.3. Drug delivery

Because the biocompatibility, degradability and stimuli responsibility, ELPs can be used as wonderful drug carrier for both systemic drug delivery and localized drug delivery.

ELP is a great candidate as a systemic drug delivery carrier. After injection,

ELPs can be accumulated at a heated location, where the local ELP coacervates will be formed due to the thermotriggered phase separation [76-78]. The radiolabeled ^{14}C-ELP was injected into the tumor containing animal. The tumor was then heated for 30 minutes to induce a local hyperthermia at the position of tumor [79]. Autoradiography of tumor sections showed that ELP accumulated to at a much greater extent at the heated tumor than non-heated tumor. In addition, ELP also showed greater preferential accumulation in the extravascular compartment of tumor. Anticancer chemotherapeutics such as doxorubicin attached to ELP backbone can be delivered to the tumor with the above heat targeting method [80].

Peptide therapeutics are a promising strategy to meet the need of more effective cancer therapy because of the specificity of peptides for their intracellular molecular targets[81]. Small therapeutic peptides fused to ELPs and cell penetrating peptide (CPP) and have good pharmacokinetic parameters and more effectively permeate through tissue and cell membrane [81]. The use of ELP and CPP for targeted therapeutic peptide delivery has a series of advantages. ELPs like other soluble macromolecules have ability to improve tumor accumulation due to a passive targeting EPR effect. The addition of CPPs to ELP carrier enhances uptake by tumor cells and also target ELP to the desired cell compartment [82-85].

Di-block ELP consisted of hydrophobic and hydrophilic blocks can form a spherical micelle with drugs loaded in its hydrophobic core [86, 87]. Recombinant chimeric polypeptides (CPs) consisted of ELP and a short Cys-

rich segment can self-assemble into nanoparticles with a size of sub-100nm. Covalently conjugating hydrophobic small molecules like chemotherapeutics to Cys residues leads to spontaneous formation of nanoparticles [88]. The chemotherapeutics have been efficiently delivered to a murine cancer model.

ELPs are also great candidates as localized drug delivery carriers. ELPs with drugs can be injected into body and form a localized coacervate. Drugs can be released out of these coacervates through solvation of the outermost ELP in the coacervate and diffusion of the drugs[89]. ELP also can be used with other biopolymers like silk to form more stable depot, aiming at a more sustained drug release[90]. In addition, ELP also can be fusioned with silk sequence to form fusion peptide, known as silk-like ELP (SELP), which is able to form a stable and injectable hydrogel. Biologically-active molecules such as DNA, RNA and proteins retain biological activity following release out of this SELP hydrogel [91].

2.1.3.4. Tissue engineering

The biocompatibility and non-immunogenicity belong with the precisely controllable amino sequence and molecular weight make ELPs a good candidate for tissue engineering applications. A variety of ELP scaffolds including injectable coacervate, hydrogel and cell sheet have been proved their ability to promote the regeneration of vascular graft, cartilage, ocular and liver tissue [1, 92-95]. ELP formed a gel-like structure,coacervate, at specific concentration without crosslinking at the temperature above T_t. ELP

coacervates allow encapsulation of cartilage cells and promote the synthesis and retention of cartilaginous matrix [96, 97]. One limitation of ELP coacervates is their mechanical property.

ELP can be crosslinked with both chemical and physical methods to obtain hydrogel with great mechanical property. ELPs with amine residues have been crosslinked with various amine active chemical crosslinkers such as glutaraldehyde, hexamethylene diisocyanate, bis(sulfosuccinimidyl)- and disuccinimidyl suberate to form hydrogel [98-103]. These hydrogels exhibit a gradual inverse phase transition, not a discrete inverse transition like pure ELP molecules do. ELP molecules inside hydrogel undergo molecular rearrangement over a much broader temperature range. The possible explanation to this difference is that crosslinking formation between inter or intra ELP chains broadens the transition by inducing a series of small ELP segments with its own discrete transition temperature [104].

Temperature-triggered physical crosslinking between ELP hydrophobic domains is very simple method to fabricate ELP hydrogel. Unlike chemical crosslinking, which always accompany with potential cell toxicity due to chemical crosslinkers used, physical crosslinking is totally biocompatible. Reversible self-assembling hydrogels based on a tri-block ELP have been fabricated [105, 106]. These ABA tri-block copolymers composed of an elastomeric B domain (VPGVG) with a higher T_t and two plastic domains (VPAVG) with a lower T_t. Hydrogels were formed by thermal aggregation of the plastic domains derived from different ELP molecules. In addition,

synthesized diblock ELP composed of tropoelastin exons 20 and 40 as the hydrophilic block and exons 21 and 23 as the hydrophobic block can form fibrillar matrices, due to alignment of ELP into fibrils [107]. Synthesized recombinant human tropoelastin composed of complex alternation hydrophilic and hydrophobic domains can also form hydrogel through intermolecular hydrophobic interactions above their T_t [108-110].

There is much interest in scaffold-free tissue engineering based on cell sheet with intact ECM structure, which can be used directly for tissue regeneration [1, 111, 112]. ELPs have been used for preparing ECM-containing cell sheet [113]. RGD-functionalized ELPs were coated on the surface of tissue culture plate, and then cells were mixed with RGD-functionalized ELP and seeded on the RGD-ELP coated surface. Cell sheet composed of cells and ECM was harvested by lower the temperature below the transition temperature of ELP [113].

2.1.3.5. Self-assembly

Protein-based self-assembly have been studied intensively due to their controlled assembly/disassembly and potential applications including switchable encapsulation, efficiently drug delivery and tissue engineering.

Amphiphilic diblock ELPs with consecutive cysteine residues have been synthesized, and these ELPs can form thermally responsive micellar nanoparticles in aqueous solutions that exhibit a spherical core shell structure.

Self-assembly is driven by a conformational transition of the hydrophobic block and stabled by intermolecular covalent cross-linking through disulfide bond formation at the core/shell interface [40].

ELP also can be fused with the other protein to create multi-stimuli-responsive system. A structural fusion protein of ELP and a viral capsid protein (CP) have been designed and its assembly properties were investigated [114]. This design combines the stimuli responsive properties of the two peptide blocks: adjusting pH triggers this fusion peptide self-assembly to form homogeneous virus-like-particles with a diameter of 28 nm, on the other hand, adjusting temperature drive ELP blocks aggregate together via hydrophobic interaction, leading to virus-like-particles with a diameter of 18 nm.

2.2. Emulsion method for polypeptide based microstructure fabrication

During the past few decades, research interest in biodegradable polymeric microspheres and microcapsules has increased steadily due to their potential in a wide range of biomedical applications such as drug delivery and tissue engineering. Among the microstructure preparation methods, emulsion method is the most common technique to fabricate microstructure [115, 116]. Microspheres can be prepared by water in oil (W/O) or oil in water (O/W) method. Generally speaking, microspheres based on oil soluble organic materials are commonly prepared with O/W method, on the other hand, microspheres based on water soluble materials are always prepared with W/O method. The size of microspheres is usually controlled by mechanical shear force.

Polysaccharide-based microspheres of chitosan, starch, and alginate can be easily prepared with water-in-oil (W/O) emulsion method [117]. Because of their biocompatibility and cheap price, polysaccharides have been widely used to prepare microspheres to delivery water-soluble drugs. Microspheres from chitosan have been prepared by chemical cross-linking in water-in-oil (W/O) emulsion. Chitosan is a polysaccharide with a lot of reactive functional amine groups and therefore can be crosslinked with aldehyde groups of the crosslinking agent [118-120]. Firstly, a water-in-oil (w/o) emulsion is established by emulsifying the chitosan aqueous solution in the oil phase with

the help of continuous stirring. And then, cross-linking agent such as glutaraldehyde was added to harden the chitosan droplets. Similarly, both the other two common polysaccharides, starch and alginate, can be prepared with this simple water in oil emulsion method [117, 121, 122].

Biodegradable poly (lactic-*co*-glycolic acid) (PLGA) polymers grab increasing attraction of researchers due to their outstanding biocompatibility and their authorization by the Food and Drug Administration (FDA) for drug delivery [123]. The most common PLGA structure used for drug delivery is microsphere, which can be simply fabricated by emulsion method [124, 125]. Schwendeman group has developed a self-healing PLGA microsphere with interconnected porous network by using emulsion method [126].The pores on the surface of microsphere can be closed by heating to 30 ^{o}C after loading protein at 4^{o}C. The dry microspheres were incubated at 4 ^{o}C (which is lower than the glass transition temperature of the hydrated polymer (T_g, 30 ^{o}C) in a concentrated lysozyme solution to enable protein flow into microspheres through the open pores. Pore healing was initiated by raising the temperature above the T_g value [126]. As a result, much more proteins have been loaded into microsphere and will be released in a very sustained way because of the closure of pores by gently heating.

Microcapsules (MCs) with shell/core strucure have attracted a lot of attentions due to their potential applications in drug delivery, cosmetics, catalysis and other extensive applications [127-131]. Particularly, MCs susceptible to environmental stimuli offer even greater versatility for

encapsulation and controlled release, which can be controlled by changing temperature, pH, and other stimuli [132-134]. Emulsion system can provide a hydrophobic/hydrophilic interface, where a lot of interesting actions are able to be triggered. Therefore, this hydrophobic/hydrophilic interface also provide a great avenue for preparing microcapsule. Recently, internal phase separation technique was found to be a suitable technique for the preparation of MCs. In this method, a polymer is dissolved in a solvent mixture containing a volatile good solvent for the polymer and a nonvolatile poor solvent for the polymer, and the resultant solution is dispersed into the aqueous phase by high shear stirring. The emulsion is then subjected to elevated temperature which will gradually remove the volatile solvent from the polymer-containing droplet. As the volatile solvent evaporates, the polymer begins to coacervate and migrate to the oil/water interface where they fuse and spread to engulf the oil droplet. When the volatile solvent has completely evaporated, the polymers coalesce at oil/water interface to form a shell [135-138]. Dinsmore, Bausch, weitz, and co-workers have developed an emulsion template directed self-assembly system to synthesis hollow capsules (colloidosomes) [139, 140]. Colloidal particles are adsorbed on emulsion droplet interface to reduce the surface energy, and eventually completely cover the droplet interface. These adsorbed particles are subsequently locked together by addition of polycations, by van der Walls force, or by sintering these particles to form elastic shells [139]. Cell like filamentous microcapsules prepared by interfacial self-assembly of peptide amphiphiles have been reported [141]. Peptide amphiphiles self-assembled at hydrophilic/hydrophobic interface to form a hierarchically

structured membrane, named the shell of microcapsule. The fibrous surface of microcapsules offers a high surface area and opportunity to introduce bioactive events through molecular design of the peptide head of peptide amphiphiles. Because of the existence of peptide domain in peptide amphiphiles nanofiber, microcapsules can be further modified with growth factors, small peptide, or DNA [141].

Microcapsule with an both oil and water core have been prepared by self-assembly of diblock copolypeptide at hydrophobic/hydrophilic interface [142]. The diblock copolypeptide has a general structure structure poly(L-lysine)x-b-poly(racemic-leucine)y, Kx(rac-L)y, where x ranged from 20 to 100, and y ranged from 5 to 30 residues [142]. Generally, poly (L-leucine) domain will form an alpha helix structure leading to hydrophobic side groups exposed outside. And these helix structure can insert into oil phase left poly (L-lysine) domain in water phase. As a result, when copolypeptide water solution was mixed with oil phase, these copolypeptides gathered together at oil/water interface and a single oil in water emulsion system formed. However, once replaced L-leucine with racemic-leucine, the copolypeptide lost its ability to form alpha helix structure. When mixed with oil phase, the double emulsion structure was able to form, leading to a microcapsule with both oil and water core formed [142]. Obviously, racemic-leucine segments play a key role in stabilizing the double emulsion structure and the corresponding microcapsule formation.

Recently, flow focusing devices based emulsion systems have been

employed to prepare core/shell microcapsules. The Weitz group has designed a microcapillary fluidic device to generate monodisperse double emulsions [143, 144]. The inner phase (core forming phase) was firstly encapsulated by middle fluid phase (shell forming phase), which was then dispersed in an outer fluid [143]. This microcapillary fluidic device can generate double emulsions dispersed in either hydrophilic or hydrophobic fluid, that is both oil-soluble and water-soluble polymer can be used as the middle phase to form the shell of capsule. Depending on what shell forming materials were used, the shells can be fixed with a broad class of methods such as chemical crosslinking [143], solvent evaporation [145], or polymer solidification [146].

2.3. Self-assembly inside water solution for polypeptide based microstructure fabrication

In nature, self-assembly of helical macromolecules into structured materials is critical to tissue formation [147-149]. A series of aqueous solution based self-assembly systems for both natural and synthesized polypeptide/protein have been widely reported.

Stupp and colleagues have designed a series of peptide-amphiphiles composed of a hydrophilic peptide block and a hydrophobic hydrocarbon block [150, 151]. These peptide-amphiphiles (PAs) can self-assemble from aqueous media into supramolecular nanofibers with high aspect ratio. The peptide block is made up of a beta-sheet forming domain and a biological signal domain. Inside water solution, the hydrophobic lipid tails drive the PAs self-assembly to form cylindrical nanofibers with several to hundreds of micrometer in length. In addition, the hydrogen bonding formed between beta-sheet peptide segments will stabilize the nanofiber structure. Furthermore, the terminal biological signal peptide becomes exposed in very high density on the surface of the nanofibers. A broad class of biosignal peptide such as growth factor binding peptide and cell binding peptide can be designed into the PAs [152]. These nanofibers can be used for drug delivery and tissue engineering. The Stupp group also reported a noddle like hydrogel prepared by PAs [153]. The PA contains the peptide sequence $V_3A_3E_3(CO_2H)$ and a C_{16} alkyl tail and self-assemble into nanofibers by screening the charged amino

acid residues via addition of ions. The PAs form a two dimensional plaques with filamentous texture when injected into salt solution after heat treatment. This supramolecular filaments can be mixed with cells at physiological temperatures and injected from a pipette into salt solutions to form hydrogels with aligned filaments [153]. After equilibration at 80 ^{o}C for 30 min, PAs formed thin plaque-like structures up to micrometres in both length and width and these plaque-like structures composed of a series of aligned nanofibres. Once cooled to room temperature, these plaque-like structures collapse into aligned nanofiber bundles, namely the noddle like microfibers.

The self-assembly of a positively charged peptide can be triggered by a oppositely charged polymer to prepare a self-supporting bioactive membrane [154]. Natural polymer hyaluronic acid (HA), an anionic polysaccharide typically existed in the connective tissues of vertebrates, was selected to drive the self-assembly of positively charged multidomain peptide. After peptide ($K_2(QL)_6$) solution was mixed with hyaluronic acid solution with a final concentration of 2 Wt% (peptide :HA, 1:1), a membrane was obtained at the interface between the two solutions. The resulting co-assembled hybrid membranes exhibited a hierarchical structure and surface microtopographies with various GRD densities [154]. In addition, the order of the combination of the two solutions (HA over the peptide or vice-versa) changed the types of the obtained hybrid membranes. Furthermore, time and temperature of incubation after mixing were also able to vary the morphologies of the finally obtained hybrid membranes [154].

Microcapsule fabricated from self-assembly of diblock copolypeptide in aqueous solution has been reported [155]. The diblock copolypeptide was composed of a poly (L-lysine), hydrophilic domain and a poly (L-leucine), hydrophobic domain, and its lysine residues were modified with ethylene glycol to form a stable rod-like conformations inside water. Unlike the conventional amphiphilic diblock copolymers with the similar sequence which would be expected to form small or cylindrical micelles in aqueous solution, the present diblock copolypeptide was able to form a microcapsule with empty core in water solution [155]. Because both the lysine and leucine domains were able to adopt rod-like conformations due to that both leucine and ethylene glycol-modified lysine domain tend to form alpha-helix structure. As a result, a flat interface on hydrophobe association was formed in water, leading to tying together copolypeptide to supramolecular structure, microcapsule. Similarly, the Deming group synthesized another diblock copolypeptide with a sequence of $R_{60}L_{20}$, which can also form micrometer-sized vesicles in water [156]. These vesicles were able to encapsulate water-soluble materials and its stability was not compromised. In addition, these vesicles were stable in both aqueous phase and neutral zwitterionic or anionic lipid containing chloroform phase [156]. Both the empty vesicles and dextran-loaded vesicles have ability to transport from aqueous phase to lipid-containing chloroform phase due to the counterion binding to the arginine residues. The vesicles were able to transport back to aqueous phase by adding sulphate ions into aqueous phase because of the much stronger affinity of sulphate ions to guanidine residues than phospholipid headgroups [156].

Various viral particles have previously been used as building blocks to create functional materials for self-assembly [157-159] and tissue engineering [160, 161]. Lee group has used bacterial virus M13 phase, a virus with helical, nanofibrous shape and multiple function motifs, to create large-area film [148]. Three kinds of strucutres, nematic orthogonal twist, cholesteric helical ribbon and smectic helicoidal nanofilament, have been prepared by dipping in and pulling substrate out of suspensions of M13 phage particles in water. Two factors were critical to the helical self-templating assembly of M13 phage on the surface of substrate, that is, the local induction of chiral liquid-crystal phase transitions at the meniscus and the competing interfacial forces acting at the meniscus [148]. The morphologies of this phage-based film can be controlled from sub-micrometer-scale to micrometer-scale, and to centimeter-scale. The sub-micrometre-scale order was controlled by liquid crystal phase transitions and their chiral twist. The micrometer-scale order was controlled by geometric constraints (confined spaces and curved menisci) and by periodic modulation of material flux (phage concentration and pulling speed). The centimeter-scale order was controlled by meniscus movement [148].

Charlotte A. E. Hauser group has reported several ultra-small peptides with only several alanine residues as the hydrophobic tail and one charged residue as the hydrophilic tail. These small peptides could undergo self-assembly to form hydrogels with remarkable mechanical strength [162, 163]. The peptide hydrogel network formation is a sequential process of self-assembly and requires at least three steps. Step I: antiparallel pairing of two peptide

monomers and structural transition to alpha-helical conformation. Step II: assembly of peptide pairs to fibers and nanostructures. Step III: condensation of peptide fibers to fibrils [163].

Amino acids are available with D- and L-forms, but all natural proteins are made of only L-amino acids and nature can only use L-form amino acid. Therefore not surprisingly, most of peptide self-assembly system has been carried out using the naturally occurring L-form amino acid but D-form. As a matter of fact, peptides and proteins made of only D-amino acids are more stable since naturally occurring proteases cannot degrade D-form peptide bonds [164-166]. Zhang and colleagues have designed a variety of D-form peptide to self-assemble into functional materials. The D-peptide d-EAK16-II forms stable beta-sheets with the exact inverted CD spectrum as its L-form counterpart l-EAK16-II. Although both d-EAK16-II and l-EAK16-II can form well-ordered nanofibers, there is an apparent structural difference between them [164, 165]. D-EAK16-II fibers weave together to form a scaffold hydrogel with >99% water content. The scaffold hydrogel not only formed in PBS but also in the tissue cell culture media DMEM [165].

2.4. Negatively and positively thermoresponsive properties

Microstructures susceptible to environmental stimuli offer even greater versatility for encapsulation and controlled release, which can be controlled by changing temperature, pH, and other stimuli [132-134]. However, from a biomedical point of view, temperature change is a considerably valuable stimulus to trigger drug release due to its simple, effective, and safe natures. Thermoresponsive drug release system can be divided into two groups: Positive thermoresponsive release system releases drugs rapidly above a certain temperature and sustains release below this temperature. And negative thermoresponsive release system releases drugs rapidly below a certain temperature and sustains release above this temperature.

2.4.1. Negative thermoresponse

As of now, almost all of the thermoresponsive hydrogel system including macro/micro/nano hydrogel have been featured with negatively thermoresponsive property, that is lowering temperature triggers hydrogel swelling and network extension. As a result, pore channels will be formed inside hydrogel, through which active molecules can easily flow into or out of the hydrogel. So far, only a handful of thermoresponsive materials have been used to prepare hydrogel, among which poly(N-isopropylacrylamide) (poly-NIPAAm) and its derivatives are the most major material [167].

A negative thermoresponsive drug release system can rapidly release loaded drugs through pore channels formed below a certain temperature and cease release above this temperature as pore channels closed. According to the literatures, poly (N-isopropylacrylamide)(pNIPAAm) has been widely used to prepare negative thermoresponsive drug release hydrogel system. pNIPAAm exhibits a lower T_t at ~32 ℃, which is not concentration dependent [168]. The hydrophilic hydrogels comprised of pNIPAAm or its copolymers have been used for the controlled release of drugs. At high temperature (above T_t), pNIPAAm hydrogel shrinks and forms a dense skin layer at the gel surface. The skin layer prevents drug diffusion, leading to the creation of an on-off pulsatile drug release in response to temperature [169-171].

Besides pNIPAAm, some biodegradable polymers such as poly (lactic-co-glycolic acid) (PLGA) and poly(ethylene glycol) (PEG) also have been designed to be used as building blocks for thermoresponsive hydrogel [172, 173]. Triblock polymer PEG–PLGA–PEG triblock copolymer with a specific composition has been synthesized, which is a free flowing solution at room temperature but becomes a hydrogel at body temperature [172, 173]. The PEG-PLGA-PEG triblock copolymer form core/shell micelles with the hydrophilic PEGs as the outer shell and the hydrophobic PLGAs as the inner core when temperature increased. Above a critical gel concentration, the micelles pack together to occupy the entire volume, resulting in gel formation. But this formed gel is not stale enough and subject to dissolution upon dilution because low concentration can weaken the interaction forces between

micelles and dissociate the hydrogel network[173].

2.4.2. Positive thermoresponse

Opposite to negative thermoresponse, a negative thermoresponsive drug release system can rapidly release loaded drugs through pore channels formed above a certain temperature and cease release below this temperature as pore channels closed. Positive thermoresponse is also realizable for pNIPAAm polymer, but needs some additional processes such as coating pNIPAAm hydrogel with release-holes-containing membrane, grafting pNIPAAm hydrogel main chains with hydrophilic polymer(HEMA) [25], copolymerizing pNIPAAm hydrogel with other polymer [26], or putting pNIPAAm hydrogel into the holes of an inert membrane [27].

PNIPAAm oligomers were grafted onto a thermally nonresponsive polymer poly(hydroxyethyl methacrylate), pHEMA. P(HEMA-g-NIPAAm) hydrogels were fabricated by crosslinking the pHEMA network [25]. Based on the sharp transition and negative thermosensitivity of pNIPAAm grafted on the surface of pHEMA network, the thermosensitivity is switched to a positive response manner. At low temperature, the grafted NIPAAms expand and block the diffusion, while at high temperature, the collapsed NIPAAMs open mesh space for drug release [25]. Composite hydrogel films with positively thermoresponsive property have been prepared by blending chitosan, PEG and pNIPAAm [26]. Because the swelling ratio was reduced by the dehydration

nature of pNIPAAm inside the hydrogel film at high temperature. The blended swollen hydrogel film exhibited a more porous structure at high temperature, that is encapsulates can flow out of the hydrogel film much more easily through these pores at high temperature [26]. Positively responsive microcapsule with a novel composite membrane composed of poly (NIPAAm) hydrogel particles dispersed in a ethylcellulose shell has been reported [27]. The hydrogel particles dispersed inside the shell of microcapsule swell and inhibit water flow at low temperature, while shrink at high temperature and create channels inside shell for water flow. As a result, drug release a high temperature will accelerate [27].

Recently, Xia group has reported two new classes of thermoresponsive materiales for positively thermoresponsive system: fatty alcohols and fatty acids [23]. A variety of colloidal particles containing drugs were encapsulated in the thermoresponsive 1-tetradecanol block matrix. The particles serve as a diffusive barrier for controlling the release kinetic of the drugs while the 1-tetradecanol block matrix serves as a thermoresponsive container of the particles [23]. Three major steps were involved in the release of encapsulated drugs: melting of 1-tetradecanol by increasing temperature, leaching out of drug containing microparticles, and release of drugs as microparticles dissolved [23].

III. Materials and Method

3.1. Synthesis and characterization of elastin-like polypeptides

3.1.1. ELP gene synthesis, expression and purification

The ELP gene $[(VPGVG)_{14}(VPGKG)]_8[VPGVG]_{40}$ was oligomerized inside pGEM-T easy vector (Promega, USA) by recursive directional ligation method and then transformed into JM-109 cells (Promega, USA) for replication. The colonies of the transformed cells were screened by blue-white screening through spreading cells on LB agar plates supplemented with ampicillin and X-gal. The plasmids from cultured cells were purified using a plasmid prep kit (SolGent, Korea).

To prepare ELP gene-containing expression plasmid, the above purified replication plasmid with ELP gene was digested with restriction enzymes, with *PflM* I (Takara, Japan) and *Bgl* I (Takara, Japan), and then inserted into a modified pET-32b vector (Novagen Inc., USA), pET-32b-*Sfi* I, which was prepared by inserting *Sfi* I cassette (Takara, Japan) into the normal pET-32b vector with the help of the restriction enzymes, *Xba* I (Takara, Japan) and *EcoR* I (Takara, Japan). Digesting with *Sfi* I made pET-32b-*Sfi* I able to conjugate with ELP gene which was separated from replication vector through digesting with *PflM* I and *Bgl* I. And then ELP gene-containing expression vectors were transformed into *E. coli* strain $BLR(DE)_3$ (Novagen) for expression.

BLR(DE3) cells transformed with ELP expression vectors were firstly inoculated into 50 mL of CircleGrow medium (Q-biogene, USA) supplemented with 100 μg/mL ampicillin and incubated for 12 h at 37 ^{o}C with shaking (150 rpm). After the preculture, the cells were restored with centrifuge at a speed of 2000 rm for 2 min. And then, the cells were again re-inoculated into the main culture media and incubated for 2 days at 37 ^{o}C with shaking (220 rpm). The main culture was carried out in 2 L flasks containing 500 mL of CircleGrow medium supplemented with 100 μ g/mL ampicillin.

After culture, the ELPs were purified by a method named inverse transition cycling (ITC). The cultured cells were restored with centrifuge with a speed of 4,000 rpm for 10 min at 4^{o}C and resuspended in phosphate buffer silane (PBS : 137 mM NaCl, 2.7 mM KCl, 4.2 mM Na_2HPO_4, 1.4 mM KH_2PO_4, pH 7.3), and then deep frozen at -70 ^{o}C. To lyse cells, the cells were rapidly thawed and sonicated in ice for 4min. The cell lysate was centrifugated at 12,000 rpm for 10 min at 4 ^{o}C to remove cell debris. The solution was centrifuged at 12,000 rpm for 10min at 4^{o}C after polyethyleneimine (0.5 % final concentration, w/v) was added into supernatant to settle nucleic acids down. And then ELPs inside the final supernatant was purified by ITC method. The ELPs were aggregated by adding NaCl and centrifugated at 12,000 rpm for 10 min at 40 ^{o}C to remove impurities like soluble proteins and remained nucleic acids. The ELP pellet was resuspended in PBS at 4 ^{o}C and centrifugated at 12,000 rpm for 10 min at 4 ^{o}C to remove insoluble contaminants. These ITC circle was repeated by 5 times and ELPs with high

purity were obtained.

3.1.2. Gene size and molecular weight determination

The ELP gene size was determined by 1% agarose gel electrophoresis. Molecular weight of the expressed ELP was determined by SDS-polyacrylamide gel electrophoresis (SDS-PAGE). The SDS-PAGE analysis used 15% acrylamide gel with a discontinuous buffer system. The 20 μL of ELP solution was mixed with 20 μL of loading buffer (20 % SDS, 10 % 2-merchptoethanol) cooled for 10 min at 4 ^{o}C, and electrophorized in polyacrylamide gel slabs. SDS-PAGE gels were visualized by a silver staining.

3.1.3. Determination of transition temperature by UV-visible spectroscopy

To determine the T_t of ELP and TOBC/ELP solution, the OD350 was monitored by using UV-visible spectrophotometer equipped with a water circulating temperature controller (Mecasys, South Korea). The samples were heated at a rate of 1 ^{o}C/min. The inverse phase transition temperature was determined as the temperature at which the turbidity of the ELP solution was 50% of its maximum.

3.1.4. Secondary structure analysis by circular dichroism (CD)

ELP secondary structure was determined by circular dischroism (CD) (Applied photophysics, UK) at different temperatures. ELP (0.5 mg/mL) solutions were prepared for CD analysis.

3.1.5. Tertiary structure analysis by fluorescence measurement

Fluorescence emission/excitation spectra were recorded by FP-8300 spectrofluorometer (Jasco, Japan). To determine the maximum excitation spectrum, ELP solution with a concentration of 0.25 mg/mL was scanned in the range of 200 nm to 500 nm, and emission spectra were recorded in the range of 220 to 750 nm. At given temperatures (10 ^{o}C) with the excitation wavelength set to 270 nm, the emissions of samples were recorded in the range of 280 to 450 nm.

3.2. ELP microcapsule prepared by water in oil emulsion

3.2.1. Microcapsule prepared by top-down method at low temperature

3.2.1.1. Preparation of microcapsules

The ELP/BSA microgel capsules (MCs) were prepared by water in oil (w/o) emulsion method with a minor modification reported by Wei et al.(Figure 3).[174] All the following processes were finished at 4℃. Firstly, 60 mg of freeze-dried ELP and BSA with different mass ratios (MC_e, 1:0; MC_1, 3:1; MC_2, 2:1; MC_3,1:1; MC_a,0:1) were dissolved in 450 μL PBS at 4 °C (Table 1), and this mixture was used as water phase. Next, this mixture was added drop-wise into oil phase, which was composed of 15 mL petroleum ether and 10mL cotton seed oil and pre-cooled to 4 ℃. And then this water/oil mixture was emulsified by magnetic stirring. After 10 min of emulsion, 100 μL of ρ-phthalaldehyde solutions (200mg mL^{-1} in DMSO) were added to crosslink the macroemulsions. After 2 h of continuing stirring, another 20 mL petroleum ether and 5 mL cotton seed oil were added into the solution followed by addition of 100 μL glutaraldehyde (25% aqueous solution). Glutaraldehyde crosslinking times were various with the ratios of ELP to BSA. Finally, crosslinked microspheres were rinsed twice with petroleum ether to remove cotton seed oil and the residual of crosslinkers. Subsequently, microspheres were washed using acetone and ethanol with forcefully shaking to destroy ρ-phthalaldehyde/ELP crosslinking, tansforming the microspheres

into MCs. Finally, the MCs were collected by centrifuge and redispersed into ethanol until use.

3.2.1.2. Characterization of microcapsules

Temperature triggered swelling-deswelling changes of MCs were observed by optical microscope. CLSM images of MCs in PBS solution were acquired using LSM510 (Carl Zeiss, Germany). All MCs were excited at 488 nm, fluorescent images were obtained at 510-540 nm (green). The relative fluorescence intensity was calculated automatically by using LSM image browser. MCs were sectioned with a cryotome HM 505 E (Microm, Germany) with a blade step setting at 50 μm.SEM images were taken with SUPRA 55VP Field-Emission Scanning Electron Microscope (Carl Zeiss, Germany). To observe the shape and surface morphology, intact and cross-sectioned MCs were immersed in deionized distilled water with 20 ℃ and 40 ℃ until equilibrium swelling state achieved and dipped into liquid nitrogen followed by freeze-drying. Freeze-dried intact and cross-sectioned MCs were coated by gold sputter prior to observation.

3.2.1.3. Temperature-dependent permeability to rhodamine b, FITC, and BSA

To confirm the thermoresponsive controlled release function, MC_1s were

loaded with rhodamine B (Aldrich) at 20 and 40 ℃. Equal amounts of MC_1s and molecules (rhodamine B, FITC or BSA-Rho) PBS solutions (1 mg mL^{-1}) were mixed together and stored at corresponding temperatures for 20 h, and this was followed by two more hours at 4 ℃, leading to pore closure. Subsequently, the molecules-loaded MC1s were washed three times with PBS at 4 ℃, and were then dispersed in PBS and directly observed by CLSM. To verify the thermoresponsive release, molecules-loaded MC1s in PBS at 20 ℃ were incubated at 40 ℃ for 20 h and imaged by CLSM. For both loading and releasing tests, the fluorescence excitation was performed at 543,495 and 543nm and fluorescent images were obtained at 650-800, 519 and 633 nm for rhodamine b, FITC and BSA-Rho, respectively.

Molecules release efficiency was calculated by using the following expressions:

Molecules release (%) = $(I_b\text{-}I_a/I_b) \times 100$

Where I_b and I_a are the fluorescence intensities of before and after release, respectively.

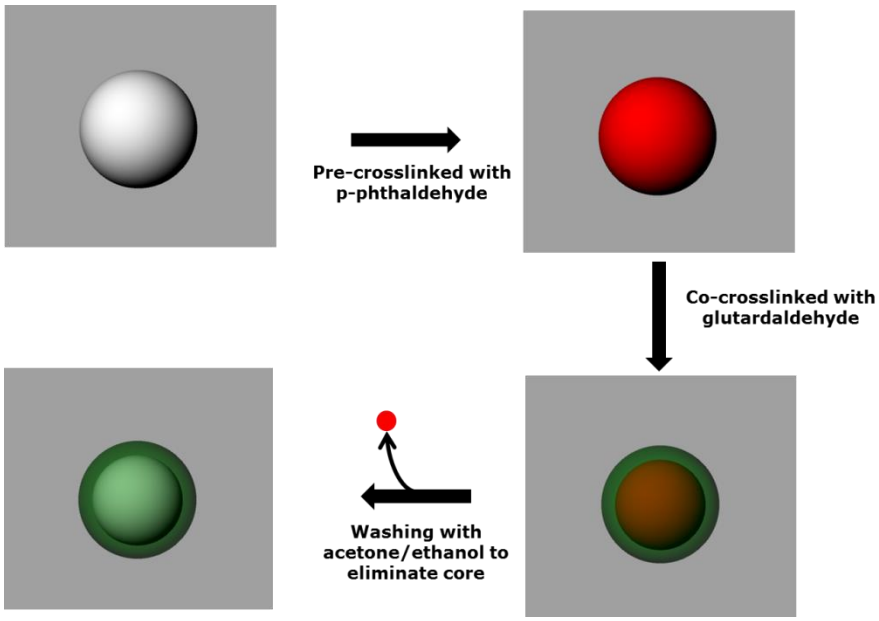

Figure 3. Schematic illustration of the preparation of ELPs microcapsule

Table 1. Composition of microcapsules (MCs)

Sample ID	ELP (mg)	Albumin (mg)	PBS (μL)
MC_e	60	--	450
MC_1	45	15	450
MC_2	40	20	450
MC_3	30	30	450
MC_a	--	60	450

3.2.2. Microstructure prepared by one step method at various temperatures

3.2.2.1. Thermal characterization of the ELP

To characterize the T_t of ELP, the optical density (OD350nm) of an ELP solution (PBS, 30 mg/ 225 μL) was monitored relative to temperature using a Cary 100 Bio UV-visible spectrophotometer (Varian) equipped with a temperature controller. To characterize the phase separation properties of the ELP, the particles' hydrodynamic diameters were determined using dynamic light scattering (DLS) (Zetasizer Nano, Malvern) as related to temperature.

3.2.2.2. Observation of the ELP phase separation inside an emulsion droplet

Firstly, ELPs were conjugated with Rhodamin B isothiocyanate (ELP-Rho) and purified with an inverse transition cycling method and subsequent freeze-drying. Next, 30 mg ELP-Rho was dissolved in 225 μL PBS at 4 ℃. The ELP-Rho solution was dispersed in an oil phase composed of 25 mL petroleum ether and 25 mL cotton seed oil at 4 ℃. The emulsion containing ELP-Rho was observed using fluorescence microscopy (Olympus, Japan).

3.2.2.3. Preparation of the crosslinked microstructures

ELP microstructures were prepared by water-in-oil emulsion method. Firstly, 30 mg freeze-dried ELPs were dissolved in 225 μL PBS at 4 °C. Subsequently, this solution was added dropwise to an oil phase composed of 25 mL petroleum ether and 25 mL cottonseed oil at 4℃. After magnetically stirring the emulsion for 1 h at various temperatures (4, 30 and 45 °C), 50 μL glutaraldehyde (25% aqueous solution) was added to the emulsion to crosslink microstructures. The crosslinked microstructures were rinsed with petroleum ether, acetone and ethanol (in the listed order) to remove any cottonseed oil or residual crosslinkers; the material was collected by centrifugation and redispersed in ethanol for storage. The steps were finished in a thermostatic chamber.

3.2.2.4. Characterization of the ELP microstructures

CLSM images of samples in deionized water (DW) solution were acquired using LSM510 (Carl Zeiss, Germany). All samples were excited at 488 nm, and the fluorescent images were obtained at 510-540 nm (green). The epi-fluorescent images were also acquired using fluorescence microscopy (Olympus, Japan). High-resolution morphological images were obtained with a SUPRA 55VP field-emission scanning electron microscope (FE-SEM Carl Zeiss, Germany). To observe the shape and surface morphology, the samples were immersed in DW at various temperatures until an equilibrium swelling state was reached; the particles were immediately dipped into liquid nitrogen

and freeze-dried. Freeze-dried ELP samples were coated with sputtered gold before observation. The ELP localization at the interface was modeled using a hydrophobically modified gold surface. First, 5 μM ELP solution was incubated with a hydrophobically modified gold surface for 1, 5, 10 and 30 min at 45 ℃. After incubation, the surface was rinsed gently with DI water and placed on the AFM imaging stage. The topographical AFM images were collected in tapping mode using silicon nitride cantilevers (DNP-S, Bruker, 0.35 N/m nominal spring constant; 65 kHz nominal resonant frequency) with Multimode (Bruker, Santa Barbara, USA) in liquid. The best images were obtained using 1 Hz scan rates. AFM images were obtained at a resolution of 512×512 pixels.

3.3. ELP microbead prepared in water solution

3.3.1. Transition temperature determination

To determine the T_t of ELP, the OD350 of ELP PBS solution was monitored with a Cary 100 Bio UV-visible spectrophotometer equipped with a temperature controller (Varian). ELP secondary structure was determined by circular dischroism (CD) (Applied photophysics).

3.3.2. ELP microbead preparation

Freeze-dried ELPs (10,5,2.5,1,and 0.5 mg) were dissolved in 1ml PBS (pH 7.4) at 4 ℃, and then increasing the ambient temperature to 40 ℃ induced the ELPs phased separation and further coacervating into microbead, and finally crosslinked these microbead with glutaraldehyde aqueous solution (Sigma, Germany).

3.3.3. ELP microbead characterization

Effect of initial ELP concentrations on the size of resulting microbeads were determined by Confocal laser scanning microscopy (CLSM) (LSM 510,Carl Zeiss, Germany). The mean size of ELP microbeads were determined by randomly measuring 30 particles in CLSM images.

Temperature-triggered swelling and deswelling changes of ELP microbeads were observed by optical microscope.

Scanning electron microscope (SEM) images were taken with a SUPRA 55VP field-emission scanning electron microscope (Carl Zeiss, Germany). To observe the shape and surface morphology, ELP microbeads were immersed in deionized distilled water at temperatures of 4 and 37 ℃ until equilibrium swelling states were achieved and then dipped into liquid nitrogen and freeze dried. Freeze-dried microbeads were coated by gold sputter prior to observation.

IV. Results and Discussion

4.1. Synthesis and characterization of elastin-like polypeptides

4.1.1. Molecular weight characterization of ELP molecule

The present ELP was made up of a lysine-containing domain and lysine-lacking domain (Figure 4a). To confirm the size of ELP gene, the pET-sfi ELPs were extracted from JM-109 cells by plasmid miniprep kit and digested by restriction enzymes of Nde I and EcoR I. And further verified by DNA agarose gel electrophoresis. Figure 4b shows the ELP gene size is consistent with the expected size, 2400bp.

For expression, ELP gene inside expression vector (pET-sfi) was transformed into BLR(DE3) cells. After culture at 37 ^{o}C with continuous shaking, the transformed cells were restored by centrifugation at 4 ^{o}C and lysed by sonication. ELP was purified by inverse transition cycling (ITC) from total protein and other impurities. The purity and molecular weight were confirmed by SDS-PAGE with Commassie brilliant blue stain. After purification by ITC method, pure ELP with high purity was obtained and the molecular weight was consistent with the expected value determined by amino acid sequence, 85kDa (Figure 4c).

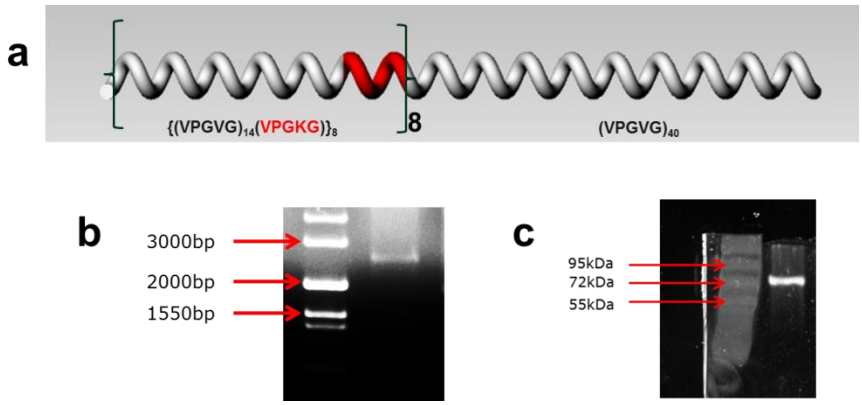

Figure 4. (a) Schematic representation of the ELP chain. (b) One percent agarose gel electrophoresis of ELP gene. (c) Fifteen percent SDS-PAGE of ELP purified by inverse transition cycling method.

4.1.2. Thermoresponsive characterization of ELP molecule

ELP is a thermoresponsive polypeptide, which undergoes reversible inverse phase transition through a characteristic temperature (T_t). ELP molecules are wrapped with water molecules by hydrophobic hydration below T_t, where water molecules are oriented at the surface of ELP molecules and take a very ordered structure. Hydrophobic hydration has the thermodynamic properties of decreased enthalpy and decreased enthalpy relative to bulk water. However the hydrophobic hydration can be interrupted by raising environmental temperature above T_t, the oriented water molecules become disordered bulk water amid intramolecular hydrophobic attraction between side groups of the ELP. This temperature triggered phase separation is a discrete process, which can be identified by the optical density at 350nm (OD350nm). The change in turbidity of ELP solution with a concentration of 200 μM as a function of temperature was measured with thermo-regulated UV/vis spectrometer at 350nm and the temperature was increased at a rate of 1 ^{o}C/min. Upon heating, the transition from transparent to turbid solution was rapidly finished within ~2 ^{o}C around 37 ^{o}C (Figure 5). Intuitively, temperature-triggered aggregation of ELPs resulted in transition of ELP solution from a transparent liquid to a turbid solution (Figure 6). Firstly, hydrophobic domains exposed outwardly via temperature-triggered collapse of ELP molecule. And then, ELP molecules aggregated with neighboring molecules through hydrophobic interactions between the exposed hydrophobic side groups to form colloidal particles, leading to the transition

to a turbid state. And, the solution can turn back to transparent as temperature decreased below T_t. Although, ELP molecules aggregated together via hydrophobic interactions to form colloidal particles, a number of water was still embedded inside these colloidal particles. And because of the unique primary sequence, the formation of intramolecular hydrogen bonding is unusual even at its collapse state. As a result, the temperature-triggered phase transition is entirely reversible.

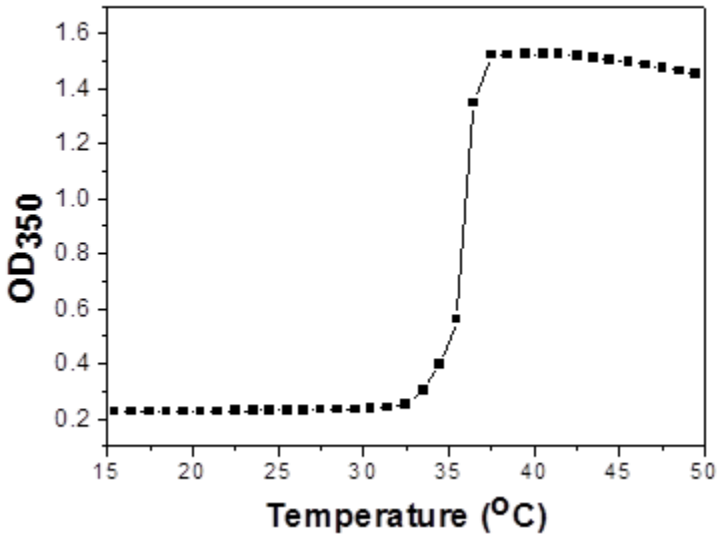

Figure 5. Turbidity profile of ELP at a concentration of 200 µM in PBS.

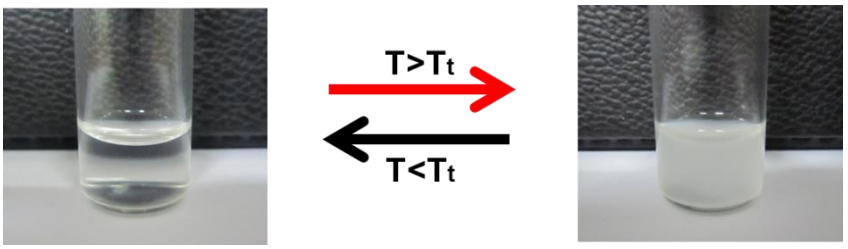

Figure 6. Photographs of temperature-related inverse phase transition of ELP

4.1.3. Structural characterization of ELP molecule

Temperature triggered folding of ELP molecules always involves changes in secondary and tertiary structure. At low temperature (below T_t), all ELP chains existed in a disordered way (random coil), once the temperature increased above T_t, ELP chains started to fold and took an ordered strucrture(β-turn/β-spiral). This change in secondary structure transition was determined by CD spectra. As shown in Figure 7, two main peaks (a band at ～198 nm and a band at ～212 nm) were clearly observed. According to literatures, the band at ~198 nm assigns to random coil structure and the band at ~212 nm should arise from type Ⅱ β–turn/β-spiral structure [30, 46, 58]. The band at 198 nm decreased in intensity and approached to zero whereas the characteristic band of type II β-turn was positively shifted as temperature increased (Figure 7).

The tertiary structure of ELP was further tracked down using fluorescence spectroscopy. Although the present ELP had only one tryptophan residue (w) at its carboxyl-terminus, the fluorescence derived from the tryptophan residue was still detectable as shown in Figure 8, leading to a maximum excitation and emission wavelength at 270 nm and 345 nm, respectively. As a result, the tertiary structure of ELP was able to be analyzed using fluorescence spectroscopy.

The typical fluorescence spectra for ELP aqueous solutions as a function of temperature were shown in Figure 9, respectively. All samples were excited

at the excitation wavelength of 270 nm to detect the ELP conformational changes along with temperature. The fluorescence intensities decreased with increasing temperature (Figure 9). The change in fluorescence intensity is usually coincident with protein unfolding. Generally, the fluorescence quantum yield of tryptophan decreases with its exposure to solvent [175, 176]. The fluorescence quenching as temperature increases was possibly due to the rearrangement of the tryptophan surroundings. In another word, the exposure of tryptophan residues to water was increased with temperature, leading to fluorescence quenching. In addition, because the tryptophan residue was located at the carboxyl-terminus where there were no positively charged lysine residues. Considering its extremely hydrophobic nature, the tryptophan residue was used to be wrapped and protected by the other ELP amino acid residues from water contacting inside pure ELP water solution at a lower temperature than T_t. While, as ELP molecule folded into beta-turn, a rigid spring-like structure, the tryptophan residue exposed to contacting with water, leading to fluorescence quenching as shown in Figure 9.

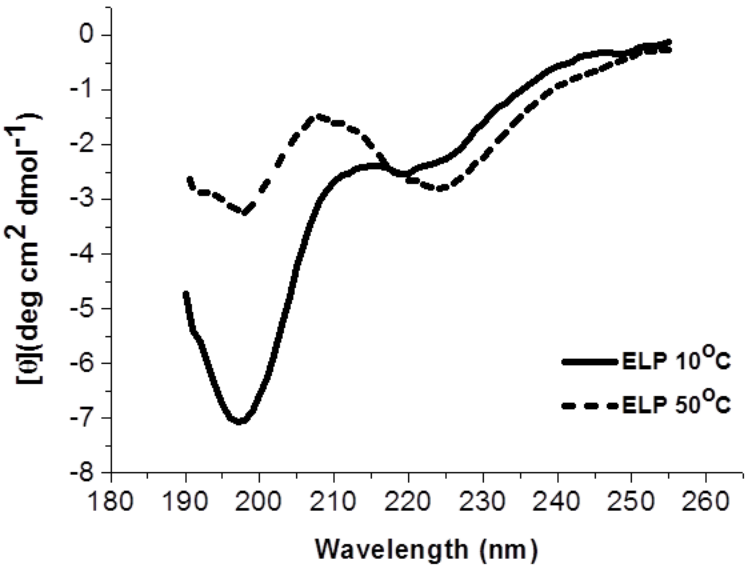

Figure 7. CD spectra of ELP taken at different temperatures in water with a concentration of ELP (c=0.5 mg/mL).

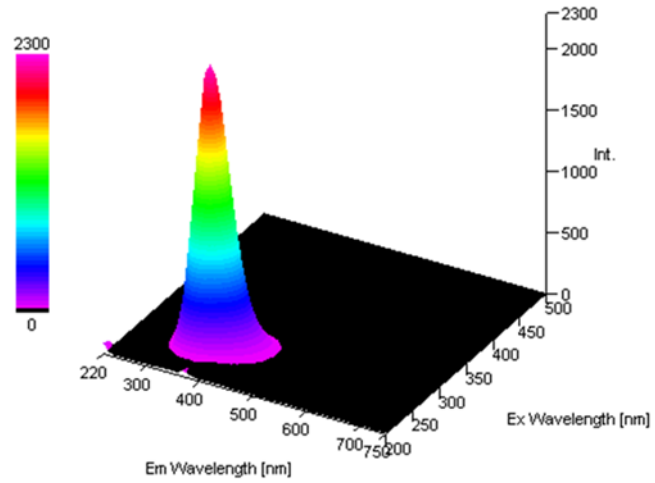

Figure 8. Fluorescence map of ELP aqueous solution.

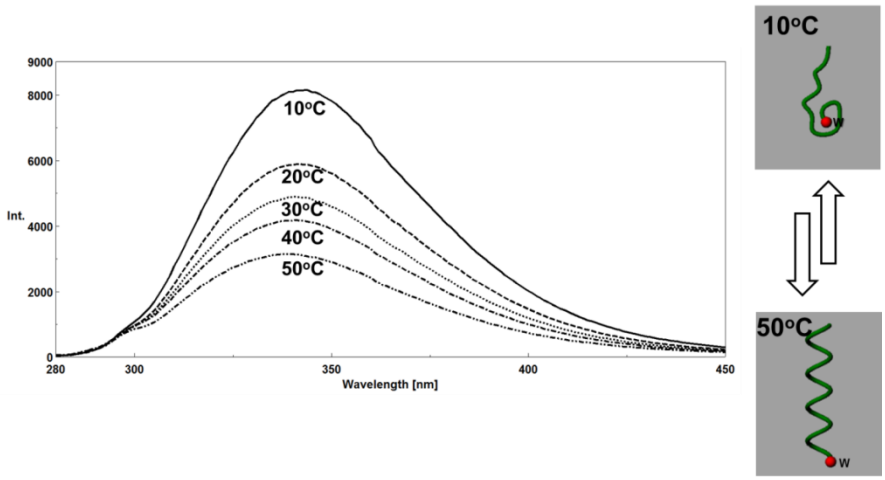

Figure 9. The fluorescence intensities of ELP water solution as a function of temperature. The excitation wavelength was 270 nm.

4.2. ELP microcapsule prepared by water in oil emulsion

4.2.1. Microcapsule prepared by two-step method at low temperature in water/oil emulsion

4.2.1.1. Preparation of ELP microcapsules

A series of polypeptide MCs were fabricated using a little modification of two-step cross-linking w/o emulsion method reported by wei et.al. In the presence of acetone and ehtanol, the instability of ρ-phthaldehyde and the stability of glutardaldehyde based Schiff bases ensure the successful preparation of microcapsules. Five different types of MCs, which consist of different ELP to BSA mass ratios (MCe,1:0;MC1,3:1; MC2,2:1;MC3,1:1;MCa,0:1), were prepared. The obvious core-shell structures of MC_1 can even be observed by optical microscope (Figure 10a) and were further confirmed by confocal laser scanning microscopy (CLSM) (Figure 10b). Due to the n-π^* transitions of C=N bonds in the Schiff bases formed during crosslinking reaction, these MCs show autofluorescent properties. The strong signal contrast between center and edge indicated that the polypeptide MC_1 were successfully fabricated (Figure 10c). The present method is based on the replacement of ρ-phthaldehyde with glutaraldehyde. Although the glutaraldehyde can crosslink primary amine groups very quickly, because of the existence of ρ-phthaldehyde based first crosslinking, the crosslinking based on glutardaldehyde has been delayed. As a result, the shell thickness can be easily adjusted by changing the glutaraldehyde crosslinking

time. In the case of glutaraldehyde crosslinking time of 30min, a very thin shell has been formed (Figure 11a). As crosslinking time increased, the shell thickness increased gradually. And when crosslinking time extended to 4h, the empty core disappeared and microbead was obtained (Figure 11). Step wise increasing glutaraldehyde crosslinking time led to a gradual growth of the shell thickness of MC1 from about 10 μm for glutaraldehyde crosslinking time of 30 min to about 80 μm for 3h (Figure 12). The overall preparation processes were performed at 4 ℃, at which temperature ELP chains are hydrophilic; therefore, the final shell of each capsule was composed of cross-linked hydrophilic ELP chains, meaning that the shell of the capsule thus obtained was a hydrogel.

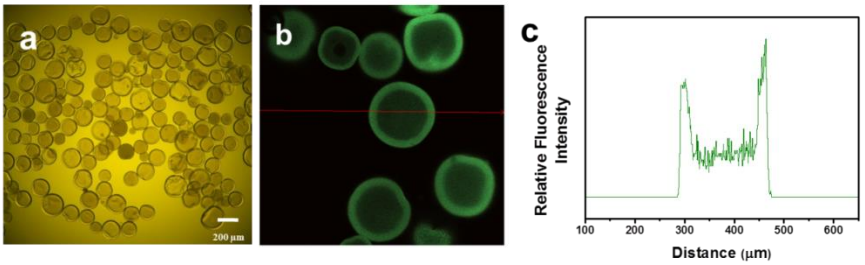

Figure 10. Optical microscopic image (a), CLSM image (b) and relative fluorescence intensity (c) of hollow microcapsules MC_1.

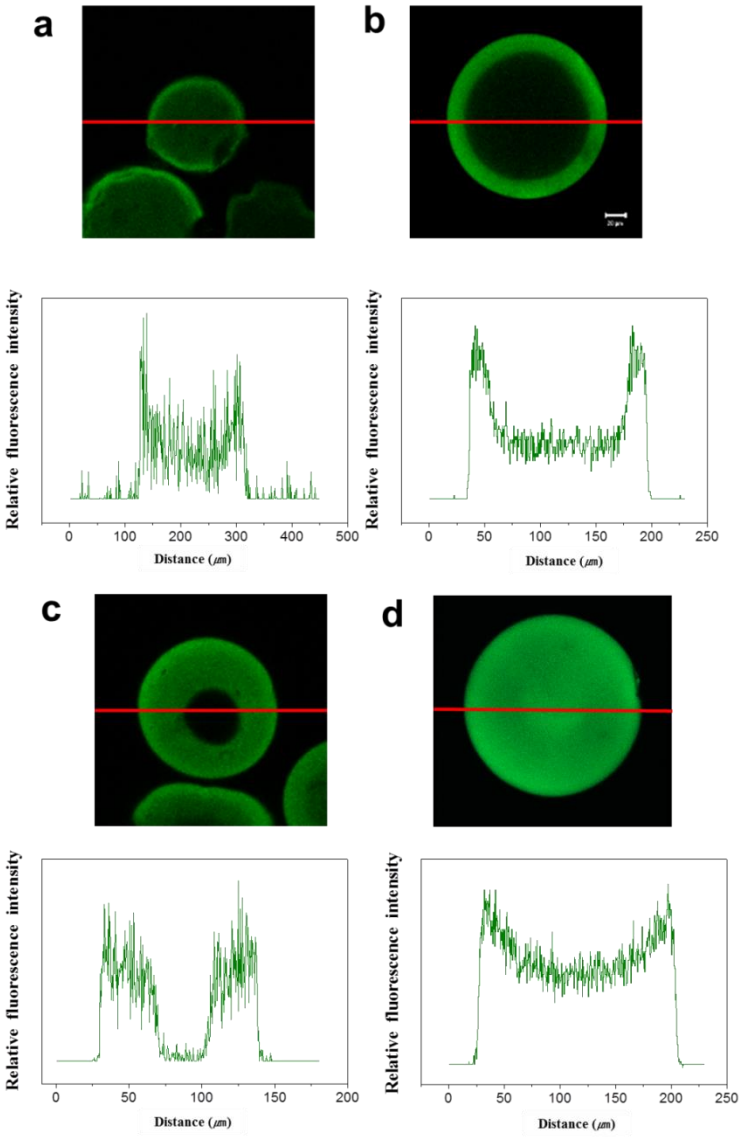

Figure 11. CLSM images and relative fluorescence intensity curves of MC_1 prepared with various glutaraldehyde cross-linking time. (a) 30 min (b) 1 h 30 min (c) 3 h (d) 4 h.

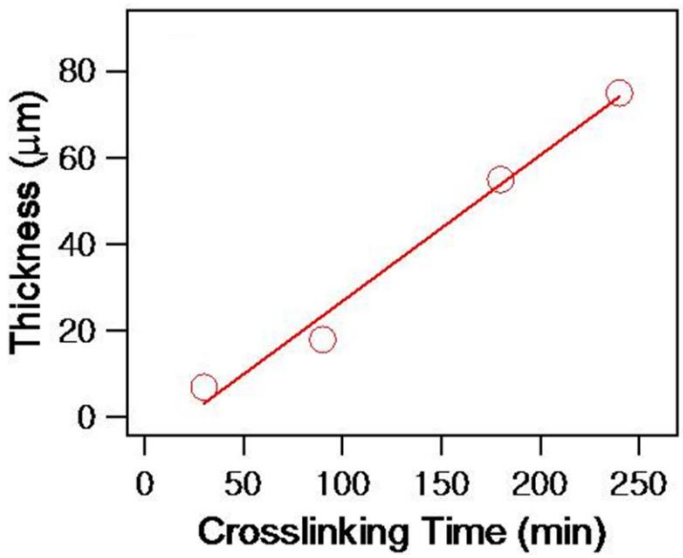

Figure 12. A gradient growth of the wall thickness of MC_1 was an expected consequence of the increased glutaraldehyde cross-linking time.

4.2.1.2. Thermoresponsive properties of ELP microcapsules

The inherent thermoresponsive nature of ELPs imbues these MCs with thermoresponsive characteristics. The diameter of MCs was monitored with optical microscopy in the temperature range from 10 ℃ to 50 ℃ (Figure 13). The rapid change of MCs diameter was observed at 35 ^{o}C, which is a lower value compared with T_t of ELP molecules (T_t=37 ^{o}C) used in the experiment probably due to the crosslinked hybrid structures. When incubated alternatively below T_t (20 ℃) and above T_t (40 ℃), MC_1 showed rapidly repetitive volume changes, which led to the formation and closure of pore windows at the surface of MC_1, and the swelling-deswelling transition occurred in just a few seconds. The thermally responsive volume changes decreased when the ratio of ELP to BSA decreased. Because of the inherent thermally insensitive property of BSA, MC_a exhibited no volume change, nor was the corresponding formation of pore windows observed.

As the BSA component increased, fewer pores were observed at the surfaces of the MCs (Figure 14). As the ratio of ELP to BSA decreased to 1:1, surface pores were no longer visible at temperatures above T_t although slight thermoresponsive volume changes could be observed. Although incorporating BSA will decrease the number of thermally responsive pores, properly added BSA could lead to more integral pores. Above T_t, the pure ELP-based MCs, MCe, showed relatively small and non-integral pores on their surfaces whereas MC_1 showed relatively integral surface pores (Figure 14).

Below T_t, both the surface and interior shell of MC_1 were filled with disordered ELP chains and exhibited no pores (Figure 15a-c). However, once the environmental temperature was higher than T_t, all of the ELP chains underwent a conformational change from a disordered structure that is mainly random coil, to a relatively ordered structure that is β-turn rich, leading to the shrinking and pore formation in the MC_1 (Figure 15d-f). Incorporating BSA into ELP-based MCs not only controls the thermally responsive changes in volume, but also the pore morphologies of the MCs.

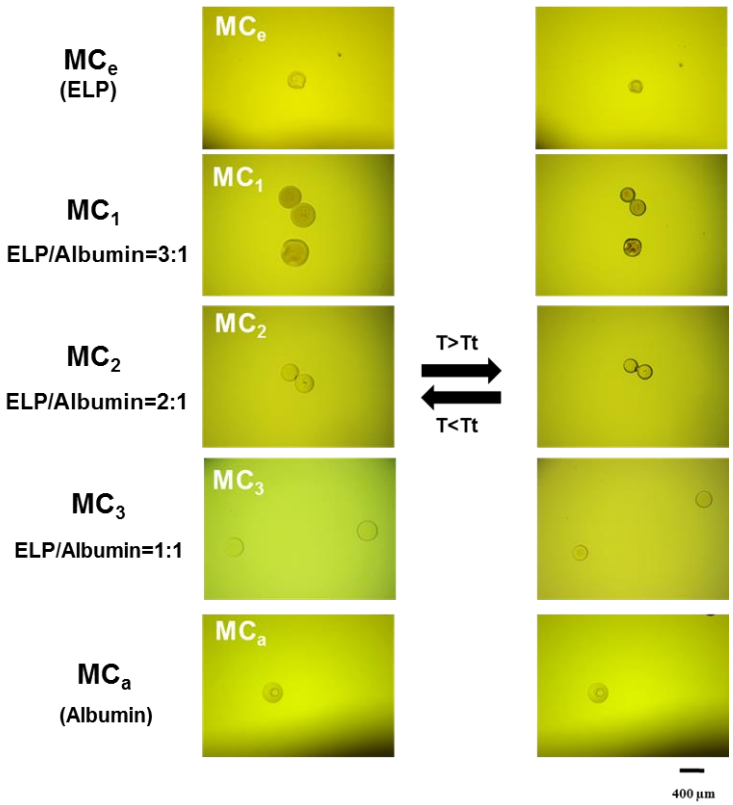

Figure 13. The thermally responsive volume changes decreased with decreasing of the ratio of ELP to BSA, the mass ratios of ELP to BSA are MC_e,1:0;MC_1,3:1; MC_2,2:1;MC_3,1:1;MC_a,0:1, respectively. (Scale bar, 400 μm).

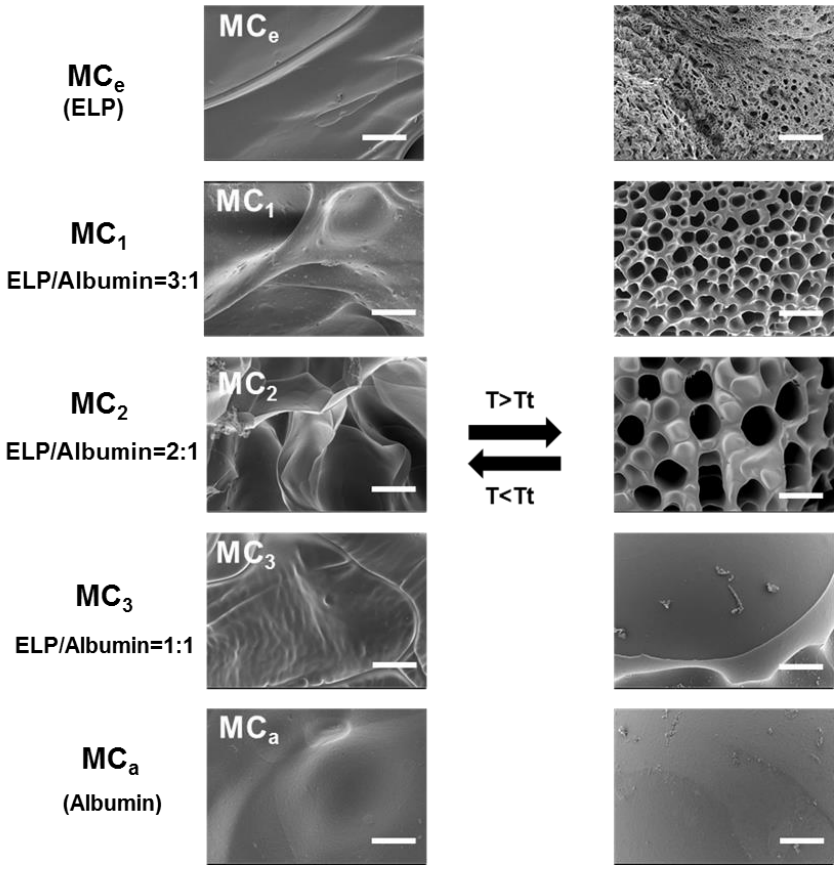

Figure 14. FE-SEM images of the surface morphology of MCs below and above T_t, the mass ratios of ELP to BSA are MC_e,1:0; MC_1,3:1; MC_2,2:1; MC_3,1:1; MC_a,0:1, respectively. (Scale bars, 6 ㎛).

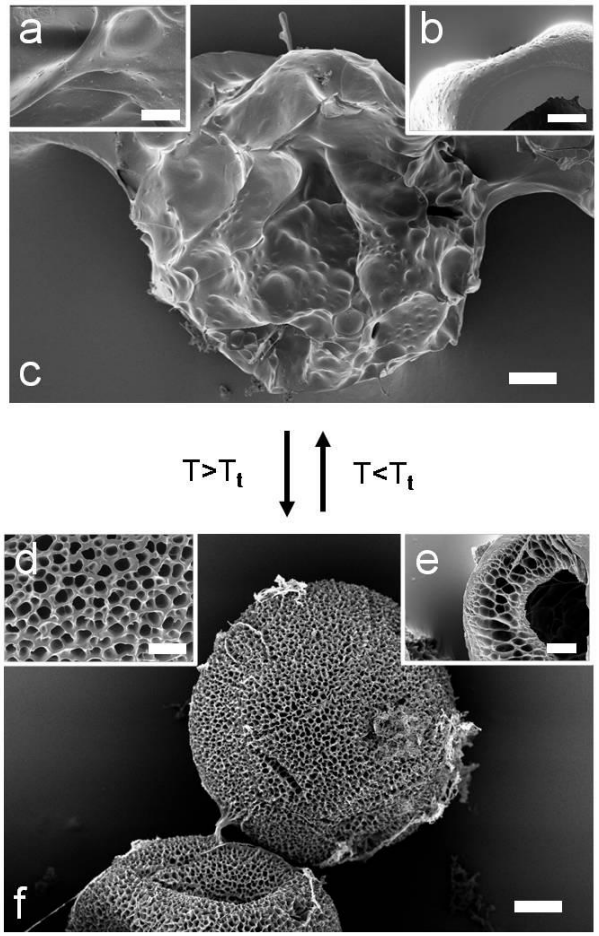

Figure 15. FE-SEM micrographs of MC_1 below (a, b, c) and above (d, e, f) transition temperature T_t. (a, d) High magnification micrographs of the surface of MC_1. (b, e) The shell internal structure of MC_1. (c, f) Overall MC_1. All scale bars denote 10 μm.

4.2.1.3. The role of BSA in control of pore morphology

To address both the character of BSA in the present capsule system and the formation mechanism of temperature responsive “pore windows”, BSAs with a Rhodamine label (molecular probe) were blended with ELPs and microcapsules have been prepared. .

The pore morphology of the MCs depends on the distribution of BSA at the oil-water interfaces in the process of emulsion. Because the interface between the phase-separated regions of the film is at a higher free energy, proteins exhibit a high propensity to migrate and bind to oil-water interfaces and decrease the interfacial tensions. BSA and ELP in the aqueous phase also migrate to the oil-water interface and rearrange and separate into regions rich in either of the species during aging of the layer (Figure 16). ELP is a disordered type polypeptide (hydrophilic) whereas BSA is a typical globular protein (hydrophobic) at the temperature below T_t. The two distinctly different groups of materials migrate to oil-water interfaces with different affinity and show, as a result, a phase separation. At the mass ratio of 9:1 (ELP:BSA), ELP-rich phase formed the continuous phase (black colored region) of the film while the BSA-rich phase existed as segregated clusters dispersed in the continuous phase (Figure 16a). At the ratio of 3:1, numerous dispersed BSA-rich clusters appeared and were closely packed forming a space inside, which was supposed to be ELP-rich regions of the continuous phase (Figure 16). At the higher fraction of BSA (1:1), it was expected that BSA would form a continuous phase with ELP clusters dispersed in the mixed layer but

hydrophilic ELP didn't aggregate at the temperature below Tt. Instead, tiny dispersed BSA-rich clusters were formed and filled the space of the layer meaning BSA was a majority on the surface and ELP migrated into the bulk (Figure 16).

The key factor to determine whether or not the two proteins in solution will separate into two phases is the free energy of mixing [177, 178]. In terms of Gibb's free energy of mixing: complete miscibility of two proteins requires the Gibb's free energy should be always negative, if it is positive the two-protein mixing system will have a tendency to separate into two phases.

$$\Delta G_{mix} = \Delta H_{mix} - T\Delta S_{mix} < 0$$

Where ΔG_{mix}, ΔH_{mix} ,ΔS_{mix}, and T are the Gibb's free energy, the enthalpy,the entropy and the mixing temperature, respectively.

The approximation of the free energy of polymers binary mixing system is known as the Flory-Huggins free energy. And the Flory-Huggins equation can be written in the following form [177].

$$\Delta G_{mix} = RT(\Phi A \ln \Phi A / r1 + \Phi B \ln \Phi B / r2 + X\, \Phi A \Phi B)$$

Where Φi is the volume fraction of the two component(A,B), ri is the Flory-Huggins number of the protein segments, R is the gas constant, and X is the Flory-Huggins binary interaction parameter. And the critical value of the interaction parameter, Xc, separates the situation whether the mixtures at all compositions are stable or not. In other words, if the value of X is less than

the critical value Xc and the binary mixing system will stable at all compositions, otherwise the binary mixing system will separate into two phase. Generally, for big molecules(polymers and proteins), the value of Xc that can be tolerated before phase separation happens is very smaller than for small molecules, this is why very few pairs of polymers with a large degree of polymerization can form single phase mixture. As mentioned above, being big molecules ELP and BSA will undergo phase separation after mixing. That is the reason why BSA molecules aggregated together to clusters which were dispersed inside ELP bulks (Figure 16).

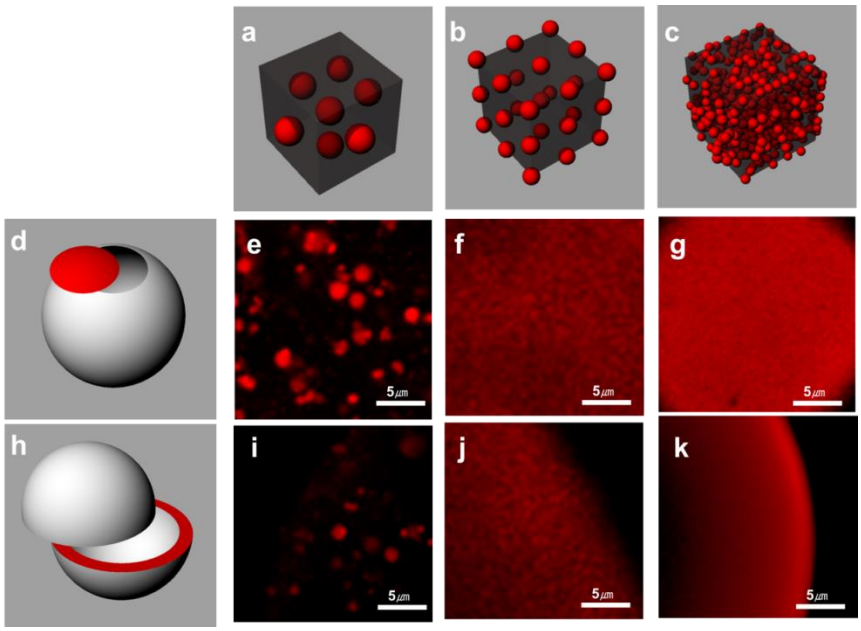

Figure 16. **(a, b, c, d, h) Schemes to explain the character of BSA, red and black represent BSAs and ELPs, respectively. (e, f, g, i, j, k) CLSM images of the surface and interior of the microcapsule. (e, f, g) Dispersion morphologies of BSAs on the surface of microcapsules made with different ELP/BSA ratios,9:1(g), 3:1(h),1:1(i). (i, j, k) Dispersion morphologies of BSAs inside the shell of microcapsules made with different ELP/BSA ratios, 9:1(i), 3:1(j), 1:1(k). Scale bars: 5 μm.**

4.2.1.4. Temperature-dependent permeability to rhodamine B, FITC and BSA

To evaluate the controlled release of thermoresponsive MC hydrogels, rhodamine B, a commonly used fluorescent dye with a molecular weight of 479.02 Da, was used as the model to carry out the loading and releasing test. MC1s were chosen as controlled release scaffolds because of their relatively integral pores both at their surfaces and inside the shells. When MC_1s were immersed in rhodamine B solution at a temperature below T_t, because all pore windows were closed, the rhodamine B could not be loaded into the MC_1 cores due to the physical barrier of the hydrogel shell (Figure 17a). In contrast, when MC1s were immersed in rhodamine B solution at a temperature above Tt, the opened pore windows provided channels through which rhodamine B could flow into the cores of the MC_1s (Figure 17b). Correspondingly, most entrapped rhodamine Bs remained inside the cores of the MC_1s when incubated at temperatures below T_t after 20 h (Figure 17c), because all of the pore windows were closed and the diffusion-based release was relatively slow, whereas, when pore windows opened at temperatures above T_t, the release rate accelerated and the entrapped rhodamine B escaped out of the MC_1s through the pore window channels (Figure 17d).

Negatively charged FITC having a similar molecular weight to rhodamin B was chosen to investigate the charge effect on the controlled release of the MCs (Figure 18a). It showed similar loading and releasing efficiency to rhodamine B which is positively charged because the pore size of MCs is

large enough to allow the fast diffusion of either cationic or anionic molecules (Figure 18b). In addition, a relatively large molecule, rhodamine-conjugated BSA (BSA-Rhod, MW. 70,000 Da) was loaded in the MC hydrogels and released by opening the pores in a controlled manner (Figure 17a). The releasing efficiency of BSA-Rhod showed a similar value to much smaller size of rhodamine B or FITC.

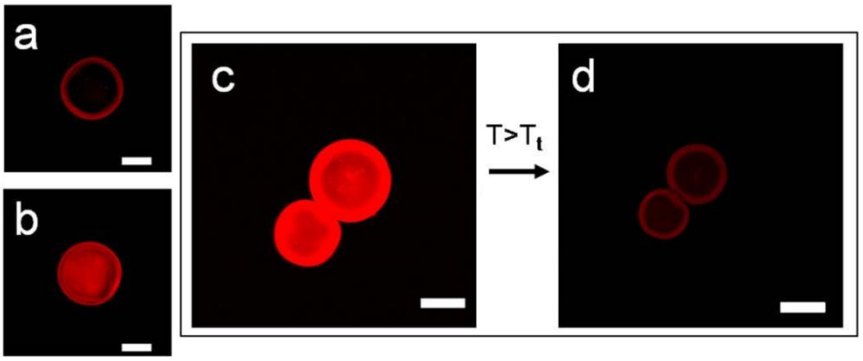

Figure 17. CLSM images illustrating that the loading and releasing of rhodamine B were controlled in a temperature-responsive manner. (a) Below T_t, most rhodamine B couldn't pass through the hydrogel shell to enter into the core of MC_1. (b) Above T_t, rhodamine B passed through the hydrogel shell with ease and the core of MC_1 was filled with rhodamine B. (c) Below T_t, most entrapped rhodamine B molecules remained inside the core of MC_1. (d) Above T_t, most entrapped rhodamine B molecules escaped out of the core of MC_1 [shown in (c)] after 20 h. All scale bars denote 50 μm.

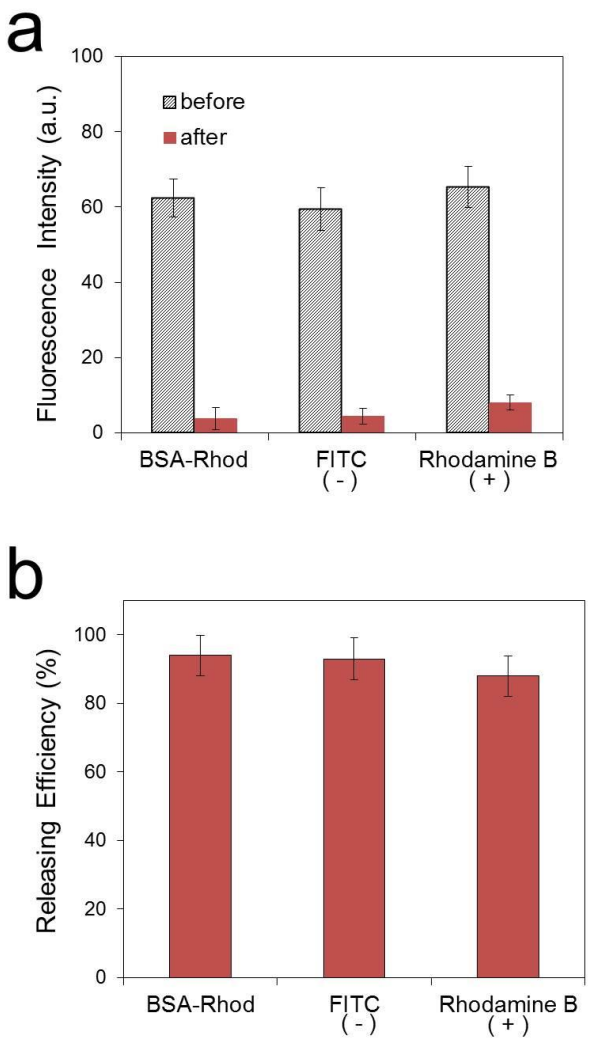

Figure 18. Releasing efficiency of BSA-rhodamine, rhodamine B and FITC controlled in a temperature-responsive manner. (a) Fluorescence intensity of inside the core of MC_1 before and after the releasing experiment and (b) releasing efficiency of MC_1 by thermal stimuli. The releasing experiment was carried out for 48 h (n=5, error bar: STD). BSA-Rhod (BSA-rhodamine), Rhodamine B(+) (positively charged rhodamin B) and FITC(-) (negatively charged FITC).

4.2.2. Microcapsule prepared by one-step method at high temperature in water/oil emulsion

4.2.2.1. The effect of the environmental temperature on thin ELP layer formation in water-in-oil emulsion

Stimuli-responsive microparticles are generally categorized into microbeads and microcapsules by morphological distinction. The former has a uniform structure without a core/shell, but the latter has an empty core and a thin shell membrane. A microbead is relatively simple to prepare because it has a simple structure. However, a microcapsule involves multiple processes to produce the empty core. One challenging aspect of smart microstructure design is controlling a structure's responsiveness. Normally, the responsiveness of a microstructure is determined by the materials making up the system. Surprisingly, we discovered that the responsiveness of a smart microstructure could also be modulated by simple parameter changes, such as reaction temperature, that overrode the material-specific behavior. Furthermore, the morphologies, types and the response of the microparticles could be varied by simple changes in temperature.

The temperature-induced formation of microcapsules utilizes the properties of thermoresponsive polymeric materials by exploiting their thermal phase transitions in emulsified systems. The emulsion method was chosen for its simplicity when applied to microparticle formulation. Hydrophobic colloidal particles move to the water-oil interface and form a

shell in emulsion after being thermally triggered. Elastin-like polypeptides (ELP) are artificial, smart polypeptides that are thermoresponsive; ELP nanoparticles can be easily prepared by heating aqueous ELP solutions [63, 86, 87, 179-182]. Consequently, we hypothesized that the behavior of ELPs in emulsion droplets could be controlled by adjusting the temperature. Maintaining the entire emulsion system at a lower temperature state (below the transition temperature, T_t) keeps the ELPs dissolved and evenly dispersed inside the water droplet. Crosslinking these ELP-containing droplets forms microbeads without any core/shell structures (Figure 19). However, increasing the temperature of the emulsion above T_t forces the ELPs to undergo phase separation and aggregation to form colloidal particles inside the droplets. The colloidal particles are adsorbed on the emulsion droplets' interfaces to reduce the surface energy, forming the ELP-based colloidosome (Figure 19). The colloidosome may be subsequently crosslinked to fabricate a stable microcapsule with core/shell structure.

Studying the effect of the environmental temperature on thin ELP layer formation in water-in-oil emulsion is a major research interest. After heating, the solution rapidly became cloudy as the ELP phases separated; the ELP solution's turbidity gradient was created between 15 ℃ and 28 ℃ at 30 mg/ 225 μL (Figure 20a). The DLS data indicated that the soluble ELP monomer (~ 11 nm in diameter) was converted into ELP colloidal particles (~300 nm) by coactivating the neighboring ELPs (Figure 20b).

The T_t was determined to be 26 ℃ or the temperature of the half

maximum of the ELP solution's turbidity gradient. Although the T_t of the ELP was 26℃, the ELP colloidal particles could be expected to form at 15 ℃ as the ELP solution's turbidity increased. Based on the turbidity gradient curve, the temperature range could be divided into three portions: 1) a hydrophilic phase below 15 ℃, 2) hydrophilic-hydrophobic transitional phase between 15 ℃ and 28 ℃, and 3) hydrophobic phase above 28 ℃ in the water-oil emulsion. We hypothesized that the ELPs' phase changes would modify their hydration, and therefore their movement toward the water-oil interface could be modulated.

To trace the ELPs using fluorescence microscopy, ELP was conjugated with rhodamine B (ELP-Rho). ELP-Rho was uniformly dispersed inside emulsions at 4 ℃, and no phase separation was observed, even after 12 h of incubation (Figure 21). The uniformly dispersed, hydrophilic ELPs were used to fabricate microbeads without core-shell structures. However, the ELP-Rho's phases separated inside the emulsion at 45 ℃ (above T_t) (Figure 22). The ELP-Rho formed colloidal particles by aggregating with neighboring ELP-Rho molecules (Figure 22). The colloidal particles formed inside emulsion tended to move toward the hydrophobic/hydrophilic interface, reducing the interfacial energy [139, 183-186]. During the phase separation, the colloidal ELP-Rho particles migrated to the water-oil interface to become completely engulfed by the interface (Figure 23). In addition, the soft nature of ELP-Rho colloidal particles facilitated their maturation because they had a high water content (~63%) [43]. As displayed in Figure 23, this process also

occurred between the colloidal ELP-Rho particles near the water-oil interface. As time progressed, the colloidal ELP-Rho particles coalesced further to generate a thin, dense shell (Figure 23).

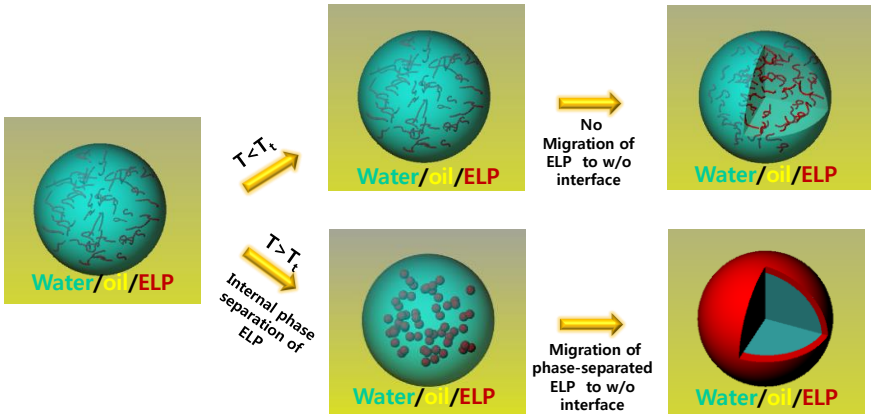

Figure 19. Migration of the colloidal ELP particles inside the emulsion droplets.

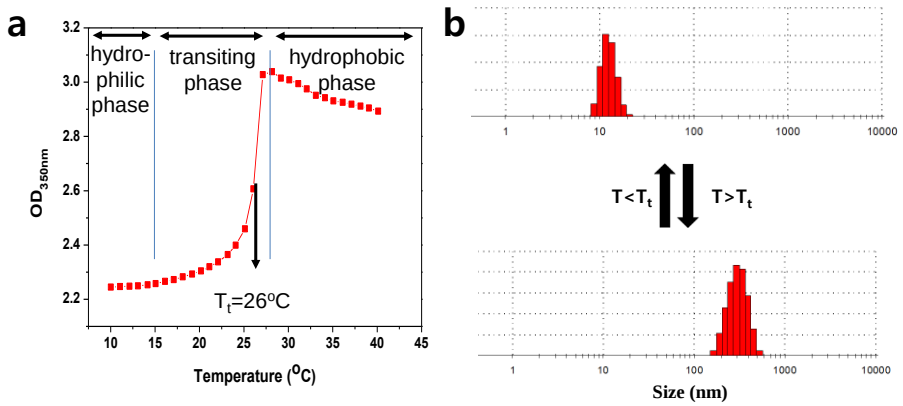

Figure 20. Phase transition of ELPs. (a) Turbidity of the ELP solution as a function of temperature. ELP concentration = 30 mg/225 µL (b) Development of ELP colloidal particles at a temperature above T_t. The ELP colloidal particles were ~ 300 nm when measured by DLS.

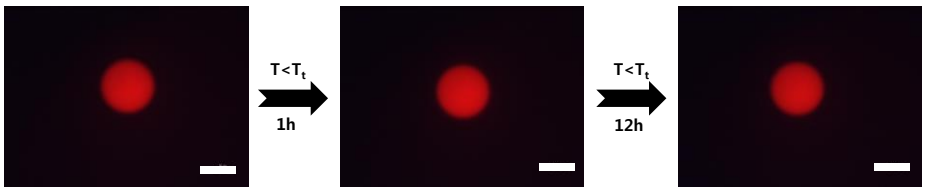

Figure 21. Fluorescence images of ELP-Rho stored at a temperature below the transition phase. ELP-Rho was uniformly dispersed inside a water droplet. Phase separation or migration of ELP-Rho was not observed, even after 12 h. Scale bars = 100 μm.

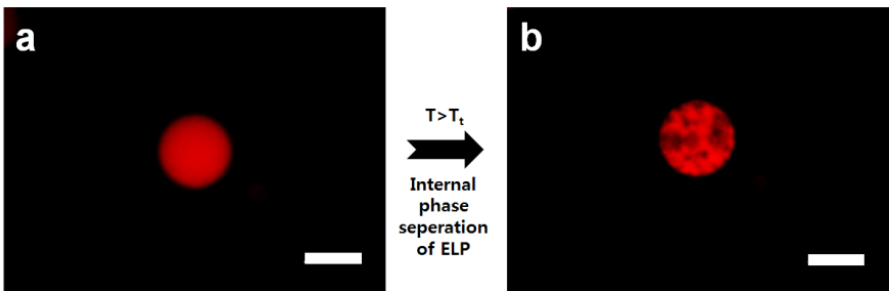

Figure 22. Phase separation of the ELP-Rho. Fluorescence image of ELP-Rho in the emulsion at temperatures (a) below the phase transition and (b) above the phase transition. Scale bars = 100 μm.

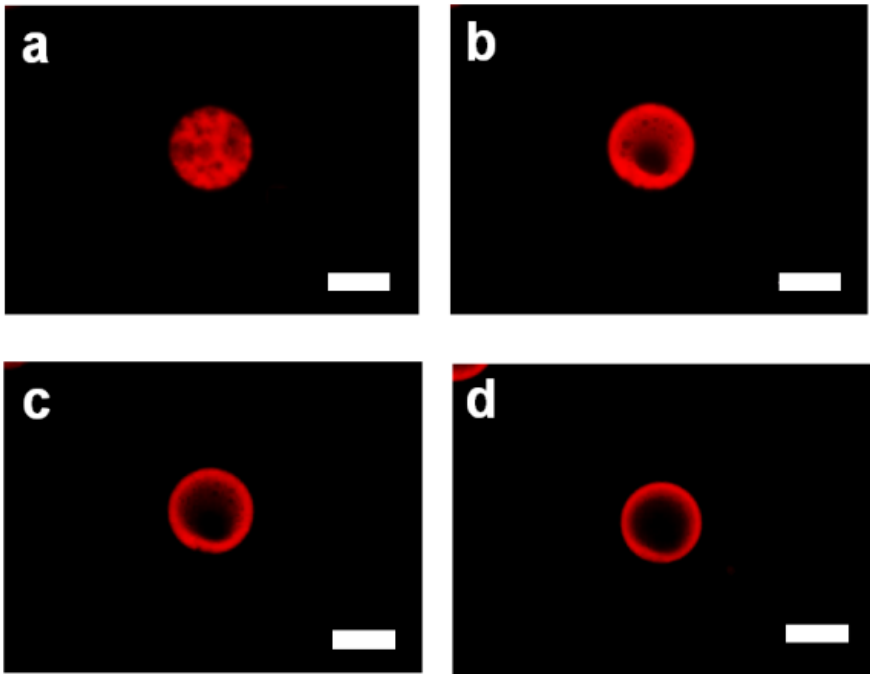

Figure 23. Migration of the ELP-Rho to the water-oil interface. Fluorescence images were taken over time at a temperature above the transition phase. Incubation time (a) 5 min, (b) 10 min, (c) 15 min and (d) 30 min. Incubation temperature = 45 °C. Scale bars = 100 μm.

4.2.2.2. Fixing ELP microstructure with glutaraldehyde

Both the ELP-based microbeads and microcapsules could be obtained by controlling the phase separation in the water-in-oil emulsion method and subsequently by crosslinking with glutaraldehyde. Schiff bases were formed while crosslinking the primary amines from the ELP and aldehyde groups from glutaraldehyde. The Schiff bases autofluoresced, and the interior of this ELP microstructures, including the microbeads and microcapsules, could be monitored by CLSM (Figure 24). The ELP microbeads prepared at low temperatures (below T_t) emitted a uniform fluorescence signal (Figure 24a), indicating that the ELPs were uniformly dispersed and crosslinked with the microbead without any visible voids. However, the ELP microcapsules prepared at higher temperatures (above T_t) exhibited a strong fluorescence signal with contrast between the center and the edge (Figure 24b) because the thin, dense ELPs shell had migrated to the interface before crosslinking with glutaraldehyde.

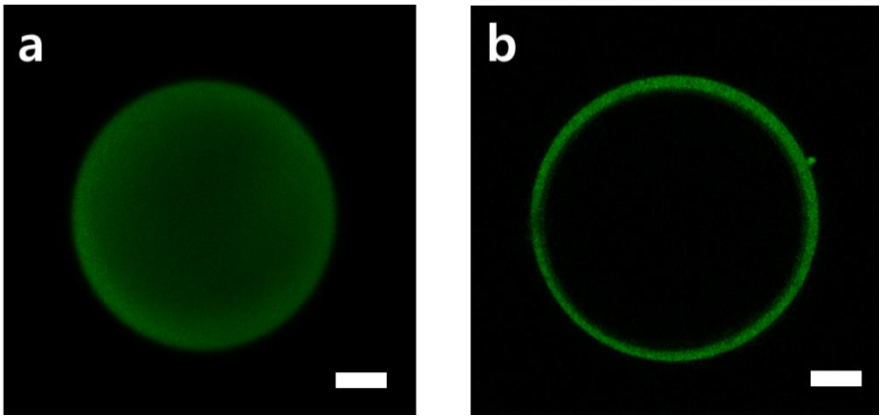

Figure 24. Cross-sectional CLSM images of the ELP microstructures. (a) An ELP microbead prepared at 4 °C and (b) a microcapsule prepared at 45 °C. The Schiff bases formed during the crosslinking between the ELP molecules and glutaraldehyde emitted green autofluorescence. Scale bars = 50 μm.

4.2.2.3. The layer formation and the maturation of the ELP colloidal particles at the interface

The layer formation and the maturation of the ELP colloidal particles at the interface created interesting surface morphologies (Figure 25). Generally, the temperature-induced self-assembly of ELP can be divided into two sequential processes: phase separation and maturation. When the environmental temperature increases, the phase separation initiates within one minute. After the phase separation, the ELP colloidal particles formed during the phase separation mature and coalesce, forming an ordered polymeric network. Although the phase separation process for the ELPs was relatively fast, the coalescence or maturation process was quite time consuming, and the maturation rate was temperature dependent. Microcapsules could only form at the temperature where ELP begins its phase transition, as presented in Figure 6a. Figure 25 reveals that all four temperatures could be used to prepare microcapsules (Figure 25a, d, g, and j), but the temperature affected the particles' surface morphologies (SEM images shown in Figure 25). The microcapsules prepared at 20 ℃ displayed a number of large pores on their surfaces (Figure 25b, c), but the surface pores decreased in size as the temperature increased (Table 2). When the preparation temperature was increased to 45 ℃, the surface pores disappeared and microcapsules with a smooth and thin shell were obtained (Figure 25k, l and Table 2).

The water content of the ELP colloidal particles formed by phase separation is temperature-dependent. Although the phase separated ELPs can

form colloidal particles when the environmental temperature is above T_t, the water content varies with temperature due to the particles' different compression levels. Colloidal particles formed at higher temperatures (well above T_t) contain less water, generating a more compressed ELP network inside the colloidal particles; these qualities may facilitate the coalescence of colloidal particles, accelerating the maturation process. However, the colloidal particles that formed at relatively low temperatures (near T_t) could still undergo phase separation but had significant water content. Therefore, a less compressed polymeric network was formed, slowing the maturation relative to the material formed at higher temperatures.

Therefore, the microcapsules prepared at 45 ℃ had a nonporous shell (Figure 25k, l) due to its rapid maturation rate. In addition, because of their rapid maturation and high compression, the microcapsules prepared at 45 ℃ had the thinnest shell (Figure 25j and Table 2). Conversely, the microcapsules prepared at 20 ℃ exhibited the largest surface pores and the highest surface porosity (Figure 25b, c and Table 2), most likely due to their slow maturation rate.

As mentioned above, higher temperatures produced microcapsules with nonporous shells. Because they matured faster, ELP colloidal particles quickly coalesced and compressed both laterally and vertically at higher temperatures. The vertical compression was crucial to forming a compact microcapsule shell. Lateral compression produced more space, leading to pore formation at the interface. Vertical compression transported more ELPs

toward the interface, increasing their concentration at the interface. As more ELPs were transported toward the interface by the vertical compression, the interface was eventually engulfed by the ELPs, forming a nonporous shell. Consequently, the amount of ELPs needed to cover the interface determined the final surface morphology of the microcapsules.

The changes in morphology related to the amount or surface density of the ELPs at the hydrophobic/hydrophilic interface was also verified by atomic force microscopy (AFM). The surface morphology was imaged in DI water using tapping mode (Figure 26). As displayed in Figure 26a, when an ELP solution (5 μM) was placed on a hydrophobic gold surface, only a few of ELP colloidal particles were observed on the surface after 1 min of incubation. As the ELP incubation lengthened to 5 min, more ELP colloidal particles were observed on the surface. As the incubation time increased to 10 min, a layer formed that contained small pores densely distributed across the surface (Figure 26c). Finally, a nonporous ELP film without pores was formed when the ELP solution was incubated for 30 min (Figure 26d).

Placing a hydrophobically modified gold surface in water might simulate the oil phase in a water-oil interface system. A similar morphological trend was observed, inferring that the interface concentration of ELP colloidal particles determined the layer's final morphology. When the interface concentration of ELP was sufficient, a film without pores was formed at the interface (Figure 26d). However, when the interface concentration was insufficient, a porous film formed (Figure 26b, c). The AFM images strongly

suggested that the differences in microcapsules' morphologies depended on the ELP concentration at the interface. Higher temperatures drove the hydrophobic ELPs toward the interface faster, leading to a high concentration at the interface. Consequently, a nonporous film formed at the interface (Figure 25k, l).

The changes in morphology related to the amount or surface density of the ELPs at the hydrophobic/hydrophilic interface was further verified by adding crosslinker at certain time point. Because the migration of phase-separated ELP to oil/water interface after internal phase separation is time consuming, when the crosslinker (glutaraldehyde) added at a given time point, three typical MCs with different morphologies can be obtained (Figure 27): (1) MCs with a porous shell consisted of only interconnected porous networks (Figure 27 a,d,g); (2) MCs with a less porous shell consisted of both interconnected porous networks and dense film (Figure 27b,e,h); (3) MCs with a nonporous shell consisted of a dense film (SM) (Figure 27c,f,i). If glutaraldehyde was added at the initial stage of ELP migration, MCs with macropores crossing the whole shell was obtained (Figure 27a,d,g). If glutaraldehyde was added at the intermediate stage of ELP migration, because ELP migrated to interface and aggragated with each other, although there were still pores both on the surface (Figure 27b,h) and inside the shell (Figure 27e) of MCs, which were no longer as big as that of MCs obtained at the initial stage (Figure 27a,d,g). And the shell of MCs obtained at intermediate stage was thinner than that of MCs obtained at initial stage. If glutaraldehyde

was added at the final stage of ELP migration, at which the whole interface was occupied with ELPs and there was no remained space for ELP further compression, instead of MCs containing a porous shell, MCs consisted of a thin and perfect ELP film was obtained (Figure 27c,f,i).

As migration time went on, it can been seen that the pores both on the surface and inside the shell were gradually reduced in size (Figure 27e,h) and finally closed (Figure 27f,i). And some semi-closed pores as shown by white circle in Figure 27h and the overall reduction in shell thickness (Figure 27d,e,f) were convincing evidences of the above demonstration for MCs formation, that is, phase-separated ELPs gradually migrated to W/O interface, at which they further compressed with each other, leading to formation of a densely packed ELP film.

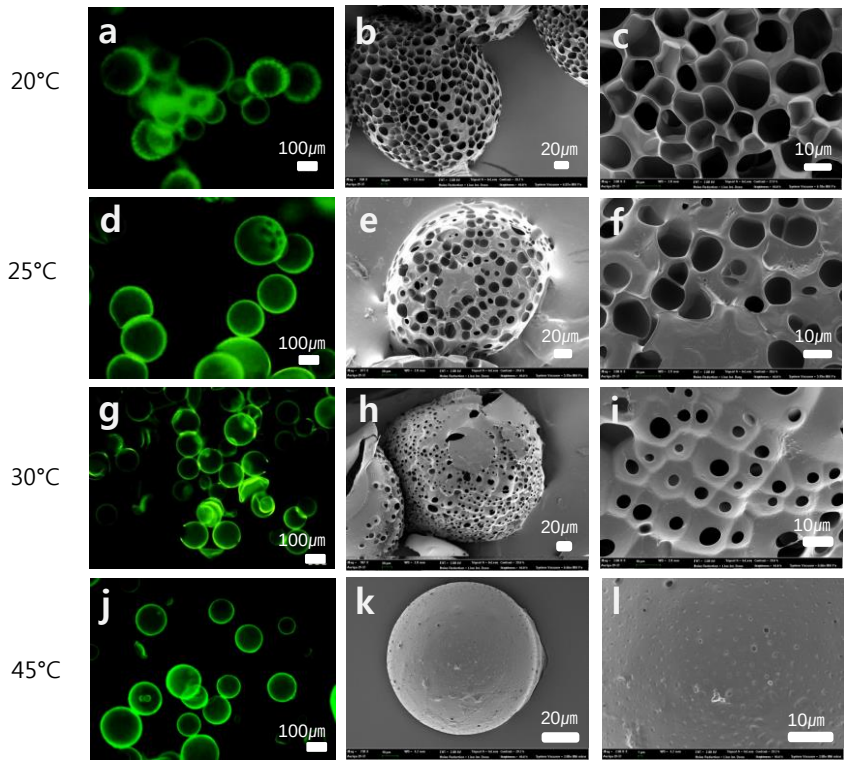

Figure 25. Morphological variations between the ELP microcapsules prepared at different crosslinking temperatures. Microcapsules were prepared at (a-c) 20 °C, (d-f) 25 °C, (g-i) 30 °C and (j-l) 45 °C. (a, d, g, i) Confocal images, (b, e, h, k) FE-SEM images and (c, f, i, Enlarged FE-SEM images of microcapsules.

Table 2. Comparison of microcapsule shells prepared at different temperatures.

	Diameter of pore (μm)	Surface porosity	Shell thickness/Diameter of microcapsule (%)
M $_{20°C}$	14.20±5.80	68.34±11.97	14.34±2.23
M $_{25°C}$	13.01±5.21	34.97±10.83	10.41±2.04
M $_{30°C}$	5.35±3.15	16.88±4.01	8.16±0.89
M $_{45°C}$	0	0	7.94±0.63

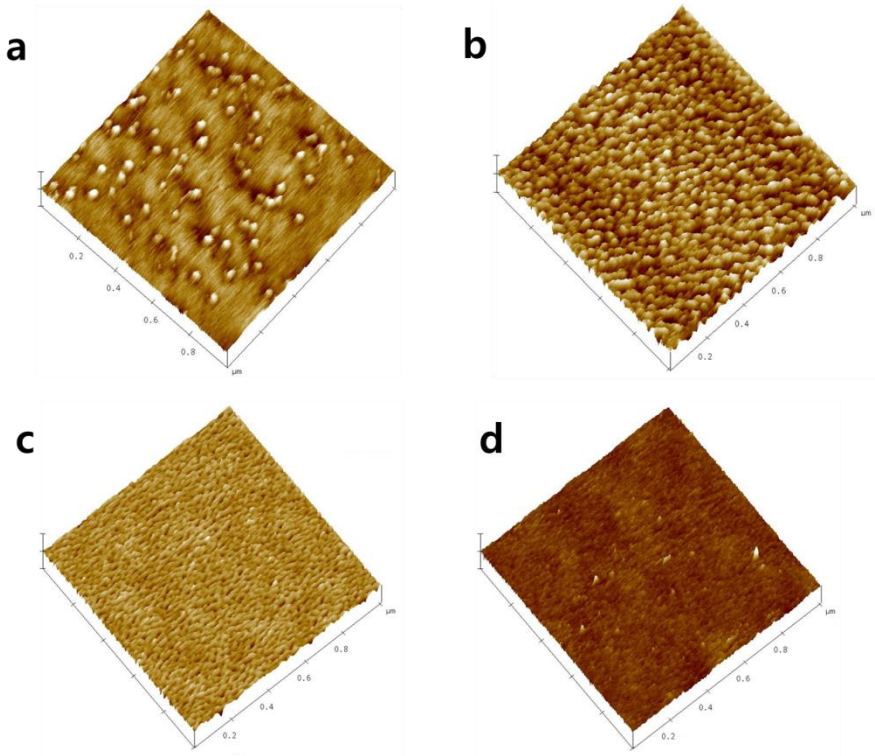

Figure 26. AFM topographic images of ELP colloidal particles adsorbed on the hydrophobically modified gold surface at different incubation times: (a) 1 min, (b) 5 min, (c) 10 min and (d) 30 min. ELP concentration of incubation solution was 5 μM. Incubation temperature = 45 °C

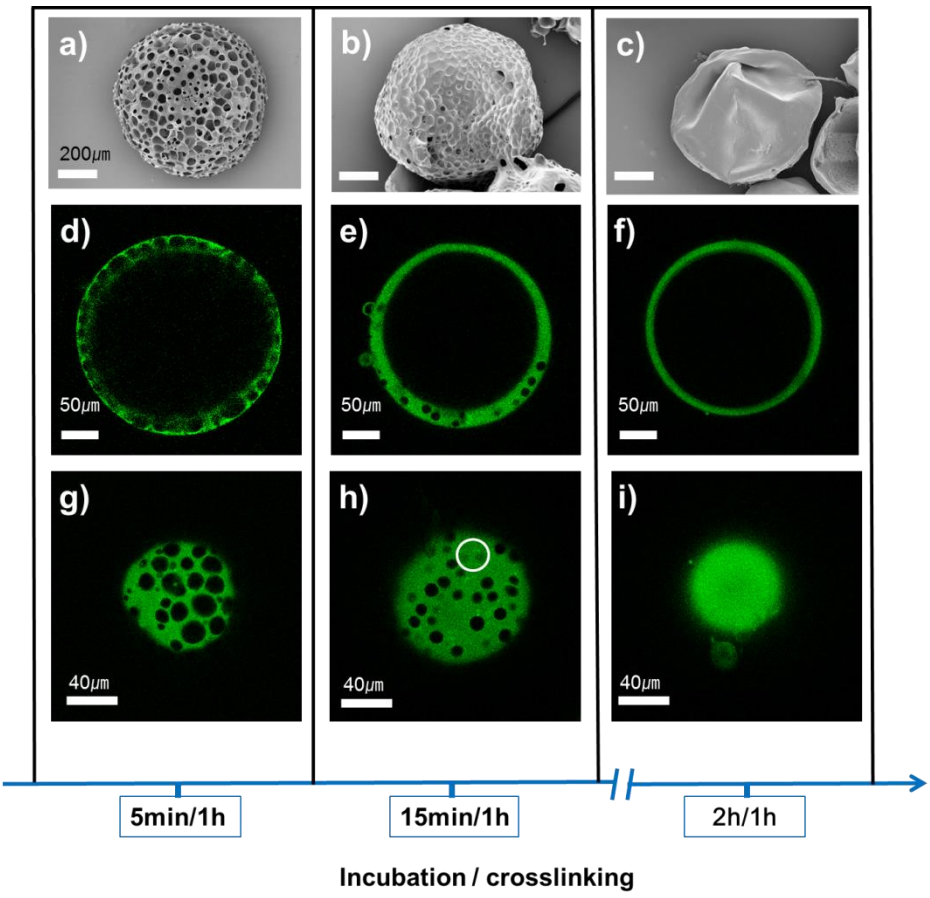

Figure 27. Three typical microcapsules with different morphologies have been obtained by changing the incubation time at 45 °C. The left, middle and right panels are microcapsule with a porous shell (a,d,g), microcapsule with a less porous shell (b,e,h) and microcapsule with nonporous shell (c,f,i), respectively. (a-c) FESEM images. (d-f) Cross-section CLSM images.(g-i)Surface CLSM images. Scale bars: 200 μm(a-c), 50 μm(d-f) and 40 μm(g-i).

4.2.2.4. Thermoresponsive properties of ELP microstructures

Due to the thermoresponsive nature of ELP, the glutaraldehyde-crosslinked ELP microstructures displayed smart behaviors, such as closing and opening the pores under thermal control. To verify that the pores were thermoresponsive, the microbeads and microcapsules were immersed in DI water at different temperatures (4 and 45 ℃) and allowed to equilibrate. Subsequently, the ELP microstructures were dipped into liquid nitrogen and freeze-dried. FE-SEM images of the frozen microbeads and microcapsules are displayed in Figure 28. The microbeads prepared at 4 ℃ possessed positively thermoresponsive properties, opening their pores at temperatures above T_t (Figure 28b) and closing them at temperatures below T_t (Figure 28a). However, the microcapsules prepared at 45℃ possessed negatively thermoresponsive properties, opening their pores at temperatures below T_t (Figure 28c) and closing them at temperatures above T_t (Figure 28d).

The type of crosslinker combined with the diblock nature and local concentration of the ELPs controlled whether the thermoresponsive properties were positive or negative. Increasing the ELP concentration promoted intermolecular, functional crosslinks, leading to shorter segment lengths between the crosslinked points. Conversely, decreasing the concentration promoted intramolecular, nonfunctional crosslinks, leading to longer segment lengths between the crosslinked points and an enhanced swelling ability. The ELPs were completely extended and had few interchain contacts due to the high hydration at temperatures below the phase transition, leading to a

relatively low interface concentration (Figure $30a_0$). Most of crosslinkings occurred intramolecularly in this state; the pores should open as the temperature increases above T_t (Figure $30a_1$).

Microcapsules with small pores could be fabricated near the temperature of the ELPs' transition state. Interestingly, the microcapsules formed in this temperature range revealed bidirectional thermoresponsiveness. The pores could be closed by either increasing or decreasing the temperature (Figure 29). When the temperature increased and reached the phase transition temperature (15 ~ 28 ℃ in this ELP system), the ELPs phase separated to form colloidal particles; these particles migrated to and packed at the interface (Figure $30b_0$). When the crosslinkers were added to this emulsion, the amount of intermolecular crosslinking was increased due to the high local ELP concentration. However, these ELP particles still contain a large amount of water due to their loose compression (Figure $30b_0$). The ELPs used to fabricate microstructures are a diblock polymer composed of a lysine-containing block and a lysine-lacking block. Lysine is a very hydrophilic amino acid because it contains a charged primary amine group that can easily entrap more water molecules through hydrogen bonding. Because the temperature near transition state can selectively induce folding in the lysine-lacking block, relatively large and loosely compressed colloidal particles are formed with their hydrophilic lysine side groups located near the particle surfaces (Figure $30b_0$). Consequently, the interface cannot be fully packed, leading to pore formation the microcapsule surface. The hydrophilic lysine

groups at the colloidal particles' surfaces facilitated intermolecular crosslinking at the edges of the colloidal particles, bridging with the neighboring colloidal particles (Figure $30b_0$). The pores close in two ways: by increasing or decreasing the temperature. Increasing temperature makes lysine-containing block fold, further compressing the ELPs and shrinking the microcapsules. Therefore, the pores formed during the transition state close above the transition temperature (Figure $30b_1$). The other way to close the pores is to decrease the temperature below the transition temperature. When the temperature decreases below the transition temperature, the folded lysine-lacking block extends, allowing the pore spaces to be occupied by ELPs. Subsequently, the pores on the ELP microcapsules close. (Figure $30b_2$)

An adequately warm hydrophobic state causes both the lysine-containing and lysine-lacking blocks to fold, forming highly compressed colloidal particles (Figure $30c_0$). Because the lysine-containing blocks are folded and embedded into the colloidal particles at high temperatures, they lose their dynamic properties and their ability to resist the coalescence of the colloidal particles; therefore, the colloidal particles coalesce more rapidly. In addition, the intermolecular crosslinking is dominant because the local concentration is much higher. Consequently, the interface is tightly packed, and the microcapsules have a nonporous shell (Figure $30c_0$). Because the ELP chains involved in the intermolecular crosslinkages have restricted extension properties, the ELPs cannot fully cover the enlarged surface area, leading to pore formation, as illustrated in Figure $30c_1$.

In conclusion, the responsiveness and morphology of ELP microstructures could be controlled through the temperature used during the crosslinking process in a water-in-oil emulsion. The ELPs' behavior inside the emulsion could be controlled by adjusting the experimental temperature. The ELP molecules are hydrophilic at low temperatures, allowing them to fully extend due to the level of hydration; these conditions generate ELP microbeads with positively thermoresponsive pores. At higher temperatures, the ELP molecules are hydrophobic, leaving them completely folded and compressed inside water droplets; these conditions generate ELP microcapsules with negatively thermoresponsive pores. ELP microcapsules were also prepared at the temperature of their transition state. Interestingly, these ELP microcapsules demonstrated bidirectional thermoresponsiveness, closing their pores at both higher and lower temperatures. The dominance of inter or intramolecular crosslinkings depended on the diblock nature and local concentration of the ELPs; this parameter determined the surface morphology of the ELP microstructures.

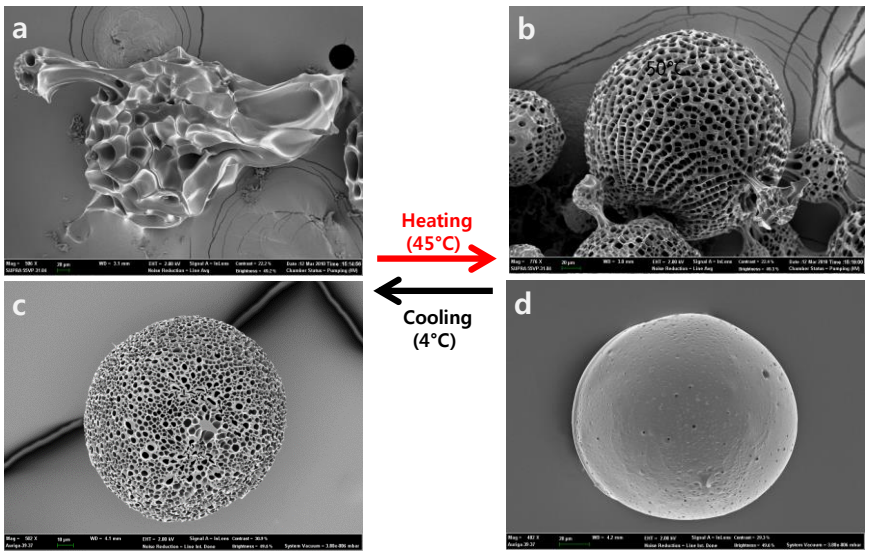

Figure 28. Thermoresponsiveness of the ELP microstructures. FE-SEM images of microbeads incubated at (a) 4 ℃ and (b) 45 ℃. FE-SEM images of microcapsules incubated at (c) 4 ℃ and (d) 45 ℃. The surface morphologies were changed as the incubation temperature changed. The microbead displayed positively thermoresponsive pores that opened when the temperature increased. Conversely, the microcapsule displayed negatively thermoresponsive pores that opened when the temperature decreased.

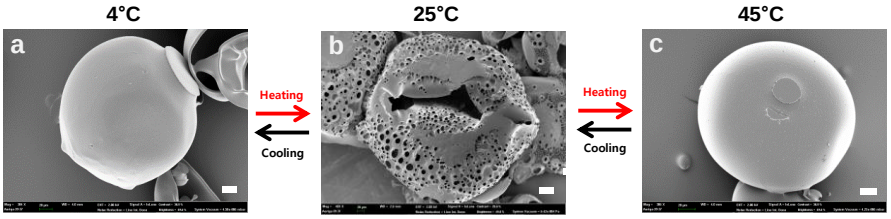

Figure 29. Bidirectional thermoresponsiveness of the microcapsules prepared at 25 °C. The pores of the microcapsule (a) could be closed by either (a) cooling the microcapsule to 4 °C, which is below the phase transition temperature or (c) by heating the microcapsule to 45 °C, which is above the phase transition temperature. Scale bars = 20 μm.

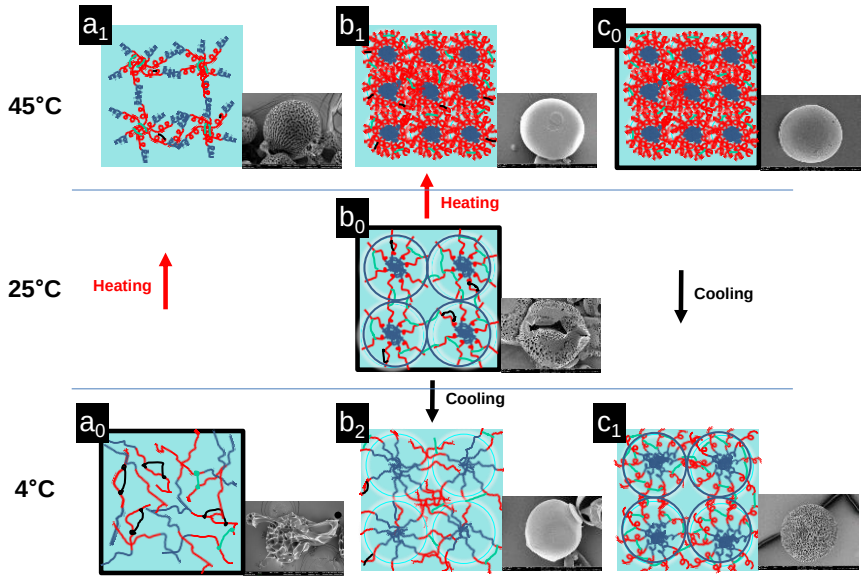

Figure 30. Schematic illustration of pore formation. The red and blue represent the lysine-containing and lysine-lacking domains, respectively. The green lines denote intermolecular crosslinks, and the black lines denote intramolecular crosslinks.

(a) Microbeads were prepared at 4 °C. The ELPs extend completely, and the intramolecular crosslinking dominates. The ELP microbeads form due to the evenly distributed ELP molecules in the bulk. The pores are opened by increasing the temperature.

(b) Microcapsules were prepared at 25 °C. The lysine-lacking ELP blocks the folding, and the ELPs are phase separated. Relatively large and loosely compressed ELP colloidal particles are formed by locating the hydrophilic lysine side groups near the surface of the neighboring colloidal particles. Both inter- and intra-molecular crosslinkings are available. The crosslinkings occur mainly on the edges of the colloidal particles while bridging the neighboring colloidal particles. The pores formed in the transition state are closed above the transition temperature. In addition, below the transition temperature, the folded lysine-lacking ELP blocks any extension, allowing the pore space to be occupied by the

(continued from the previous page)

ELPs. Subsequently, the pores of the ELP microcapsules are closed.

(c) Microcapsules were prepared at 45 °C. Lysine-containing blocks also folded and embedded themselves into the colloidal particles, causing the colloidal particles to become tightly compressed. The intermolecular crosslinkages are dominant. Because the ELP colloidal particles are tightly compressed, the intermolecular crosslinkages occur mainly on the surfaces of the neighboring colloidal particles. Because the intermolecular crosslinkings restrict the extension of the ELP chains, the ELPs cannot fully cover the enlarged surface area, leading to pore formation.

(a_0, b_0 and c_0)The ELP molecules have been crosslinked.

4.3. ELP microbead prepared in water solution

4.3.1. Preparation of ELP microbead

Negative thermoresponsive polypeptide microbeads were simply prepared by temperature induced elastin like polypeptide (ELP) phase separation. Crosslinking these microbeads with glutaraldehyde gave them negative thermoresponsive pores, which closed at high temperature (above transition temperature) and opened at low temperature (below transition temperature). These smart polypeptide microbeads have great potential applications in biomedicine.

Firstly, freeze-dried ELPs were dissolved in PBS(pH 7.4) at 4 ℃, and then increasing the ambient temperature to 40 ℃ (above T_t) (Figure 31) induced the ELPs phased separation and further coacervation into microbeads. The size of the microbeads could be easily controlled by changing the initial concentration of ELP. As shown in Figure 32 and Figure 33, the size of microbeads increased with ELP concentration, and the detailed changing in size as a function of ELP concentration was summarized in Figure 33. As the ELP concentration was increased, the mean diameter of the microbeads increased from 9.58 (at 0.5 mg/mL) to 31.29㎛ (at 10 mg/mL). The size of microbead increased with ELP concentrations in a nonlinear way. The size of the microbeads prepared by low ELP concentration focused in a relatively narrow size range, on the contrary, the microbeads prepared by high ELP concentration had a very broad size distribution (see Figure 33 error bars).

Effect of concentration on microbead size was particularly strong at lower concentrations. Increased concentration of ELP could lower the coacervation temperature (Figure 31) and coacervation velocity, correspondingly leading to influencing the size of the final droplet/microbead [108, 180, 187]. With time, the droplet grew until reached a stable size, where ELP chains aligned along with the outer layer surface of the droplet with lysines directed toward the aqueous phase. The presence of lysine residues in the droplet surface protected droplets from further coalescence by charge-charge repulsion.

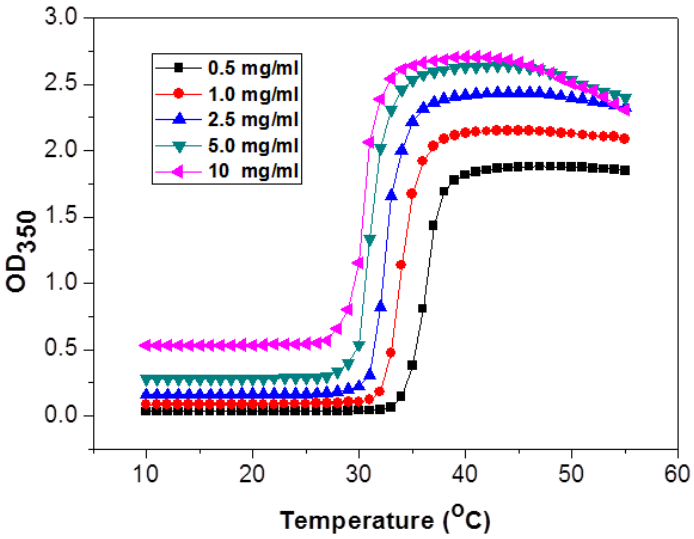

Figure 31. UV-visible spectra of the ELP solutions at various concentrations as a function of temperature.

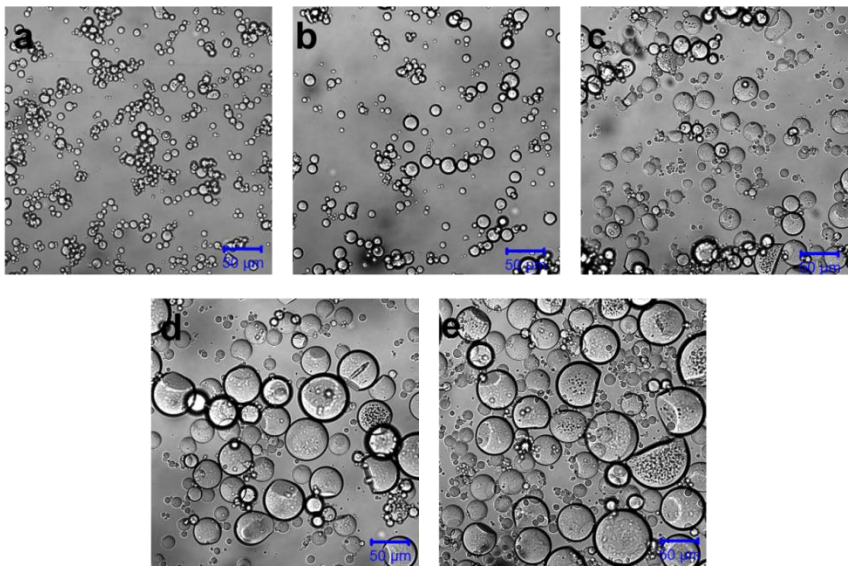

Figure 32. CLSM images of ELP microbeads formed under various initial ELP concentrations.(a) 0.5, (b) 1, (c) 2.5, (d) 5 and (e) 10 mg/mL. Scale bars, 50 µm.

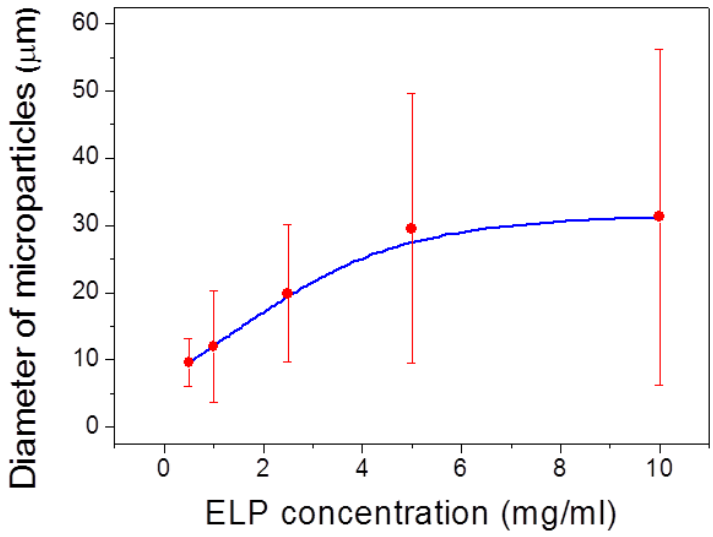

Figure 33. Effect of the initial ELP concentration on the size of microbeads (n=30).

4.3.2. Thermoresponsive properties of ELP microbead

Though the as-prepared microbeads were fabricated by temperature induced ELPs aggregation and crosslinking with glutardaldehyde at high temperature, the thermoresponsive property was still remained and imparted it to these as-prepared microbeads. The change in diameter of microbeads was monitored with optical microscopy at the given temperature. As shown in Figure 34, when incubated alternatively below T_t (4 ℃) and above T_t (37℃), microbeads showed rapidly repetitive volume changes, which led to the formation and closure of pores at the surface of microbeads (Figure 35), and this swelling-deswelling transition occurred in just a few seconds(~30s). Figure 35 clearly shows that two totally different surface morphologies have been obtained when the ambient temperature was changed. At 37 ℃ (above T_t), the surface of microbeads was relatively smooth and no pores could be seen (Figure 35c and d). On the contrary, the surface was no longer smooth and bestrewn with pores once the temperature decreased to 4 ℃ (below T_t) (Figure 35a and b).

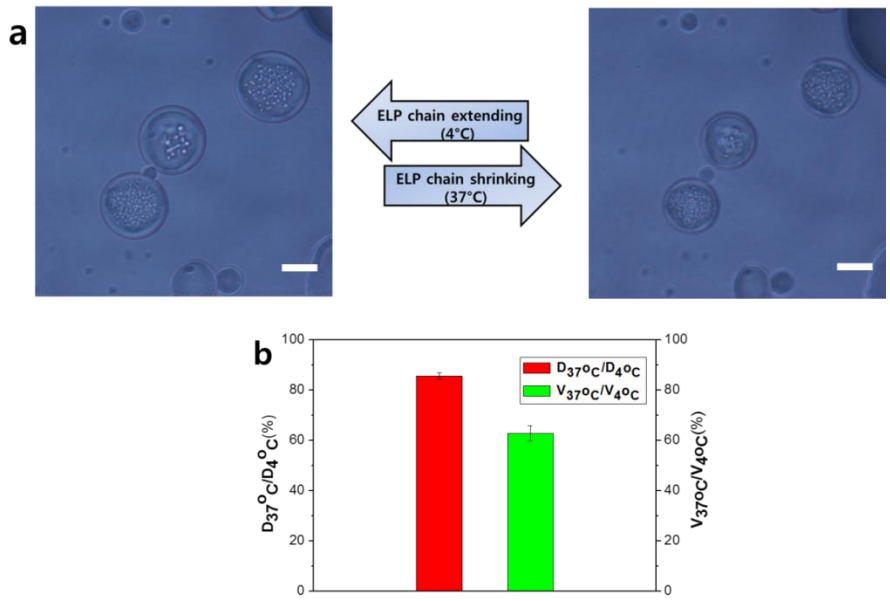

Figure 34. Optical images (a) for changing in size as the function of temperature and the corresponding changing in diameter and volume (b). Scale bar, 20 ㎛.

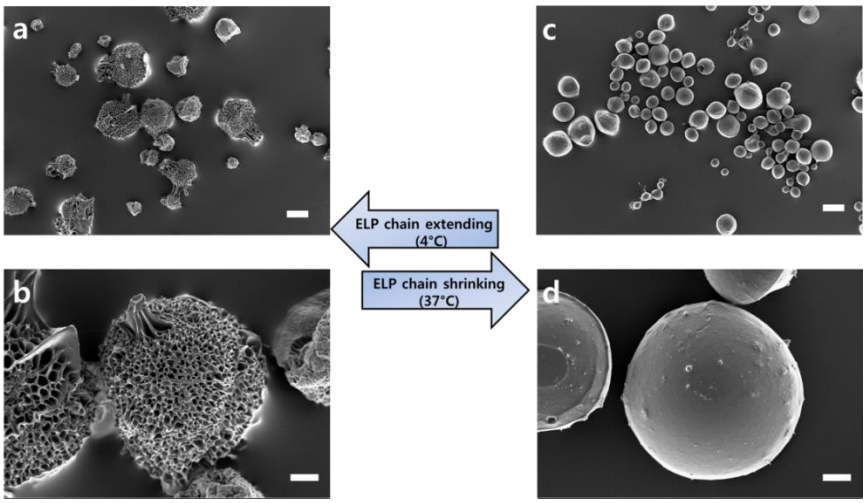

Figure 35. FESEM images of ELP microparticles at low temperature (a,b) and high temperature (c,d). Scale bars: 20 ㎛(a,c) and 5 ㎛ (b,d).

4.3.3. Proposed mechanisms for ELP microbead fabrication and morphology transition

To clearly describe the morphology change of ELP microbead as a function of temperature, the proposed mechanisms for ELP microbead fabrication and morphology transitions were summarized in Figure 36. At low temperature (below T_t), all ELP chains existed in a disordered way (random coil) (Figure 36a), once the temperature increased above T_t, ELP chains started to fold and took an ordered strucrture (β-turn/β-spiral), and then these folded ELP chains coacervated to form micro-scale particles (Figure 36b). This changing from free chains to a micro-scale particle involved a secondary structure transition which was determined by CD spectra. As shown in Figure 36a, two main peaks (a band at ～198 nm and a band at ～212 nm) were clearly observed. According to literatures, the band at ~198nm assigns to random coil structure and the band at ~212 nm should arise from type Ⅱ β–turn/β-spiral structure. However, forming of the ELP microbead caused the 198 nm band to decrease and the 212 nm band to increase (Figure 36b), meaning the ELP chains inside the microbeads took a β-turn/β-spiral structure. The folded ELPs with a β–spiral structure composing the microbead were just like compressed "springs" (Figure 36b), which were able to extend once the temperature decreased to a relatively low temperature (below T_t). To preserve the outline when temperature changed, the microbeads were crosslinked with glutaraldehyde. Considering the ELP sequence $[(VPGVG)_{14}(VPGKG)]_8[VPGVG]_{40}$, in the same ELP chain the distance

between two lysine residues was too far to crosslink with glutaraldehyde, so we believed that most the crosslinking happened between lysine residues coming from different ELP chains(red bonds shown in Figure 36c and d), which is also the reason why these ELP chains composing the microbead can freely shrinking and extending and the corresponding size transition of the whole microbead as temperature changed. At high temperature (at 37 ℃, above T_t), ELP chains folded and compressed with each other so tightly that no pores could be observed (Figure 36c and Figure 35c,d). On the contrary, decreasing temperature to 4 ℃ (below T_t) drove the compressed ELP chains extend, giving rise to pores formation (Figure 36d, and Figure 35a,b).

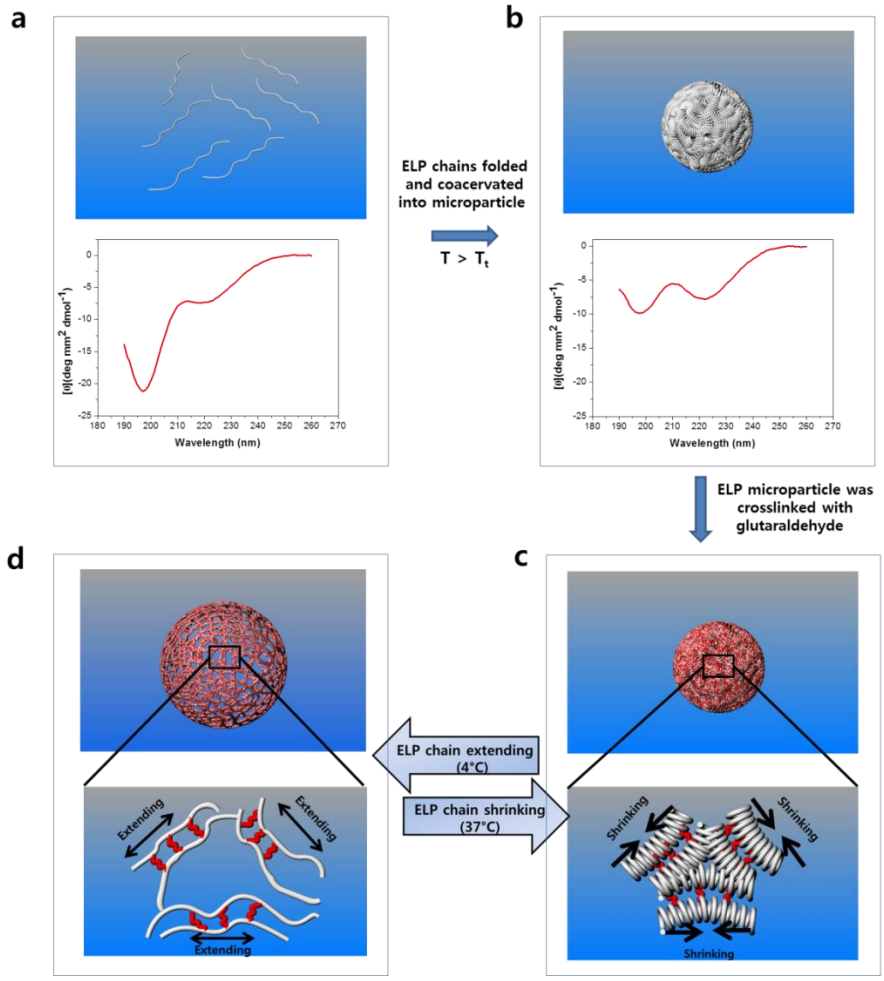

Figure 36. Proposed mechanisms for ELP microbead fabrication and morphology transition. (a) ELP with a random coil structure at low temperature. (b) As temperature raised above T_t, ELP folded to form β-spiral structure and these folded ELP chains associated with neighbors to form micro-scale particles. (c) ELP microparticle was further crosslinked with glutaraldehyde. (d) As temperature decreased below T_t, ELP chains extended and formed pores at the surface of microparticle. Red bonds shown in (c) and (d) denoted glutaraldehyde.

V. Conclusions

The ELP containing both a lysine-rich domain and a lysine-lacking domain was synthesized by recombinant DNA technology. An ELP gene inside the expression vector (pET-sfi) was transformed into BLR (DE3) cells and expressed by shaking culture at 37 ^{o}C. The purity and molecular weight (85kDa) were confirmed by SDS-PAGE with Commassie brilliant blue staining of ELP. The T_t of ELP was determined to be 37 ^{o}C at a concentration of 200 μM with thermo-regulated UV/vis spectrometer at 350 nm. Temperature-triggered folding of ELP molecules resulted in the changes in secondary and tertiary structure. At the temperature below T_t, ELP chains were disordered (random coil), but they became ordered to β-turn/β-spiral as the temperature increased above T_t. In addition, it was confirmed that the exposure of tryptophan residues to water was increased with temperature, leading to fluorescence quenching.

Due to the thermoresponsive nature of ELP, the glutaraldehyde-crosslinked ELP microstructures displayed smart behaviors, such as closing and opening the pores under thermal control.

Firstly, a series of polypeptide microcapsules (MCs) were fabricated using two-step cross-linking water-in-oil emulsion method. In the presence of acetone and ethanol, the instability of ρ-phthaldehyde and the stability of glutardaldehyde based Schiff bases ensured the successful preparation of microscapsules. The shell thickness could be easily adjusted by changing the

glutaraldehyde crosslinking time. The MCs prepared in this method had positively thermoresponsive pores, and the pore morphology could be adjusted by adding BSA. The thermal responsiveness decreased when the ratio of ELP to BSA decreased because of the inherent thermally insensitive property of BSA. The pore morphology of the MCs depended on the distribution of BSA at the oil-water interfaces in the process of emulsion. Because the interface between the phase-separated regions of the film was at a higher free energy, proteins exhibited a high propensity to migrate and bind to oil-water interfaces. The two distinctly different groups of materials migrated to oil-water interfaces with different affinity and showed a phase separation. The BSA-rich phase existed as segregated clusters dispersed in the ELP continuous phase. As the mass ratio of BSA to ELP increased, BSA-rich clusters were formed and filled the space of the layer meaning that BSA was a majority on the surface and ELP migrated into the bulk. As a result, MCs could not form a porous surface structure.

Secondly, Both the ELP-based microbeads and MCs could be obtained by controlling the phase separation in the water-in-oil emulsion method. The responsiveness and morphology of ELP microstructures could be controlled through the temperature used during the crosslinking process in a water-in-oil emulsion. The ELPs' behavior inside the emulsion could be controlled by adjusting the experimental temperature. The ELP molecules were hydrophilic at low temperatures, allowing them to fully extend due to the level of hydration; these conditions generated ELP microbeads with positively

thermoresponsive pores. At higher temperatures, the ELP molecules were hydrophobic, leaving them completely folded and compressed inside water droplets; these conditions generated ELP MCs with negatively thermoresponsive pores. ELP MCs were also prepared at the temperature of transiting. Interestingly, these ELP microcapsules demonstrated bidirectional thermoresponsiveness, closing their pores at both higher and lower temperatures. The dominance of inter- or intramolecular crosslinkings depended on the diblock nature and local concentration of the ELPs; this parameter determined the surface morphology of the ELP microstructures.

Thirdly, ELP microbeads were prepared by temperature triggered phase separation of ELP molecules in water solution at a temperature above T_t. Though the as-prepared microbeads were fabricated by temperature induced ELPs aggregation and crosslinking with glutardaldehyde at high temperature, the thermoresponsive property was still remained and imparted it to these as-prepared microparticles. The folded ELPs with a β–spiral structure composing the microparticle were just like compressed "springs", which were able to extend once the temperature decreased to a relatively low temperature (below T_t). Considering the ELP sequence $[(VPGVG)_{14}(VPGKG)]_8[VPGVG]_{40}$, in the same ELP chain, the distance between two lysine residues was too far to crosslink with glutaraldehyde, so most the crosslinking happened between lysine residues from different ELP chains. It was a reason why ELP chains composing the microbead could shrink and extend. The microbead prepared in this method had negatively thermoresponsive pores. Above T_t,

ELP chains folded and were compressed so tightly that no pores could be observed. On the contrary, below T_t, the compressed ELP chains extended, giving rise to pores formation.

The temperature, at which ELP microstructures were crosslinked, controlled the thermoresponsive properties of ELP microstructures. ELP microstructures prepared and crosslinked below T_t had positively thermoresponsive pores. ELP microstructures prepared and crosslinked above T_t had negatively thermoresponsive pores. ELP microstructures prepared at transiting state demonstrated bidirectional thermoresponsiveness.

Because the temperature change is able to induce the on-off morphological transition of ELP microstructures, these ELP microstructures have great potential in controlled release. The encapsulated molecules can be released on demand in response to changing environmental temperatures. In addition, the present ELP microstructures could be applicable for a scaffold for cell carrier and tissue engineering, as well as *in situ* encapsulation.

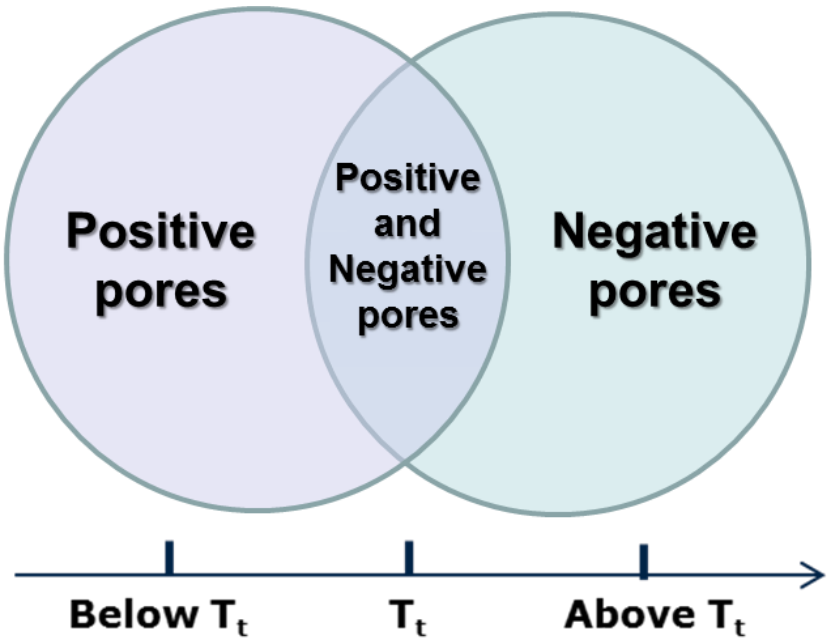

The thermoresponsive property of ELP microstructures was controlled by the experimental temperatures at which ELP microstructures were prepared.

VI.References

[1] D.L. Nettles, A. Chilkoti, L.A. Setton, Applications of elastin-like polypeptides in tissue engineering, *Advanced Drug Delivery Reviews*, **62**, 1479-1485 (2010).

[2] J.R. McDaniel, D.J. Callahan, A. Chilkoti, Drug delivery to solid tumors by elastin-like polypeptides, *Advanced Drug Delivery Reviews*, **62**, 1456-1467 (2010).

[3] D.M. Lynn, M.M. Amiji, R. Langer, pH-responsive polymer microspheres: Rapid release of encapsulated material within the range of intracellular pH, *Angewandte Chemie-International Edition*, **40**, 1707-1710 (2001).

[4] Y. L. Yu, M. J. Zhang, R. Xie, X. J. Ju, J. Y. Wang, S. W. Pi, L. Y. Chu, Thermo-responsive monodisperse core–shell microspheres with PNIPAM core and biocompatible porous ethyl cellulose shell embedded with PNIPAM gates, *Journal of Colloid and Interface Science*, **376**, 97-106 (2012).

[5] X. Wang, G. Li, J. Wei, W. Guan, A novel method to control microcapsule release behavior via photo-crosslink polyurethane acrylate shells, *Journal of Applied Polymer Science*, **113**, 1008-1016 (2009).

[6] J. Sankaranarayanan, E. A. Mahmoud, G. Kim, J.M. Morachis, A. Almutairi, Multiresponse Strategies To Modulate Burst Degradation and Release from Nanoparticles, *ACS Nano*, **4**, 5930-5936 (2010).

[7] J. You, R. Shao, X. Wei, S. Gupta, C. Li, Near-Infrared Light Triggers Release of Paclitaxel from Biodegradable Microspheres: Photothermal Effect and Enhanced Antitumor Activity, *Small*, **6**, 1022-1031 (2010).

[8] A. M. Javier, P. del Pino, M. F. Bedard, D. Ho, A.G. Skirtach, G.B. Sukhorukov, C. Plank, W.J. Parak, Photoactivated Release of Cargo from the Cavity of Polyelectrolyte Capsules to the Cytosol of Cells, *Langmuir*, **24**, 12517-12520 (2008).

[9] K. Katagiri, K. Koumoto, S. Iseya, M. Sakai, A. Matsuda, F. Caruso, Tunable UV-Responsive Organic-Inorganic Hybrid Capsules, *Chemistry of Materials*, **21**, 195-197 (2009).

[10] T. Hoare, J. Santamaria, G.F. Goya, S. Irusta, D. Lin, S. Lau, R. Padera, R. Langer, D.S. Kohane, A Magnetically Triggered Composite Membrane for On-Demand Drug Delivery, *Nano Letters*, **9**, 3651-3657 (2009).

[11] Z. Lu, M.D. Prouty, Z. Guo, V.O. Golub, C.S.S.R. Kumar, Y.M. Lvov, Magnetic Switch of Permeability for Polyelectrolyte Microcapsules Embedded with Co@Au Nanoparticles, *Langmuir*, **21**, 2042-2050 (2005).

[12] S. H. Hu, C. H. Tsai, C. F. Liao, D. M. Liu, S. Y. Chen, Controlled Rupture of Magnetic Polyelectrolyte Microcapsules for Drug Delivery, *Langmuir*, **24**, 11811-11818 (2008).

[13] H.Y. Koo, S.T. Chang, W.S. Choi, J.H. Park, D.Y. Kim, O.D. Velev, Emulsion-based synthesis of reversibly swellable, magnetic nanoparticle-embedded polymer microcapsules, *Chemistry of Materials*, **18**, 3308-3313 (2006).

[14] I. Lentacker, S.C. De Smedt, N.N. Sanders, Drug loaded microbubble design for ultrasound triggered delivery, *Soft Matter*, **5**, 2161-2170 (2009).

[15] S. Hernot, A.L. Klibanov, Microbubbles in ultrasound-triggered drug and gene delivery, *Advanced Drug Delivery Reviews*, **60**, 1153-1166 (2008).

[16] J. Yun, J.S. Im, Y. S. Lee, T. S. Bae, Y. M. Lim, H. I. Kim, pH and electro-responsive release behavior of MWCNT/PVA/PAAc composite microcapsules, *Colloids and Surfaces A: Physicochemical and Engineering Aspects*, **368**, 23-30 (2010).

[17] M. Yoshida, T. Matsui, Y. Hatate, T. Takei, K. Shiomori, S. Kiyoyama, Permeability control in electro-sensitive microcapsules with immobilized ferroelectric liquid crystalline segments, *Journal of Polymer Science Part A: Polymer Chemistry*, **46**, 1749-1757 (2008).

[18] M.S. Wong, J.N. Cha, K.S. Choi, T.J. Deming, G.D. Stucky, Assembly of nanoparticles into hollow spheres using block copolypeptides, *Nano Letters*, **2**, 583-587 (2002).

[19] H. Kukula, H. Schlaad, M. Antonietti, S. Forster, The formation of polymer vesicles or "peptosomes" by polybutadiene-block-poly(L-glutamate)s in dilute aqueous solution, *Journal of the American Chemical Society*, **124**, 1658-1663 (2002).

[20] K.D. Hermanson, D. Huemmerich, T. Scheibel, A.R. Bausch, Engineered microcapsules fabricated from reconstituted spider silk, *Advanced Materials*, **19**, 1810-1815 (2007).

[21] J.B. Li, H. Mohwald, Z.H. An, G. Lu, Molecular assembly of biomimetic microcapsules, *Soft Matter*, **1**, 259-264 (2005).

[22] M. Horecha, V. Senkovskyy, M. Stamm, A. Kiriy, One-Pot Synthesis of Thermoresponsive PNIPAM Hydrogel Microcapsules Designed to Function in Apolar Media, *Macromolecules*, **42**, 5811-5817 (2009).

[23] S.W. Choi, Y. Zhang, Y.N. Xia, A Temperature-Sensitive Drug Release

System Based on Phase-Change Materials, *Angewandte Chemie-International Edition*, **49**, 7904-7908 (2010).

[24] X.Z. Zhang, X.D. Xu, S.X. Cheng, R.X. Zhuo, Strategies to improve the response rate of thermosensitive PNIPAAm hydrogels, *Soft Matter*, **4**, 385-391 (2008).

[25] I. Ankareddi, C.S. Brazel, Synthesis and characterization of grafted thermosensitive hydrogels for heating activated controlled release, *International Journal of Pharmaceutics*, **336**, 241-247 (2007).

[26] G.M. Sun, X.Z. Zhang, C.C. Chu, Formulation and characterization of chitosan-based hydrogel films having both temperature and pH sensitivity, *Journal of Materials Science-Materials in Medicine*, **18**, 1563-1577 (2007).

[27] H. Ichikawa, Y. Fukumori, A novel positively thermosensitive controlled-release microcapsule with membrane of nano-sized poly(N-isopropylacrylamide) gel dispersed in ethylcellulose matrix, *Journal of Controlled Release*, **63**, 107-119 (2000).

[28] D.W. Urry, Free-energy transduction in polypeptides and proteins based on inverse temperature transitions, *Progress in Biophysics & Molecular Biology*, **57**, 23-57 (1992).

[29] D.W. Urry, C.H. Luan, C. Harris, T. Parker, Protein-based materials with a profound range of properties and applications: the elastin ΔTt hydrophobic paradigm, in: K. McGrath, D. Kaplan (Eds.) Protein-Based Materials, Birkhäuser Boston, 1996, pp. 133-177.

[30] D.E. Meyer, A. Chilkoti, Genetically encoded synthesis of protein-based polymers with precisely specified molecular weight and sequence by recursive directional ligation: Examples from the elastin-like polypeptide system, *Biomacromolecules*, **3**, 357-367 (2002).

[31] D.T. McPherson, C. Morrow, D.S. Minehan, J.G. Wu, E. Hunter, D.W. Urry, Production and purification of a recombinant elastomeric polypeptide, G-(VPGVG)19-VPGV, from Escherichia-coli, *Biotechnology Progress*, **8**, 347-352 (1992).

[32] A. Girotti, A. Fernandez-Colino, I.M. Lopez, J.C. Rodriguez-Cabello, F.J. Arias, Elastin-like recombinamers: Biosynthetic strategies and biotechnological applications, *Biotechnology Journal*, **6**, 1174-1186 (2011).

[33] D.C. Chow, M.R. Dreher, K. Trabbic-Carlson, A. Chilkoti, Ultra-high expression of a thermally responsive recombinant fusion protein in E-coli, *Biotechnology Progress*, **22**, 638-646 (2006).

[34] H. Kurihara, T. Morita, M. Shinkai, T. Nagamune, Recombinant extracellular matrix-like proteins with repetitive elastin or collagen-like functional motifs, *Biotechnology Letters*, **27**, 665-670 (2005).

[35] L.X. Mi, Molecular cloning of protein-based polymers, *Biomacromolecules*, **7**, 2099-2107 (2006).

[36] J.H. Lee, P.M. Skowron, S.M. Rutkowska, S.S. Hong, S.C. Kim, Sequential amplification of cloned DNA as tandem multimers using class-IIS restriction enzymes, *Genetic Analysis-Biomolecular Engineering*, **13**, 139-145 (1996).

[37] S. Stahl, A. Sjolander, M. Hansson, P.A. Nygren, M. Uhlen, A general strategy for polymerization, assembly and expression of epitope-carrying peptides applied to the Plasmodium-falciparum antigen Pf155/RESA, *Gene*, **89**, 187-193 (1990).

[38] R.A. McMillan, T.A.T. Lee, V.P. Conticello, Rapid assembly of synthetic genes encoding protein polymers, *Macromolecules*, **32**, 3643-3648 (1999).

[39] M.R. Dreher, W.G. Liu, C.R. Michelich, M.W. Dewhirst, A. Chilkoti, Thermal cycling enhances the accumulation of a temperature-sensitive biopolymer in solid tumors, *Cancer Research*, **67**, 4418-4424 (2007).

[40] W. Kim, J. Thevenot, E. Ibarboure, S. Lecommandoux, E.L. Chaikof, Self-assembly of thermally responsive amphiphilic diblock copolypeptides into spherical micellar nanoparticles, *Angewandte Chemie-International Edition*, **49**, 4257-4260 (2010).

[41] J.R. McDaniel, J.A. MacKay, F.G. Quiroz, A. Chilkoti, Recursive directional ligation by plasmid reconstruction allows rapid and seamless cloning of oligomeric genes, *Biomacromolecules*, **11**, 944-952 (2010).

[42] D.W. Urry, T.L. Trapane, K.U. Prasad, Phase-structure transitions of the elastin polypentapeptide water-system within the framework of composition temperature studies, *Biopolymers*, **24**, 2345-2356 (1985).

[43] D.W. Urry, K.D. Urry, W. Szaflarski, M. Nowicki, Elastic-contractile model proteins: Physical chemistry, protein function and drug design and delivery, *Advanced Drug Delivery Reviews*, **62**, 1404-1455 (2010).

[44] Y.H. Cho, Y.J. Zhang, T. Christensen, L.B. Sagle, A. Chilkoti, P.S.

Cremer, Effects of hofmeister anions on the phase transition temperature of elastin-like polypeptides, *Journal of Physical Chemistry B*, **112**, 13765-13771 (2008).

[45] N. Nath, A. Chilkoti, Interfacial phase transition of an environmentally responsive elastin biopolymer adsorbed on functionalized gold nanoparticles studied by colloidal surface plasmon resonance, *Journal of the American Chemical Society*, **123**, 8197-8202 (2001).

[46] T. Yamaoka, T. Tamura, Y. Seto, T. Tada, S. Kunugi, D.A. Tirrell, Mechanism for the phase transition of a genetically engineered elastin model peptide (VPGIG)(40) in aqueous solution, *Biomacromolecules*, **4**, 1680-1685 (2003).

[47] D.E. Meyer, A. Chilkoti, Purification of recombinant proteins by fusion with thermally-responsive polypeptides, *Nature Biotechnology*, **17**, 1112-1115 (1999).

[48] J. Reguera, D.W. Urry, T.M. Parker, D.T. McPherson, J.C. Rodriguez-Cabello, Effect of NaCl on the exothermic and endothermic components of the inverse temperature transition of a model elastin-like polymer, *Biomacromolecules*, **8**, 354-358 (2007).

[49] R. Flamia, P.A. Zhdan, M. Martino, J.E. Castle, A.M. Tamburro, AFM study of the elastin-like biopolymer poly(VaIGIyGlyValGly), *Biomacromolecules*, **5**, 1511-1518 (2004).

[50] K.K. Kumashiro, T.L. Kurano, W.P. Niemczura, M. Martino, A.M. Tamburro, C-13 CPMAS NMR studies of the elastin-like polypeptide (LGGVG)(n), *Biopolymers*, **70**, 221-226 (2003).

[51] K. Ohgo, T.L. Kurano, K.K. Kumashiro, T. Asakura, Structure of the model peptides of Bombyx mori silk-elastin like protein studied with solid state NMR, *Biomacromolecules*, **5**, 744-750 (2004).

[52] P. Schmidt, J. Dybal, J.C. Rodriguez-Cabello, V. Reboto, Role of water in structural changes of poly(AVGVP) and poly(GVGVP) studied by FTIR and Raman spectroscopy and ab initio calculations, *Biomacromolecules*, **6**, 697-706 (2005).

[53] B. Li, D.O.V. Alonso, B.J. Bennion, V. Daggett, Hydrophobic hydration is an important source of elasticity in elastin-based biopolymers, *Journal of the American Chemical Society*, **123**, 11991-11998 (2001).

[54] Y. Cho, L.B. Sagle, S. Iimura, Y. Zhang, J. Kherb, A. Chilkoti, J.M. Scholtz, P.S. Cremer, Hydrogen bonding of β-turn structure is stabilized in D_2O, *Journal of the American Chemical Society*, **131**, 15188-15193 (2009).

[55] D.E. Meyer, A. Chilkoti, Genetically encoded synthesis of protein-based polymers with precisely specified molecular weight and sequence by recursive directional ligation: Examples from the elastin-like polypeptide system, *Biomacromolecules*, **3**, 357-367 (2002).

[56] H. Reiersen, A.R. Clarke, A.R. Rees, Short elastin-like peptides exhibit the same temperature-induced structural transitions as elastin polymers: implications for protein engineering, *Journal of Molecular Biology*, **283**, 255-264 (1998).

[57] T. Yamaoka, T. Tamura, Y. Seto, T. Tada, S. Kunugi, D.A. Tirrell, Mechanism for the phase transition of a genetically engineered elastin

model peptide $(VPGIG)_{40}$ in aqueous solution, *Biomacromolecules*, **4**, 1680-1685 (2003).

[58] Y. Cho, L.B. Sagle, S. Iimura, Y.J. Zhang, J. Kherb, A. Chilkoti, J.M. Scholtz, P.S. Cremer, Hydrogen bonding of beta-turn structure is stabilized in D_2O, *Journal of the American Chemical Society*, **131**, 15188-15193 (2009).

[59] C. Nicolini, R. Ravindra, B. Ludolph, R. Winter, Characterization of the temperature- and pressure-induced inverse and reentrant transition of the minimum elastin-like polypeptide GVG(VPGVG) by DSC, PPC, CD, and FT-IR spectroscopy, *Biophysical Journal*, **86**, 1385-1392 (2004).

[60] Y. Cho, L.B. Sagle, S. Iimura, Y.J. Zhang, J. Kherb, A. Chilkoti, J.M. Scholtz, P.S. Cremer, Hydrogen bonding of beta-turn structure is stabilized in D_2O, *Journal of the American Chemical Society*, **131**, 15188-15193 (2009).

[61] V. Serrano, W. Liu, S. Franzen, An infrared spectroscopic study of the conformational transition of elastin-like polypeptides, *Biophysical Journal*, **93**, 2429-2435 (2007).

[62] A.M. Salvi, P. Moscarelli, G. Satriano, B. Bochicchio, J.E. Castle, Influence of amino acid specificities on the molecular and supramolecular organization of glycine-rich elastin-like polypeptides in water, *Biopolymers*, **95**, 702-721 (2011).

[63] L.D. Muiznieks, F.W. Keeley, Proline periodicity modulates the self-assembly properties of elastin-like polypeptides, *Journal of Biological Chemistry*, **285**, 39779-39789 (2010).

[64] K. Trabbic-Carlson, D.E. Meyer, L. Liu, R. Piervincenzi, N. Nath, T. LaBean, A. Chilkoti, Effect of protein fusion on the transition temperature of an environmentally responsive elastin-like polypeptide: a role for surface hydrophobicity?, *Protein Engineering Design & Selection*, **17**, 57-66 (2004).

[65] X. Ge, D.S.C. Yang, K. Trabbic-Carlson, B. Kim, A. Chilkoti, C.D.M. Filipe, Self-cleavable stimulus responsive tags for protein purification without chromatography, *Journal of the American Chemical Society*, **127**, 11228-11229 (2005).

[66] F.J. Xu, S.P. Zhong, L.Y.L. Yung, E.T. Kang, K.G. Neoh, Surface-active and stimuli-responsive polymer-Si(100) hybrids from surface-initiated atom transfer radical polymerization for control of cell adhesion, *Biomacromolecules*, **5**, 2392-2403 (2004).

[67] M. Ebara, M. Yamato, M. Hirose, T. Aoyagi, A. Kikuchi, K. Sakai, T. Okano, Copolymerization of 2-carboxyisopropylacrylamide with N-isopropylacrylamide accelerates cell detachment from grafted surfaces by reducing temperature, *Biomacromolecules*, **4**, 344-349 (2003).

[68] Y. Ito, Surface micropatterning to regulate cell functions, *Biomaterials*, **20**, 2333-2342 (1999).

[69] D. Falconnet, G. Csucs, H.M. Grandin, M. Textor, Surface engineering approaches to micropattern surfaces for cell-based assays, *Biomaterials*, **27**, 3044-3063 (2006).

[70] W. Frey, D.E. Meyer, A. Chilkoti, Thermodynamically reversible addressing of a stimuli responsive fusion protein onto a patterned surface

template, *Langmuir*, **19**, 1641-1653 (2003).

[71] W. Frey, D.E. Meyer, A. Chilkoti, Dynamic addressing of a surface pattern by a stimuli-responsive fusion protein, *Advanced Materials*, **15**, 248-251 (2003).

[72] N. Nath, A. Chilkoti, Fabrication of a reversible protein array directly from cell lysate using a stimuli-responsive polypeptide, *Analytical Chemistry*, **75**, 709-715 (2003).

[73] S.H. Hsu, S.C. Chuang, C.H. Chen, D.C. Chen, Endothelial cell attachment to the gamma irradiated small diameter polyurethane vascular grafts, *Bio-Medical Materials and Engineering*, **16**, 397-404 (2006).

[74] J.F. Alvarez-Barreto, M.C. Shreve, P.L. Deangelis, V.I. Sikavitsas, Preparation of a functionally flexible, three-dimensional, biomimetic poly(L-lactic acid) scaffold with improved cell adhesion, *Tissue Engineering*, **13**, 1205-1217 (2007).

[75] K. Na, J. Jung, O. Kim, J. Lee, T.G. Lee, Y.H. Park, J. Hyun, "Smart" biopolymer for a reversible stimuli-responsive platform in cell-based biochips, *Langmuir*, **24**, 4917-4923 (2008).

[76] D.E. Meyer, G.A. Kong, M.W. Dewhirst, M.R. Zalutsky, A. Chilkoti, Targeting a genetically engineered elastin-like polypeptide to solid tumors by local hyperthermia, *Cancer Research*, **61**, 1548-1554 (2001).

[77] M.R. Dreher, W.G. Liu, C.R. Michelich, M.W. Dewhirst, F. Yuan, A. Chilkoti, Tumor vascular permeability, accumulation, and penetration of macromolecular drug carriers, *Journal of the National Cancer Institute*, **98**, 335-344 (2006).

[78] D.E. Meyer, B.C. Shin, G.A. Kong, M.W. Dewhirst, A. Chilkoti, Drug targeting using thermally responsive polymers and local hyperthermia, *Journal of Controlled Release*, **74**, 213-224 (2001).

[79] W.E. Liu, M.R. Dreher, D.Y. Furgeson, K.V. Peixoto, H. Yuan, M.R. Zalutsky, A. Chilkoti, Tumor accumulation, degradation and pharmacokinetics of elastin-like polypeptides in nude mice, *Journal of Controlled Release*, **116**, 170-178 (2006).

[80] D. Raucher, A. Chilkoti, Enhanced uptake of a thermally responsive polypeptide by tumor cells in response to its hyperthermia-mediated phase transition, *Cancer Research*, **61**, 7163-7170 (2001).

[81] G.L. Bidwell, D. Raucher, Cell penetrating elastin-like polypeptides for therapeutic peptide delivery, *Advanced Drug Delivery Reviews*, **62**, 1486-1496 (2010).

[82] G.L. Bidwell, D. Raucher, Application of thermally responsive polypeptides directed against c-Myc transcriptional function for cancer therapy, *Molecular Cancer Therapeutics*, **4**, 1076-1085 (2005).

[83] G.L. Bidwell, A.N. Davis, D. Raucher, Targeting a c-Myc inhibitory polypeptide to specific intracellular compartments using cell penetrating peptides, *Journal of Controlled Release*, **135**, 2-10 (2009).

[84] G.L. Bidwell, I. Fokt, W. Priebe, D. Raucher, Development of elastin-like polypeptide for thermally targeted delivery of doxorubicin, *Biochemical Pharmacology*, **73**, 620-631 (2007).

[85] I. Massodi, G.L. Bidwell, D. Raucher, Evaluation of cell penetrating peptides fused to elastin-like polypeptide for drug delivery, *Journal of*

Controlled Release, **108**, 396-408 (2005).

[86] S.R. MacEwan, A. Chilkoti, Digital switching of local arginine density in a genetically encoded self-assembled polypeptide nanoparticle controls cellular uptake, *Nano Letters*, **12**, 3322-3328 (2012).

[87] W. Hassouneh, K. Fischer, S.R. MacEwan, R. Branscheid, C.L. Fu, R.H. Liu, M. Schmidt, A. Chilkoti, Unexpected multivalent display of proteins by temperature triggered self-assembly of elastin-like polypeptide block copolymers, *Biomacromolecules*, **13**, 1598-1605 (2012).

[88] J.A. MacKay, M.N. Chen, J.R. McDaniel, W.G. Liu, A.J. Simnick, A. Chilkoti, Self-assembling chimeric polypeptide-doxorubicin conjugate nanoparticles that abolish tumours after a single injection, *Nature Materials*, **8**, 993-999 (2009).

[89] D.W. Urry, Preprogrammed drug delivery systems using chemical triggers for drug release by mechanochemical coupling, *Abstracts of Papers of the American Chemical Society*, **200**, 74-PMSE (1990).

[90] J. Cappello, J. Crissman, M. Dorman, M. Mikolajczak, G. Textor, M. Marquet, F. Ferrari, Genetic-engineering of structural protein polymers, *Biotechnology Progress*, **6**, 198-202 (1990).

[91] J. Cappello, J.W. Crissman, M. Crissman, F.A. Ferrari, G. Textor, O. Wallis, J.R. Whitledge, X. Zhou, D. Burman, L. Aukerman, E.R. Stedronsky, In-situ self-assembling protein polymer gel systems for administration, delivery, and release of drugs, *Journal of Controlled Release*, **53**, 105-117 (1998).

[92] A. Chilkoti, T. Christensen, J.A. MacKay, Stimulus responsive elastin

biopolymers: applications in medicine and biotechnology, *Current Opinion in Chemical Biology*, **10**, 652-657 (2006).

[93] T.G. Kim, H. Shin, D.W. Lim, Biomimetic scaffolds for tissue engineering, *Advanced Functional Materials*, **22**, 2446-2468 (2012).

[94] N. Annabi, S.M. Mithieux, A.S. Weiss, F. Dehghani, Cross-linked open-pore elastic hydrogels based on tropoelastin, elastin and high pressure CO2, *Biomaterials*, **31**, 1655-1665 (2010).

[95] A.J. Simnick, D.W. Lim, D. Chow, A. Chilkoti, Biomedical and biotechnological applications of elastin-like polypeptides, *Polymer Reviews*, **47**, 121-154 (2007).

[96] H. Betre, L.A. Setton, D.E. Meyer, A. Chilkoti, Characterization of a genetically engineered elastin-like polypeptide for cartilaginous tissue repair, *Biomacromolecules*, **3**, 910-916 (2002).

[97] H. Betre, S.R. Ong, F. Guilak, A. Chilkoti, B. Fermor, L.A. Setton, Chondrocytic differentiation of human adipose-derived adult stem cells in elastin-like polypeptide, *Biomaterials*, **27**, 91-99 (2006).

[98] K. Di Zio, D.A. Tirrell, Mechanical properties of artificial protein matrices engineered for control of cell and tissue behavior, *Macromolecules*, **36**, 1553-1558 (2003).

[99] P.J. Nowatzki, D.A. Tirrell, Physical properties of artificial extracellular matrix protein films prepared by isocyanate crosslinking, *Biomaterials*, **25**, 1261-1267 (2004).

[100] A. Panitch, T. Yamaoka, M.J. Fournier, T.L. Mason, D.A. Tirrell, Design and biosynthesis of elastin-like artificial extracellular matrix

proteins containing periodically spaced fibronectin CS5 domains, *Macromolecules*, **32**, 1701-1703 (1999).

[101] E.R. Welsh, D.A. Tirrell, Engineering the extracellular matrix: A novel approach to polymeric biomaterials. I. Control of the physical properties of artificial protein matrices designed to support adhesion of vascular endothelial cells, *Biomacromolecules*, **1**, 23-30 (2000).

[102] R.A. McMillan, V.P. Conticello, Synthesis and characterization of elastin-mimetic protein gels derived from a well-defined polypeptide precursor, *Macromolecules*, **33**, 4809-4821 (2000).

[103] M. Martino, A.M. Tamburro, Chemical synthesis of cross-linked poly(KGGVG), an elastin-like biopolymer, *Biopolymers*, **59**, 29-37 (2001).

[104] K. Trabbic-Carlson, L.A. Setton, A. Chilkoti, Swelling and mechanical behaviors of chemically cross-linked hydrogels of elastin-like polypeptides, *Biomacromolecules*, **4**, 572-580 (2003).

[105] E.R. Wright, R.A. McMillan, A. Cooper, R.P. Apkarian, V.P. Conticello, Thermoplastic elastomer hydrogels via self-assembly of an elastin-mimetic triblock polypeptide, *Advanced Functional Materials*, **12**, 149-154 (2002).

[106] E.R. Wright, V.P. Conticello, Self-assembly of block copolymers derived from elastin-mimetic polypeptide sequences, *Advanced Drug Delivery Reviews*, **54**, 1057-1073 (2002).

[107] C.M. Bellingham, M.A. Lillie, J.M. Gosline, G.M. Wright, B.C. Starcher, A.J. Bailey, K.A. Woodhouse, F.W. Keeley, Recombinant human elastin polypeptides self-assemble into biomaterials with elastin-

like properties, *Biopolymers*, **70**, 445-455 (2003).

[108] B. Vrhovski, S. Jensen, A.S. Weiss, Coacervation characteristics of recombinant human tropoelastin, *European Journal of Biochemistry*, **250**, 92-98 (1997).

[109] B. Vrhovski, A.S. Weiss, Biochemistry of tropoelastin, *European Journal of Biochemistry*, **258**, 1-18 (1998).

[110] S.G. Wise, S.M. Mithieux, M.J. Raftery, A.S. Weiss, Specificity in the coacervation of tropoelastin: solvent exposed lysines, *Journal of Structural Biology*, **149**, 273-281 (2005).

[111] J. Yang, M. Yamato, C. Kohno, A. Nishimoto, H. Sekine, F. Fukai, T. Okano, Cell sheet engineering: Recreating tissues without biodegradable scaffolds, *Biomaterials*, **26**, 6415-6422 (2005).

[112] I. Elloumi-Hannachi, M. Yamato, T. Okano, Cell sheet engineering: a unique nanotechnology for scaffold-free tissue reconstruction with clinical applications in regenerative medicine, *Journal of Internal Medicine*, **267**, 54-70 (2010).

[113] M. Mie, Y. Mizushima, E. Kobatake, Novel extracellular matrix for cell sheet recovery using genetically engineered elastin-like protein, *Journal of Biomedical Materials Research Part B-Applied Biomaterials*, **86B**, 283-290 (2008).

[114] M.B. van Eldijk, J.C.Y. Wang, I.J. Minten, C.L. Li, A. Zlotnick, R.J.M. Nolte, J. Cornelissen, J.C.M. van Hest, Designing Two Self-Assembly Mechanisms into One Viral Capsid Protein, *Journal of the American Chemical Society*, **134**, 18506-18509 (2012).

[115] S. Freitas, H.P. Merkle, B. Gander, Microencapsulation by solvent extraction/evaporation: reviewing the state of the art of microsphere preparation process technology, *Journal of Controlled Release*, **102**, 313-332 (2005).

[116] E. Campos, J. Branquinho, A.S. Carreira, A. Carvalho, P. Coimbra, P. Ferreira, M.H. Gil, Designing polymeric microparticles for biomedical and industrial applications, *European Polymer Journal*, **49**, 2005-2021 (2013).

[117] Y. Baimark, Y. Srisuwan, Preparation of polysaccharide-based microspheres by a water-in-oil emulsion solvent diffusion method for drug carriers, *International Journal of Polymer Science*, (2013).

[118] B.C. Thanoo, M.C. Sunny, A. Jayakrishnan, Cross-linked chitosan microspheres - preparation and evaluation as a matrix for the controlled release of pharmaceuticals, *Journal of Pharmacy and Pharmacology*, **44**, 283-286 (1992).

[119] J. Akbuga, G. Durmaz, Preparation and evaluation of cross-linked chitosan microspheres containing furosemide, *International Journal of Pharmaceutics*, **111**, 217-222 (1994).

[120] S.A. Agnihotri, N.N. Mallikarjuna, T.M. Aminabhavi, Recent advances on chitosan-based micro- and nanoparticles in drug delivery, *Journal of Controlled Release*, **100**, 5-28 (2004).

[121] Y.Y. Fang, L.J. Wang, D. Li, B.Z. Li, B. Bhandari, X.D. Chen, Z.H. Mao, Preparation of crosslinked starch microspheres and their drug loading and releasing properties, *Carbohydrate Polymers*, **74**, 379-384

(2008).

[122] X.L. Zhang, Z.Y. Hui, D.X. Wan, H.T. Huang, J. Huang, H. Yuan, J.H. Yu, Alginate microsphere filled with carbon nanotube as drug carrier, *International Journal of Biological Macromolecules*, **47**, 389-395 (2010).

[123] A. Aubert-Pouessel, M.C. Venier-Julienne, P. Saulnier, M. Sergent, J.P. Benoit, Preparation of PLGA microparticles by an emulsion-extraction process using glycofurol as polymer solvent, *Pharmaceutical Research*, **21**, 2384-2391 (2004).

[124] N. Faisant, J. Siepmann, J.P. Benoit, PLGA-based microparticles: elucidation of mechanisms and a new, simple mathematical model quantifying drug release, *European Journal of Pharmaceutical Sciences*, **15**, 355-366 (2002).

[125] B.S. Zolnik, D.J. Burgess, Effect of acidic pH on PLGA microsphere degradation and release, *Journal of Controlled Release*, **122**, 338-344 (2007).

[126] S.E. Reinhold, K.G.H. Desai, L. Zhang, K.F. Olsen, S.P. Schwendeman, Self-healing microencapsulation of biomacromolecules without organic solvents, *Angewandte Chemie-International Edition*, **51**, 10800-10803 (2012).

[127] Q.C. Yuan, O.J. Cayre, S. Fujii, S.P. Armes, R.A. Williams, S. Biggs, Responsive core-shell latex particles as colloidosome microcapsule membranes, *Langmuir*, **26**, 18408-18414 (2010).

[128] T. Trongsatitkul, B.M. Budhlall, Multicore-shell PNIPAm-co-PEGMa microcapsules for cell encapsulation, *Langmuir*, **27**, 13468-13480 (2011).

[129] R. Chandrawati, P.D. Odermatt, S.F. Chong, A.D. Price, B. Stadler, F. Caruso, Triggered cargo release by encapsulated enzymatic catalysis in capsosomes, *Nano Letters*, **11**, 4958-4963 (2011).

[130] A. Corma, H. Garcia, Supported gold nanoparticles as catalysts for organic reactions, *Chemical Society Reviews*, **37**, 2096-2126 (2008).

[131] A.D. Price, A.N. Zelikin, Y.J. Wang, F. Caruso, Triggered enzymatic degradation of dna within selectively permeable polymer capsule microreactors, *Angewandte Chemie-International Edition*, **48**, 329-332 (2009).

[132] L.J. De Cock, S. De Koker, B.G. De Geest, J. Grooten, C. Vervaet, J.P. Remon, G.B. Sukhorukov, M.N. Antipina, Polymeric multilayer capsules in drug delivery, *Angewandte Chemie-International Edition*, **49**, 6954-6973 (2010).

[133] K.A. Bogdanowicz, B. Tylkowski, M. Giamberini, Preparation and characterization of light-sensitive microcapsules based on a liquid crystalline polyester, *Langmuir*, **29**, 1601-1608 (2013).

[134] A.P. Esser-Kahn, S.A. Odom, N.R. Sottos, S.R. White, J.S. Moore, Triggered release from polymer capsules, *Macromolecules*, **44**, 5539-5553 (2011).

[135] R. Atkin, P. Davies, J. Hardy, B. Vincent, Preparation of aqueous core/polymer shell microcapsules by internal phase separation, *Macromolecules*, **37**, 7979-7985 (2004).

[136] X. Yu, Z.L. Zhao, W. Nie, R.H. Deng, S.Q. Liu, R.J. Liang, J.T. Zhu, X.L. Ji, Biodegradable polymer microcapsules fabrication through a

template-free approach, *Langmuir*, **27**, 10265-10273 (2011).

[137] A. Shulkin, H.D.H. Stover, Photostimulated phase separation encapsulation, *Macromolecules*, **36**, 9836-9839 (2003).

[138] P.J. Dowding, R. Atkin, B. Vincent, P. Bouillot, Oil core-polymer shell microcapsules prepared by internal phase separation from emulsion droplets. I. Characterization and release rates for microcapsules with polystyrene shells, *Langmuir*, **20**, 11374-11379 (2004).

[139] A.D. Dinsmore, M.F. Hsu, M.G. Nikolaides, M. Marquez, A.R. Bausch, D.A. Weitz, Colloidosomes: Selectively permeable capsules composed of colloidal particles, *Science*, **298**, 1006-1009 (2002).

[140] M.F. Hsu, M.G. Nikolaides, A.D. Dinsmore, A.R. Bausch, V.D. Gordon, X. Chen, J.W. Hutchinson, D.A. Weitz, Self-assembled shells composed of colloidal particles: Fabrication and characterization, *Langmuir*, **21**, 2963-2970 (2005).

[141] D.I. Rozkiewicz, B.D. Myers, S.I. Stupp, Interfacial self-assembly of cell-like filamentous microcapsules, *Angewandte Chemie-International Edition*, **50**, 6324-6327 (2011).

[142] J.A. Hanson, C.B. Chang, S.M. Graves, Z.B. Li, T.G. Mason, T.J. Deming, Nanoscale double emulsions stabilized by single-component block copolypeptides, *Nature*, **455**, 85-88 (2008).

[143] A.S. Utada, E. Lorenceau, D.R. Link, P.D. Kaplan, H.A. Stone, D.A. Weitz, Monodisperse double emulsions generated from a microcapillary device, *Science*, **308**, 537-541 (2005).

[144] H.C. Shum, J.W. Kim, D.A. Weitz, Microfluidic fabrication of

monodisperse biocompatible and biodegradable polymersomes with controlled permeability, *Journal of the American Chemical Society*, **130**, 9543-9549 (2008).

[145] E. Lorenceau, A.S. Utada, D.R. Link, G. Cristobal, M. Joanicot, D.A. Weitz, Generation of polymerosomes from double-emulsions, *Langmuir*, **21**, 9183-9186 (2005).

[146] B.J. Sun, H.C. Shum, C. Holtze, D.A. Weitz, Microfluidic melt emulsification for encapsulation and release of actives, *Acs Applied Materials & Interfaces*, **2**, 3411-3416 (2010).

[147] E.S. Place, N.D. Evans, M.M. Stevens, Complexity in biomaterials for tissue engineering, *Nature Materials*, **8**, 457-470 (2009).

[148] W.J. Chung, J.W. Oh, K. Kwak, B.Y. Lee, J. Meyer, E. Wang, A. Hexemer, S.W. Lee, Biomimetic self-templating supramolecular structures, *Nature*, **478**, 364-368 (2011).

[149] C.M. Nelson, M.M. VanDuijn, J.L. Inman, D.A. Fletcher, M.J. Bissell, Tissue geometry determines sites of mammary branching morphogenesis in organotypic cultures, *Science*, **314**, 298-300 (2006).

[150] J.D. Hartgerink, E. Beniash, S.I. Stupp, Self-assembly and mineralization of peptide-amphiphile nanofibers, *Science*, **294**, 1684-1688 (2001).

[151] J.D. Hartgerink, E. Beniash, S.I. Stupp, Peptide-amphiphile nanofibers: A versatile scaffold for the preparation of self-assembling materials, *Proceedings of the National Academy of Sciences of the United States of America*, **99**, 5133-5138 (2002).

[152] R.N. Shah, N.A. Shah, M.M.D. Lim, C. Hsieh, G. Nuber, S.I. Stupp, Supramolecular design of self-assembling nanofibers for cartilage regeneration, *Proceedings of the National Academy of Sciences of the United States of America*, **107**, 3293-3298 (2010).

[153] S.M. Zhang, M.A. Greenfield, A. Mata, L.C. Palmer, R. Bitton, J.R. Mantei, C. Aparicio, M.O. de la Cruz, S.I. Stupp, A self-assembly pathway to aligned monodomain gels, *Nature Materials*, **9**, 594-601 (2010).

[154] A.C. Mendes, K.H. Smith, E. Tejeda-Montes, E. Engel, R.L. Reis, H.S. Azevedo, A. Mata, Co-assembled and microfabricated bioactive membranes, *Advanced Functional Materials*, **23**, 430-438 (2013).

[155] E.G. Bellomo, M.D. Wyrsta, L. Pakstis, D.J. Pochan, T.J. Deming, Stimuli-responsive polypeptide vesicles by conformation-specific assembly, *Nature Materials*, **3**, 244-248 (2004).

[156] E.P. Holowka, V.Z. Sun, D.T. Kamei, T.J. Deming, Polyarginine segments in block copolypeptides drive both vesicular assembly and intracellular delivery, *Nature Materials*, **6**, 52-57 (2007).

[157] S.W. Lee, C.B. Mao, C.E. Flynn, A.M. Belcher, Ordering of quantum dots using genetically engineered viruses, *Science*, **296**, 892-895 (2002).

[158] T. Douglas, M. Young, Host-guest encapsulation of materials by assembled virus protein cages, *Nature*, **393**, 152-155 (1998).

[159] K.T. Nam, D.W. Kim, P.J. Yoo, C.Y. Chiang, N. Meethong, P.T. Hammond, Y.M. Chiang, A.M. Belcher, Virus-enabled synthesis and assembly of nanowires for lithium ion battery electrodes, *Science*, **312**,

885-888 (2006).

[160] A. Merzlyak, S. Indrakanti, S.W. Lee, Genetically engineered nanofiber-like viruses for tissue regenerating materials, *Nano Letters*, **9**, 846-852 (2009).

[161] L.Y. Wu, J.F. Zang, L.A. Lee, Z.W. Niu, G.C. Horvatha, V. Braxtona, A.C. Wibowo, M.A. Bruckman, S. Ghoshroy, H.C. zur Loye, X.D. Li, Q. Wang, Electrospinning fabrication, structural and mechanical characterization of rod-like virus-based composite nanofibers, *Journal of Materials Chemistry*, **21**, 8550-8557 (2011).

[162] A. Mishra, Y.H. Loo, R.H. Deng, Y.J. Chuah, H.T. Hee, J.Y. Ying, C.A.E. Hauser, Ultrasmall natural peptides self-assemble to strong temperature-resistant helical fibers in scaffolds suitable for tissue engineering, *Nano Today*, **6**, 232-239 (2011).

[163] C.A.E. Hauser, R.S. Deng, A. Mishra, Y.H. Loo, U. Khoe, F.R. Zhuang, D.W. Cheong, A. Accardo, M.B. Sullivan, C. Riekel, J.Y. Ying, U.A. Hauser, Natural tri- to hexapeptides self-assemble in water to amyloid beta-type fiber aggregates by unexpected alpha-helical intermediate structures, *Proceedings of the National Academy of Sciences of the United States of America*, **108**, 1361-1366 (2011).

[164] Z.L. Luo, X.J. Zhao, S.G. Zhang, Structural dynamic of a self-assembling peptide d-EAK16 made of only d-amino acids, *Plos One*, **3**, e2364(2008).

[165] Z.L. Luo, X.J. Zhao, S.G. Zhang, Self-organization of a chiral D-EAK16 designer peptide into a 3D nanofiber scaffold, *Macromolecular*

Bioscience, **8**, 785-791 (2008).

[166] K.J. Nagy, M.C. Giano, A. Jin, D.J. Pochan, J.P. Schneider, Enhanced mechanical rigidity of hydrogels formed from enantiomeric peptide assemblies, *Journal of the American Chemical Society*, **133**, 14975-14977 (2011).

[167] J.Y. Wu, S.Q. Liu, P.W.S. Heng, Y.Y. Yang, Evaluating proteins release from, and their interactions with, thermosensitive poly (N-isopropylacrylamide) hydrogels, *Journal of Controlled Release*, **102**, 361-372 (2005).

[168] O. Chiantore, M. Guaita, L. Trossarelli, Solution properties of poly(n-isopropylacrylamide), *Makromolekulare Chemie-Macromolecular Chemistry and Physics*, **180**, 969-973 (1979).

[169] R. Yoshida, K. Sakai, T. Okano, Y. Sakurai, Surface-modulated skin layers of thermal responsive hydrogels as on off switches .2. drug permeation, *Journal of Biomaterials Science-Polymer Edition*, **3**, 243-252 (1992).

[170] K.S. Soppimath, T.M. Aminabhavi, A.M. Dave, S.G. Kumbar, W.E. Rudzinski, Stimulus-responsive "smart" hydrogels as novel drug delivery systems, *Drug Development and Industrial Pharmacy*, **28**, 957-974 (2002).

[171] A. Kikuchi, T. Okano, Pulsatile drug release control using hydrogels, *Advanced Drug Delivery Reviews*, **54**, 53-77 (2002).

[172] B. Jeong, Y.H. Bae, S.W. Kim, Drug release from biodegradable injectable thermosensitive hydrogel of PEG-PLGA-PEG triblock copolymers, *Journal of Controlled Release*, **63**, 155-163 (2000).

[173] B. Jeong, Y.H. Bae, S.W. Kim, Thermoreversible gelation of PEG-PLGA-PEG triblock copolymer aqueous solutions, *Macromolecules*, **32**, 7064-7069 (1999).

[174] W. Wei, L. Yuan, G. Hu, L.Y. Wang, H. Wu, X. Hu, Z.G. Su, G.H. Ma, Monodisperse chitosan microspheres with interesting structures for protein drug delivery, *Advanced Materials*, **20**, 2292-2296 (2008).

[175] Y.A. Antonov, B.A. Wolf, Calorimetric and structural investigation of the interaction between bovine serum albumin and high molecular weight dextran in water, *Biomacromolecules*, **6**, 2980-2989 (2005).

[176] L. D'Alfonso, M. Collini, G. Baldini, Does beta-lactoglobulin denaturation occur via an intermediate state?, *Biochemistry*, **41**, 326-333 (2002).

[177] X. Hu, P. Cebe, A.S. Weiss, F. Omenetto, D.L. Kaplan, Protein-based composite materials, *Materials Today*, **15**, 208-215 (2012).

[178] W.J. Frith, Mixed biopolymer aqueous solutions - phase behaviour and rheology, *Advances in Colloid and Interface Science*, **161**, 48-60 (2010).

[179] P.C. Bessa, R. Machado, S. Nurnberger, D. Dopler, A. Banerjee, A.M. Cunha, J.C. Rodriguez-Cabello, H. Redl, M. van Griensven, R.L. Reis, M. Casal, Thermoresponsive self-assembled elastin-based nanoparticles for delivery of BMPs, *Journal of Controlled Release*, **142**, 312-318 (2010).

[180] J.T. Cirulis, F.W. Keeley, Kinetics and morphology of self-assembly of an elastin-like polypeptide based on the alternating domain arrangement of human tropoelastin, *Biochemistry*, **49**, 5726-5733 (2010).

[181] T.A.T. Lee, A. Cooper, R.P. Apkarian, V.P. Conticello, Thermo-

reversible self-assembly of nanoparticles derived from elastin-mimetic polypeptides, *Advanced Materials*, **12**, 1105-1110 (2000).

[182] M.R. Dreher, A.J. Simnick, K. Fischer, R.J. Smith, A. Patel, M. Schmidt, A. Chilkoti, Temperature triggered self-assembly of polypeptides into multivalent spherical micelles, *Journal of the American Chemical Society*, **130**, 687-694 (2008).

[183] D. Ershov, J. Sprakel, J. Appel, M.A.C. Stuart, J. van der Gucht, Capillarity-induced ordering of spherical colloids on an interface with anisotropic curvature, *Proceedings of the National Academy of Sciences of the United States of America*, **110**, 9220-9224 (2013).

[184] J. Huo, M. Marcello, A. Garai, D. Bradshaw, MOF-polymer composite microcapsules derived from pickering emulsions, *Advanced Materials*, **25**, 2717-2722 (2013).

[185] S. Jiang, Q. Chen, M. Tripathy, E. Luijten, K.S. Schweizer, S. Granick, Janus particle synthesis and assembly, *Advanced Materials*, **22**, 1060-1071 (2010).

[186] T. Chen, P.J. Colver, S.A.F. Bon, Organic-inorganic hybrid hollow spberes prepared from TiO2-stabilized pickering emulsion polymerization, *Advanced Materials*, **19**, 2286-2289 (2007).

[187] C.M. Bellingham, K.A. Woodhouse, P. Robson, S.J. Rothstein, F.W. Keeley, Self-aggregation characteristics of recombinantly expressed human elastin polypeptides, *Biochimica Et Biophysica Acta-Protein Structure and Molecular Enzymology*, **1550**, 6-19 (2001).

초 록

본 논문에서는 분자 간 가교결합을 위해 라이신이 포함된 ELP (MW: 85kDa)를 생합성 하였으며, 에멀젼과 비 에멀젼 방법을 이용하여 온도 민감성 ELP 마이크로 입자를 제조하였다. ELP의 상전이 현상은 온도에 의한 ELP 분자들의 이차와 삼차 구조의 변화에 기반하며, 200 μM에서 ELP의 상전이 온도(T_t)는 ~37°C로 측정되었다. 첫번째, 에멀젼 상태에서 두 단계의 가교결합을 이용하여 양성 온도 민감성의 ELP/알부민 복합 마이크로 캡슐을 제조하였다. 제조된 캡슐은 T_t 이상의 온도에서 캡슐막에 공극이 형성되는 구조 변화를 보였으며 온도 민감성이 없는 알부민의 혼합률에 따라 구조 변화율을 조절 할 수 있었다. 또한, 글루타알데하이드를 이용한 가교반응시간의 변화로 마이크로 캡슐막의 두께를 조절하였다. 두번째, 에멀젼 상태에서 ELP의 상분리를 제어하고 글루타알데하이드를 가교제로 사용하여 마이크로 비드 또는 마이크로 캡슐을 제조하였다. 가교 과정에서 사용된 온도에 의해 ELP 마이크로 입자의 형태와 온도 감응성이 조절되었다. T_t 보다 높은 온도에서 제조된 ELP 마이크로 캡슐은 T_t 이하의 온도에서 공극이 형성되는 음성 온도 민감성을 보였으며, T_t 보다 낮은 온도에서 제조된 ELP 마이크로 비드는 T_t 이상의 온도에서 공극이 형성되는 양성 온도 민감성을 보였다. 특히, 상전이가 일어나는 온도 범위에서 제조된 ELP 마이크로 캡슐은 양방향 온도 민감성을 나타내었다. 세번째, 온도에 따른 ELP의 상분리 현상을 이용하여 수용액 상에서 ELP 마이크로 비드를

제조하였다. 마이크로 비드는 ELP 분자의 이차구조 변화에 의해 T_t 이하의 온도에서 공극이 생성되는 양성 온도 민감성을 보였다. T_t 이상의 온도에서, ELP 사슬들이 접히고 빽빽하게 압축되기 때문에 공극이 관찰되지 않았다. 반대로 압축된 ELP 사슬들은 T_t 이하의 온도에서 펴지게 되고, 공극을 형성하게 되었다.

색인어: 엘라스틴 유래 폴리펩타이드, 마이크로 입자, 양성과 음성 온도 민감성, 마이크로 캡슐, 마이크로 비드.

학 번: 2009-31280

감사의 글

나노바이오소재연구실에서 공부한지 어느덧 4년반이란 시간이 흘렀습니다. 좋은 경험도 많이 하고 많은 것을 배웠지만, 너무 부족한 제 자신을 채우기에는 짧은 시간이었던 것 같습니다.

그 동안 학문적 연구에 많은 조언을 해 주었을 뿐만 아니라 제가 이 자리에 오기까지 잘 이끌어주시고 제 취업까지 걱정해주신 지도교수님 현진호 교수님께 무한한 감사 드립니다. 그리고 제 논문에 충고와 조언을 해 주신 학과 교수님들, 탁태문 교수님, 박영환교수님, 박종신교수님, 이기훈 교수님, 김태일교수님께 감사 드립니다. 그리고 먼 곳까지 오셔서 심사해 주시고, 많은 조언을 해 주신 한양대 임동우 교수님과 제 실험에 큰 도움을 주신 한양대 이재상님께도 깊은 감사의 말씀을 드립니다.

또한 부경대학교에 있던 시절 석사과정을 지도 해주신 양지영 교수님께도 진심으로 감사 드립니다. 석사 공부를 할 때 저에게 많은 조언과 호의를 베풀어 주신 김진희 박사님께도 고마운 마음을 전합니다.

박사 공부하는 동안 항상 격려해주시고 너무나 큰 사랑을 주신 선배님들, 나경아박사님, 이종환박사님, 정재연박사님, 김유진 선배님, 박수범 선배님께 감사 드립니다.

지난 4년 반 동안 저에게 아낌없는 도움을 주시고 훌륭한 조언과 많은 관심을 주셨던 박종보 형님께도 진심으로 감사의 마음을

전합니다.

실험실 생활 동안 가장 오랜 시간을 같이 해온 울 나노바이오 소재실 식구들, 최재유, 박민성, 안성민, 이다정, 신성철, 정은수. 다들 너무 고맙고 하는 실험 다 잘 되길 바랍니다. 민성아 힘들겠지만 성철이 잘 부탁한다~. 그리고 바이오소재과 모든 식구들에게도 고마운 마음을 전합니다.

最后，把感激献给我的家人.已逝的姥爷和岳父愿你们在天堂安详的生活．感谢岳母对我的关怀与帮助,感谢我伟大的母亲,风风雨雨几十年,养育之恩毕生无以回报．最后献给我的未婚妻吴灵,谢谢你这么多年陪伴在我身边,谢谢你改变我的人生.

정걸（程杰）올림